Sveriges lantbruksuniversitet
Swedish University of Agricultural Sciences
Faculty of Natural Resources and Agricultural Sciences

UNIVERSITÄT BONN

Removal of per- and polyfluoroalkyl substances from drinking water using ozonation

Miriam Dorothea Schäfers

Master's Thesis in Environmental science
As part of the Food Chemistry Programme, Bonn University
Uppsala, 2017

Examensarbete, [45] hp, Institutionen för Vatten och Miljö

Removal of per- and polyfluoroalkyl substances from drinking water using ozonation

Miriam Dorothea Schäfers

Supervisor: **Vera Franke,** Swedish University of Agricultural Sciences, Department of Aquatic Sciences and Assessment

Assistant supervisor: **Dr. Lutz Ahrens,** Swedish University of Agricultural Sciences, Department of Aquatic Sciences and Assessment

Examiner: **Prof. Dr. Karin Wiberg,** Swedish University of Agricultural Sciences, Department of Aquatic Sciences and Assessment

Prof. Dr. Matthias Wüst, Rheinische Friedrich-Wilhelms-Universität Bonn, Institut für Ernährungs- und Lebensmittelwissenschaften

Credits: 45 hec
Level: Master of science
Course title: Independent project in Environmental Science – Master thesis
Course code: EX 0828
Course responsible department: Department of Aquatic Sciences and Assessment

Place of publication: Uppsala
Year of publication: 2017
Online publication: https://stud.epsilon.slu.se

Keywords: Per- and polyfluoroalkyl substances, drinking water, advanced oxidation processes, ozonation, persulfate, heterogeneous catalysis, water treatment

Sveriges lantbruksuniversitet
Swedish University of Agricultural Sciences

Faculty of Natural Resources and Agricultural Sciences Department of Aquatic Sciences and Assessment Environmental Chemistry

Abstract

Per- and polyfluoroalkyl substances (PFASs) are a broad group of man-made chemicals which are persistent, bioaccumulative and toxic. Due to their unique physicochemical properties PFASs are used in various industrial processes and consumer products. Their environmental persistence and ability to undergo long-range transport have made PFASs compounds of concern as they have been found in various matrices all over the world. Concerning PFASs concentrations in blood, breast milk and organs are caused by several exposure routes i.a. contaminated drinking water. Since PFASs are not affected by conventional drinking water treatment techniques, further research on new approaches for water purification is highly needed.
In this study several advanced oxidation processes (AOPs) based on ozonation were tested for their efficiency to degrade PFASs in water. Among other an established method based on heterogeneous catalysis was evaluated in pilot scale. Prior all treatment experiments, adsorption of PFASs to the catalyst surface in MilliQ, tap and water with dissolved organic carbon were evaluated. A fit according to the Freundlich adsorption isotherm model was found. Additional investigations on the adsorption velocity showed that most PFASs adsorb within 10 min to the catalyst material, whereby the adsorption process is superimposed by equilibrium adjustment processes that occur slower. In the pilot scale trial drinking water was fortified with 18 different PFASs (1 000 ng L^{-1}). Removal of more than 98 % was found for PFASs with seven to eleven perfluorinated carbon atoms independent of the functional group. All spiked compounds were removed significantly. In a subsequent approach, all possible combinations of ozone (0.3 unit), catalyst (5 g) and persulfate (1:50 mole ratio spike:ammoniumpersulfate) were evaluated in MilliQ water in a 500 mL laboratory scale set-up. The following trends could be observed: Results comparable to the pilot scale experiment were obtained for the combination of ozone and catalyst; ozone and persulfate as well as ozone, persulfate and catalyst. Surprisingly, the treatment with ozone only led to a removal of perfluorinated carboxylic acids (PFCAs) and perfluorooctane sulfonamide (FOSA). Thus, it has been sown, that there is potential for an improvement of already applied AOP treatment via ozone and catalyst by a combination with persulfate. Further research is needed to determine the optimal reaction conditions for this new approach.

Keywords: Per- and polyfluoroalkyl substances; drinking water; advanced oxidation processes; ozonation; persulfate; heterogeneous catalysis; water treatment

Contents

List of Figures

List of Tables

Acknowledgment

This master thesis is the final part of my studies at the Rheinische-Friedrich-Wilhelms-University in Bonn, Germany. It was carried out at the Swedish University of Agricultural Sciences (SLU) in Uppsala, Sweden.

Luckily, my journey with this thesis project was accompanied and there are many people I would like to thank.
First and foremost I would like to thank Vera Franke for her outstanding supervision. You had a feeling for situations where I needed assistance but you also knew when I could figure out the solution myself (Espresso House presentation). In doing so I learned so much in many ways, technically and personally but especially in time and stress management. It was much fun to work with you and I will really miss our fits of laughter (magnetic, oxygen exclusion, stirrer and cable).
I would also like to thank Dr. Lutz Ahrens who gave me the opportunity to finish my studies at SLU and who acted as my co-supervisor. Thank you for providing insight during the project and answering lots of e-mails when I had problems with Erasmus or with finding an accommodation before I came to Sweden.
Without Prof. Dr. Matthias Wüst I would not have spent this wonderful semester in Sweden. You encouraged me in the decision to do my master thesis abroad and you helped me to make contact with Dr. Lutz Ahrens. For that I am very grateful.
Since this master project is a cooperation with the company Ozonetech in Stockholm, I would like to especially thank Johan Joos Lindberg and Ramnath Lakshmanan who supported me during the preparation and performance of the pilot-scale experiments as well as with the afterward work.
My thanks also go to Lisa Vogel, who always found time to help me during the development of the lab scale set-up for example when a glass cutter or a hot air gun were needed.
Thanks also to Claudia Cascone for the DOC measurement.
Further I would like to thank Nadine Belkouteb, Peter Müller, Anna-Lena Öhmann and Bonnie Baillet for general support and all the other wonderful people at SLU who made this seven months into a precious experience.
Finally the biggest thank is going to Clemens and my parents who never let me down. Thank you for always being there for me!

List of abbreviations

6:2 FTSA	6:2 fluorotelomer sulfonic acid
8:2 FTSA	8:2 fluorotelomer sulfonic acid
AFFF	Aqueous film forming foams
AOP	Advanced oxidation process
b	Adsorption energy
BET	Surface area determination
BPA	Bisphenol A
C_e	Equilibrium concentration
DDT	Dichlordiphenyltrichlorethan
diPAP	Polfluoroalkyl phosphoric acid diester
DOC	Dissolved organic carbon
ECF	Electrochemical flourination process
EFSA	European Food Safety Authority
e.g.	exempli gratia
Et-FOSA	n-Ethyl perfluorooctylsulfonamide
FOSA	Perfluorooctane sulfonamide
FOSA br	Perfluorooctane sulfonamide branched isomers
FOSE	Fluorosulfonamidoethanol
FTOH	Fuorotelomer alcohol
GAC	Granulat activated carbon
HDPE	High density polyethylene
Hg-porosimetry	Mercury intrusion porosimetry
i.a.	inter alia
IS	Internal standard
K_f	Adsorption capacity
K_{OW}	Octanol-water partitioning coefficient
LOD	Limit of detection
LOQ	Limit of quantification
M	Molecular weight
N	Number of samples e.g. 2 for a duplicate

n	Adsorption intensity
N	Number of replicate samples
OECD	Organization for Economic Co-operation and Development
PAC	Powdered activated carbon
PFAA	Perfluoroalkyl acid
PFAS	Per- and polyfluoro alkyl substance
PFBA	Perfluorobutyric acid
PFBS	Perfluorobutane sulfonic acid
PFCA	Perfluorinated carboxylic acid
PFDA	Pefluorodecanoic acid
PFDoDA	Perfluorododecanoic acid
PFHpA	Perfluoroheptanoic acid
PFHxA	Perfluorohexanoic acid
PFHxDA	Perfluorohexadecanoic acid
PFHxS	Perfluorohexane sulfonic acid
PFHxS br	Perfluorohexane sulfonic acid branched isomers
PFNA	Perfluorononanoic acid
PFOA	Perfluorooctanoic acid
PFOcDA	Perfluorooctadecanoic acid
PFOS	Perfluorooctane sulfonic acid
PFOS br	Perfluorooctane sulfonic acid branched isomers
PFPeA	Perfluoropentanoic acid
PFSA	Perfluorinated sulfonic acid
PFTeDA	Perfluorotetradecanoic acid
PFUnDA	Perfluoroundecanoic acid
pH_{pzc}	Point of zero charge
pK_a	Acid dissociaton constant
POP	Persistent organic pollutant
PP	Poly propylene
Q_e	Amount of adsorbate at the equilibrium
q_{max}	Maximum adsorption capacity

R^2	Coefficient of determination
RI-A	Redox potential detected before the catalytic bed
RI-B	Redox potential detected behind the catalytic bed
SEM-EDS	Scanning electron microscopy with energy-dispersive X-ray spectroscopy
SPE	Solid phase extraction
S_w	Waters solubility
UHPLC-MS/MS	Ultra high performance liquid chromatography tandem mass spectrometry
UV	Ultra violet radiation
V	Volume
VUV	Vacuum ultra violet radiation
wt%	Mass fraction
WWTP	Wastewater treatment plant

1 Introduction

1.1 Background

1.1.1 Production and use of PFASs

In the 1950s the production of per- and polyfluoroalkyl substances (PFASs) has been started by the 3M company making use of the electrochemical fluorination process (ECF) (3M, 1999). ECF and the method of telomerization are the two major manufacturing processes of PFASs (Buck et al., 2011; Post et al., 2012). Production and use increased until the 1990s due to their particular features such as their excellent thermal stability and chemical inertness as well as exceedingly low surface tension (Paul et al., 2009; Krafft and Riess, 2015; Zaggia et al., 2016). PFASs are widely applied for example as surfactants, as surface coatings for textile or packaging products because of their oil and water repellency or as processing additives during fluoropolymer production (Ahrens, 2011; Thompson et al., 2011; Arias Espana et al., 2015). Another important utilization is the use of PFASs in aqueous film forming foams (AFFF) as fire extinguisher for hydrocarbon fires (Schröder and Meesters, 2005; Arias Espana et al., 2015). Considerable concerns about the bioaccumulation and toxicity of perfluorooctane sulfonate (PFOS) and their derivates lead the principle manufacturer 3M to an unsolicitous phase out of the PFOS production in 2002 (Paul et al., 2009; Ahrens, 2011; Zaggia et al., 2016). Due to their global distribution, persistence and toxicity, PFOS and its salts were added to the Stockholm convention as a persistent organic pollutant (POP) in May 2009 (United Nations Environment Programme, 2009; Ahrens, 2011; Arias Espana et al., 2015; Merino et al., 2016). Despite those restrictions, PFASs are still used for various products since their unique properties make them irreplaceable in many applications (Schröder and Meesters, 2005). In general, the applied type of PFASs has changed from long chain to short- or rather ultra-short chain PFASs (with five or less fluorinated carbons) as well as new PFASs classes like perfluoroalkyl phosphonates (PAPs) (Ahrens, 2011; Zaggia et al., 2016).

1.1.2 Classification of PFASs

PFASs consist of a per- or polyfluorinated carbon backbone with different chain length (Post et al., 2012; Anumol et al., 2016). Perfluorinated PFASs contain no hydrogen atoms in the perfluorinated carbon backbone, whereas in polyfluorinated PFASs, for example 6:2 FTSA or 8:2 FTSA, not all hydrogen atoms are replaced by fluorine. The general molecular formula of these compounds is $C_nF_{2n+1}R$, where R refers to a terminal functional group or a partly fluorinated molecular part and n to the number of perfluorinated carbon atoms (Buck et al., 2011; Zaggia et al., 2016). PFASs are a wide group of different chemicals (Ahrens, 2011; Post et al., 2012). Depending on structure, they can be categorized in different families like fluorotelomer based products or perfluoroalkyl acids (PFAAs) (Buck et al., 2011). The latter includes e.g. the two most famous groups of carboxylic (C_nF_{2n+1}-COOH) and sulfonic acids (C_nF_{2n+1}-SO_3H),

Fig. 1. Here, the compounds comprising eight carbon atoms (PFOS and PFOA) have drawn the most attention in recent years (Buck et al., 2011; Thompson et al., 2011). Since PFOS and PFOA are frequently detected in water samples much research has focused on those two compounds showing a high detection frequency and high concentrations in the environment for these two PFASs (Thompson et al., 2011; Rahman et al., 2014). An additional important PFASs family is perfluoroalkane sulfonamides (C_nF_{2n+1}-SO_2N<) and their derivates for example perfluorooctanesulfonamide (FOSA) as shown in Fig. 1 (Buck et al., 2011).
Another way to classify PFASs is based on the number of carbon atoms comprising the fluorinanted alkyl chain (Buck et al., 2011; Post et al., 2012). The Organization for Economic Co-operation and Development (OECD) provided the following definition in 2011: PFCAs with greater or equal eight carbons and PFSAs with greater or equal six carbon atoms are referred to long-chain PFASs (Organisation for Economic Co-operation and Development, 2017). Depending on their manufacturing method, PFASs occur in linear, branched or cyclic forms (Post et al., 2012). While products of ECF contain all forms, products of a telomerization process consist of linear PFASs with an even number of carbon atoms only (de Silva and Mabury, 2006; Post et al., 2012). The analysis of isomer profiles thus allows a distinction between historical PFASs production by ECF or a current PFASs release originated from the telomerization process (Ahrens, 2011).

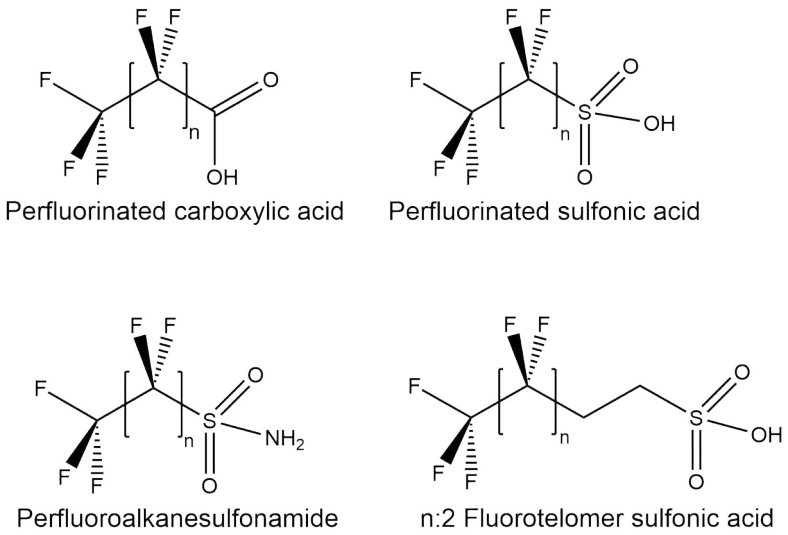

Fig. 1: Structural formula of PFCAs, PFSAs, FOSA and n:2 FTSA. n refers to the number of secondary perfluorocarbon atoms which is ≥ 0.

1.1.3 Physicochemical properties

The versatile application of PFASs for example as high-performance surface-active agents is based on their unique physico-chemical properties (Zhi and Liu, 2015; Zaggia et al., 2016). These include the extremely low surface tension attributable to the lipophilic per- or polyfluorinated carbon backbone and a hydrophilic functional group (Ahrens, 2011; Post et al., 2012; Zaggia et al., 2016). Oil- and water- repellency is a result of this structure (Post et al., 2012). The excellent stability against external influences like heat, acids, bases, oxidizing and reduc-

ing agents as well as stability against radiation or biological degradation is ascribable to the carbon-fluorine-bond, which is the strongest bond in organic chemistry with a C-F bond energy of 552 kJ mol^{-1} (Schröder and Meesters, 2005; O'Hagan, 2008; Giri et al., 2012; Rahman et al., 2014; Zaggia et al., 2016). The binding strength rises with an increasing number of fluorine atoms bound to a carbon atom (Rahman et al., 2014). Thereby this causes an increase in stability and inertness for higher fluorinated PFASs (Rahman et al., 2014). Fluorine resists oxidation because it is the element with the highest electronegativity and has a redox potential of 3.06 V (Rahman et al., 2014; Arias Espana et al., 2015). In other words, fluorine is the strongest oxidation agent except from a few fluorine compounds (Holleman et al., 2007). The fluorine atoms furthermore insulate the carbon-carbon-bonds from chemical or physical impact (Zaggia et al., 2016). Water solubility of PFASs depends on the functional group and the chain length of the lipophilic part of the molecule. Under environmental conditions, PFCAs and PFSAs occur mainly in their dissociated form (compare pK_a values in Tab. 1) with a negative charge located at the functional group. In comparison to PFAS precursors like FOSA or fluorotelomer alcohols (FTOHs) with an undissociated and therefore uncharged hydrophilic functional group, PFCAs and PFSAs have a considerably higher water solubility. Moreover, the water solubility also increases with a decreasing number of fluorinated carbon atoms (Rahman et al., 2014). The vapor pressure decreases with an increasing carbon chain length for PFCAs and PFSAs (Rahman et al., 2014). The outstanding stability of PFASs, one of many useful properties which lead to the widespread use of this compound class, made them compounds of concern: they are persistent, bioaccumulative and they have diverse health effects (Schröder and Meesters, 2005; Rahman et al., 2014; Merino et al., 2016). In comparison to highly persistent ionic PFASs, the less persistent PFASs, among other things those which are called precursor compounds, could be transformed by biodegradation, hydrolysis or photolysis (Ahrens, 2011; Post et al., 2012). The partial degradation of FTOHs, polyfluoroalkyl phosphoric acid diesters (diPAPs) and further neutral precursor compounds could lead to a release of the more persistent ionic PFCAs and PFSAs (Ahrens, 2011; Post et al., 2012). diPAPs for example could be transformed to FTOH. In a second step occurring in soil, sludge or wastewater through biodegradation or caused by chemical reactions in the atmosphere, FTOH could break down to PFOA (Post et al., 2012). Since it is proven, that long-chain PFCAs and PFSAs as well as the respective PFAS precursor degradation products are highly persistent, global producers replaced those compounds with short- or rather ultra-short chain PFASs, i.e. five or less fluorinated carbons (Wang et al., 2013; Zaggia et al., 2016). With their voluntary phase-out, 3M replaced C_6, C_8 and C_{10} based PFASs with PFASs based on C_4 perfluorinated carbon chains (Weppner, 2000; Wang et al., 2013). Hereby bioaccumulation and health risks should be reduced (Krafft and Riess, 2015). Though, the short and ultra-short chain PFASs exhibit environmentally persistent and therefore a reduction of the total amount in the environment would not be achievable (Zaggia et al., 2016).

1.1.4 Sources and distribution in the environment

Generally, there are two pathways through which PFASs can be released into the environment: emission from point and nonpoint sources as well as direct and indirect sources (Ahrens, 2011; Buck et al., 2011). The classification into point and nonpoint sources is related to the size of the affected area. The distribution through nonpoint sources is diffuse. On the contrary, the terminology direct - indirect source refers to the release of non-degraded and degraded compounds, respectively. Examples for point sources are effluents from wastewater treatment plants (WWTPs), fluorine processing industry, or unleash from AFFF. Surface runoff and atmospheric deposition are known as typical nonpoint sources (Ahrens, 2011; Post et al., 2012; Krafft and Riess, 2015). The terminology direct source stands for the release of PFASs directly from one of the diverse steps in the product life cycle like production, use or disposal of a PFASs containing object (Buck et al., 2011). Buck et al. (2011) differentiates the specification as an indirect source since another way of PFASs emission into the environment is the formation by degradation of a precursor compound for example of fluorotelomer alcohols which takes place in biota.
Long-range transport of PFASs occurs through the aquatic and atmospheric path depending on chemical and physical properties, for example water solubility, volatility, chain length and functional group (Ahrens, 2011; Krafft and Riess, 2015). The percentage of each pathway to the distribution of PFASs is not known (Post et al., 2012). PFAS precursors like fluorosulfonamidoethanols (FOSEs) or FTOHs are nonpolar, volatile and thereby disseminated by air (Post et al., 2012; Krafft and Riess, 2015). PFASs containing a polar functional group, like a carboxylic or a sulfonic acid, are highly water soluble and dissociate under environmental pH-conditions (Ahrens, 2011). The ionic forms have a low vapor pressure and remain in the water phase or are accumulated to particles (Ahrens, 2011). This leads to a detection of PFASs in remote places like the Arctic Ocean (Arias Espana et al., 2015). Groundwater contamination can amongst other be caused by surface runoff, firefighting training making use of AFFF or deposition of air emissions on soil with a subsequent migration of the PFASs into the groundwater (Ahrens, 2011; Post et al., 2012).

1.1.5 Human exposure and effects

Worldwide, PFASs were found in human blood, breast milk and organs (Buck et al., 2011; Post et al., 2012; Krafft and Riess, 2015; Zaggia et al., 2016). Of all PFASs, PFOS is most abundantly detected in humans, followed by PFOA and PFHxS (Schröter-Kermani et al., 2013). A daily intake ranging from 3 - 220 ng kg_{bw}^{-1} PFOS and 1 - 130 ng kg_{bw}^{-1} PFOA for the population of North America and Europe was calculated for different scenarios by Trudel et al. (2008). A more recent estimation conducted by EFSA (2012), stated a daily ingestion of 5 - 10 ng kg_{bw}^{-1} for PFOS and 4 - 7 ng kg_{bw}^{-1} for PFOA from dietary intake. On this occasion fish, seafood, fruit and fruit products were identified as the main nutritional sources by the European Food Safety Authority (EFSA, 2012). In general, contaminated food and drinking water were found to be the main intake sources of human exposure for the common population (Fromme et al., 2009;

Haug et al., 2010; Krafft and Riess, 2015). In contaminated drinking water areas, drinking water was observed to be the major exposure source (Vestergren and Cousins, 2009). Further intake occurs via diverse pathways as e.g. inhalation of in- and outdoor air, house durst or treated fabrics (Post et al., 2012; Krafft and Riess, 2015). Moreover, specific professorial groups like fluorochemical plant workers, ski waxing technicians or fire fighters exhibit an occupational related higher exposure (reviewed by Krafft and Riess, 2015).
For PFHxS, PFOS and PFOA serum half-lives of 8.5, 5.4 and 2.3 - 3.8 years, respectively, were reported by United States Environmental Protection Agency (2009) and Seals et al. (2011). Even low concentrations may lead to negative health effects due to long half-lives and concomitant slow excretion. Adverse health effects are enhanced by metabolic generation of PFOA from FTOH and diPAPS (D'eon and Mabury, 2011; Lee and Mabury, 2011; Krafft and Riess, 2015). PFASs can act as endocrine disruptors, possible carcinogens, reproductive and developmental toxins (Ding and Peijnenburg, 2013; Gorrochategui et al., 2014; Merino et al., 2016). As reviewed by Rahman et al. (2014) diverse health effects like low semen quality, delayed puberty in children, testicular and kidney cancer or low birth weight are associated with the exposure to certain PFASs.

1.2 Treatment techniques

Detected PFASs concentrations in water vary usually between $pg\,L^{-1}$ to $ng\,L^{-1}$ while firefighting activities or fluorochemical production sites could lead to increased amounts in the range of $\mu g\,L^{-1}$ to $mg\,L^{-1}$ (Rahman et al., 2014). Conventional primary and secondary water treatment techniques like coagulation, sand filtration, sedimentation or active sludge treatment do not remove PFASs efficiently (Sinclair and Kannan, 2006; Loganathan et al., 2007; Rahman et al., 2014). Further, (bio-)degradation of precursor compounds could lead to increasing PFCAs and PFSAs concentrations in the effluent relative to the influent (Sinclair and Kannan, 2006; Ahrens, 2011; Rahman et al., 2014). The adsorption on granular activated carbon (GAC) is the most common and frequently used treatment technique for PFASs.
AOPs describe a group of treatment techniques that are based on *in-situ* generation of hydroxyl radicals ($OH^{\bullet}$). AOPs are widely applied in water treatment to degrade a large number of different organic pollutants (Suty et al., 2004). In the ideal case, the treatment leads to an outright mineralization of the pollutant (Schröder and Meesters, 2005; Ribeiro et al., 2015). Diverse combinations of reactants and technologies like ozone (O_3), hydrogen peroxide (H_2O_2), ultra violet radiation (UV), persulfate ($S_2O_8^{2-}$) and others have been applied (Glaze et al., 1987; Andreozzi, 1999; Kasprzyk-Hordern, 2003; Oturan and Aaron, 2014; Yang et al., 2016). Miscellaneous reaction conditions could also lead to a generation of further radicals like $SO_4^{\bullet-}$, $O_2^{\bullet-}$ or $CO_3^{\bullet-}$ (Merino et al., 2016). According to the applied technology, a classification into homogeneous or heterogeneous processes is feasible. A general characteristic of homogeneous AOPs is the occurrence in a single phase (Ribeiro et al., 2015). Proceeding reactions are depending on direct interactions between target components and reactive species. Heterogeneous reactions are characterized by mass transfer limited adsorption and desorption processes on the

catalyst surface (Soon and Hameed, 2011; Ribeiro et al., 2015).

1.2.1 AOP with ozone

Ozone is a very selective oxidant and therefore primary reacts with electron rich organic molecule parts like double bonds or activated aromatic compounds (von Gunten, 2003; Kasprzyk-Hordern, 2003; Ribeiro et al., 2015). The main driver influencing the stability of ozone is the water matrix, in particular its pH, temperature and concentrations of natural organic matter (von Gunten, 2003; Kasprzyk-Hordern, 2003). In a pH range from 7 to 10, the half-life of ozone could reach values from 15 to 25 min (Kasprzyk-Hordern, 2003, and references therein).
Further, pH has a great influence on the degradation pathway of organic contaminants: Low pH values lead to direct ozonation whereas indirect ozonation is affected by hydroxyl radicals at pH values > 8. This is because ozone decomposition increases with an increase in pH. At high pH values hydroxyl radicals are generated by radical chain reactions between hydroxyl ions and ozone as shown in the following mechanism (Hoigné, 1998).

$$O_3 + OH^- \longrightarrow O_2 + HO_2^- \quad (1)$$

$$HO_2^- + H^+ \rightleftharpoons H_2O_2 \quad (2)$$

$$HO_2^- + O_3 \longrightarrow HO_2\cdot + O_3\cdot^- \quad (3)$$

$$HO_2\cdot \rightleftharpoons H^+ + O_2\cdot^- \quad (4)$$

$$O_2\cdot^- + O_3 \longrightarrow O_2 + O_3\cdot^- \quad (5)$$

$$O_3\cdot^- + H^+ \longrightarrow HO_3\cdot \quad (6)$$

$$HO_3\cdot \longrightarrow HO\cdot + O_2 \quad (7)$$

$$HO\cdot + O_3 \longrightarrow HO_2\cdot + O_2 \quad (8)$$

Non-selectivity and exceeding high reactivity are the main features of hydroxyl radicals (von Gunten, 2003; Ikehata and El-Din, 2004; Schröder and Meesters, 2005). Hydroxyl radicals react 10^6 - 10^{11} times faster with diverse organic compounds or functional groups than molecular ozone (see Tab. 2 Munter, 2001, and references therein). Compared to molecular ozone which has an redox potential of $E^0 = 2.07$ V hydroxyl radicals are even more powerful ($E^0 = 2.80$ V) (Langlais, 1991).
As reviewed by Ribeiro et al. (2015) many AOPs making use of ozone are broadly applied for the treatment of various micropollutants, for example atrazine, alachlor or dichlordiphenyltrichlorethan (DDT).
A limited number of studies have been conducted for PFASs treatment with AOPs as well (Ribeiro et al., 2015). Schröder and Meesters (2005) found that PFOS resists degradation with ozone as well as O_3/H_2O_2 and O_3/UV. All trials were conducted under alkaline conditions (pH = 11). The same result was found by Yang et al. (2014a) for PFOS treated under alkaline ozonation. Under the same conditions 6:2 FTSA was transformed to a residual amount of 13 %. Lin et al. (2012) reproduced the experimental conditions of Schröder's alkaline ozonation and reported a successful degradation of PFOA and PFOS with 33 % and 43 % removal, respec-

tively. The authors observed an increase in elimination to 90 % PFOA and 85 % PFOS by a 15 min initial ozonation at pH = 4 - 5 and a subsequent adjustment to pH 11. Further, Lin et al. (2012) found a reduction of > 99 % within four hours for both compounds via perozone treatment (O_3/H_2O_2).
Schröder et al. (2010) investigated PFASs destruction via a combination of ozone treatment and heterogeneous catalysis as a part of multiple approaches. The catalyst material celite, a 80 % TiO_2, 20 % rutile mixture, was applied. Compared to Fenton/UV, GAC and reverse osmosis treatment with removal rates of 73 %, 96 %, 90 % for PFOA and 62 %, 97 %, 86 % for PFOS respectively, low removals to about 14 % (PFOA) and 53 % (PFOS) were reported by Schröder et al. (2010) regarding the ozone/celite approach. In this study research on ozone activation with a heterogeneous catalyst is continued.
The following steps represent the ongoing processes during a classical heterogeneous catalysis (Soon and Hameed, 2011; Dalrymple et al., 2010):

1. Transport of dissolved ozone and PFASs to the catalyst surface
2. Adsorption of reactants to the active sites
3. Catalyzed reaction between the adsorbed compounds
4. Desorption of reaction products from the surface
5. Transfer of products from the solid phase into the surrounding liquid phase

1.2.2 AOP with persulfate

The sulfate radical ($SO_4 \cdot^-$, E°=2.6 V) is an oxidizing agent applied in novel AOPs (Huling and Pivetz, 2006). This highly oxidative radical species can for instance be generated by heat, UV-radiation, transition metals or hydrogen peroxide activated homolytical bond cleavage of persulfate ions ($S_2O_8^{2-}$, E°=2.1 V) (Tsitonaki et al., 2010; Merino et al., 2016).
Hori et al. (2005) and Wang et al. (2010) found that the application of highly reactive sulfate radicals in combination with UV and vacuum ultra violet radiation (VUV) irradiation leads to an efficient degradation of PFCAs. This showed that F^-, CO_2 and small quantities of shorter chain PFCAs, were the main reaction products. Further studies on PFASs degradation with persulfate and diverse persulfate activation techniques are reviewed by Arias Espana et al. (2015).
Combinations of ozone and persulfate have been tested by Abu Amr et al. (2014) and Yang et al. (2016) for the degradation of different chemical oxygen demand fractions from landfill leachates and bisphenol A (BPA). Abu Amr et al. (2014) found an enhanced PFASs removal compared to a treatment with ozone only. Further, for BPA a removal rate of 62 % was reached. For the reaction of various aromatic compounds with sulfate radicals, reactions rates in the magnitude of 10^6-10^9 were found by (Neta et al., 1977).

1.3 Aims and research questions

The overall aim of this study was the investigation and evaluation of the removal efficiency of PFASs in water by ozonation. The practical part of this thesis is divided into the following three segments.

1. Pretest on the catalyst material to calculate adsorption isotherms and sorption behavior of PFASs over time,
2. Pilot scale degradation trial with a combination of ozone and catalyst using tap water,
3. Laboratory scale degradation trial with various combinations of ozone, catalyst and persulfate using MilliQ water.

The following research questions are aimed to be answered with this thesis:

Ia How do the different PFASs behave regarding to adsorption on the catalyst surface?

Ib How quickly do the different PFASs adsorb on the catalyst surface?

II Is it possible to treat PFASs contaminated drinking water by catalyzed ozonation, making use of a heterogeneous and inorganic catalyst material?

III Is it possible to enhance the removal efficiency of the previously tested combination of catalyst and ozone by adding persulfate?

2 Materials and Methods

The pilot scale trials were conducted at the facility of the company Ozonetech in Stockholm, Sweden. Pretests on the catalyst material (2.3), the lab-scale trials (2.5) as well as the evaluation of the pilot scale trial (2.4) were performed at the Department of Aquatic Sciences and Assessment at the Swedish University of Agricultural Science (SLU), Uppsala, Sweden.

2.1 Chemicals and materials

2.1.1 PFASs standards

Analytical standards shown in Tab. 1 were used to spike the water. A detailed list containing the relative manufacturer and the purity is displayed in Tab. A.1. Further a mix of 16 mass labeled internal standards (IS), purchased from Wellingon Laboratories (Canada) with a purity > 98 %, was applied for internal calibration. A list of the corresponding compounds is shown in Tab. A.2.

2.1.2 Chemicals

Methanol (99.9 % hypergrade for LC-MS, LiChrosolv®, Merck, Germany) was used for cleaning of glassware and vials as well as for sample preparation for ultra high performance liquid chromatography tandem mass spectrometry (UHPLC-MS/MS) analyses. All experiments were conducted in tap, dissolved organic carbon (DOC) or MilliQ water (Millipak® Express 20, 0.22 µm filter, Merck Millipore). Ammoniumpersulfate (99.5 %, Peroxy Chem, USA), in the following just referred to as persulfate, was used during the lab scale trials. All lab scale trial samples were purged with nitrogen gas, provided from a house-made production.

2.1.3 Equipment

Tab. A.3 shows a list of the during the experiments used equipment.

2.2 Overview of experiments on catalyst and ozonation treatment in pilot- and lab-scale

An overview of the set-up parameter of the conducted pretest (2.3), pilot scale trial (2.4) as well as the the lab-scale trials (2.5) is given in Tab. 2:

Tab. 1: Physicochemical characteristics of selected PFASs investigated in this thesis including their acronyms, molecular formula, molecular weight (**M**), water solubility (**lg S_w**), octanol-water partitioning coefficient (**lg K_{OW}**) and the acid dissociation constant (**pK_a**).

.

Compound	Acronym	Molekular formula	M [g/mol]	lg S_w [mol/L]	lg K_{OW}	pK_a
PFCAs						
Perfluorobutyric acid*	PFBA	$C_3H_7CO_2H$	214.04	0.42[b]	2.91[a]	0.85[b]
					2.82[b]	0.05[e]
Perfluoropentanoic acid*	PFPA	$C_4H_9CO_2H$	264.05	-0.37[b]	3.69[a]	0.81[b]
					3.43[b]	-0.10[c,e]
Perfluorohexanoic acid*	PFHxA	$C_5F_{11}CO_2H$	314.05	-1.16[b]	4.50[a]	0.84[b]
					4.06[b]	-0.16[c]
						-0.17[d]
Perfluoroheptanoic acid*	PFHpA	$C_6F_{13}CO_2H$	364.06	-1.94[b]	5.36[a]	0.82[b]
					4.67[b]	-0.19[c]
						-0.20[d]
Perfluorooctanoic acid*	PFOA	$C_7F_{15}CO_2H$	414.07	-2.73[b]	6.26[a]	0.90[b]
					5.30[b]	-0.2[c]
						-0.21[d]
Perfluorononanoic acid*	PFNA	$C_8F_{16}CO_2H$	464.08	-3.55[b]	7.23[a]	0.82[b]
					5.92[b]	-0.21[c,d]
Perfluorodecanoic acid*	PFDA	$C_9F_{19}CO_2H$	514.08	-4.31[b]	8.26[a]	-0.21[c]
					6.50[b]	-0.22[d]
Perfluoroundecanoic acid	PFUnDA	$C_{10}F_{21}CO_2H$	564.1	-5.13[b]	7.15[b]	-0.21[c]
						-0.22[d]
Perfluorododecanoic acid	PFDoDA	$C_{11}F_{23}CO_2H$	614.1	-5.94[b]	7.77[b]	-0.21[c]
						-0.22[d]
Perfluorotetradecanoic acid	PFTeDA	$C_{13}F_{27}CO_2H$	714.11	-7.42[b]	8.90[b]	0.21[c]
						-0.22[d]
Perfluorohexadecanoic acid	PFHxDA	$C_{15}F_{31}CO_2H$	814.14	n.a.	n.a.	-0.22[d]
Perfluorooctadecanoic acid	PFOcDA	$C_{17}F_{35}CO_2H$	914.15	n.a.	n.a.	-0.22[d]
PFSAs						
Perfluorobutane sulfonic acid*	PFBS	$C_4F_9SO_3H$	300.1	-1.00[b]	3.90[b]	-3.94[b]
						0.14[c,d]
Perfluorohexane sulfonic acid*	PFHxS	$C_6F_{13}SO_3H$	400.11	-2.24[b]	5.17[b]	-3.45[b]
						0.14[c,d]
Perfluorooctane sulfonic acid*	PFOS	$C_8F_{17}SO_3H$	500.13	-3.92[b]	4.67 [a]	-3.41[b]
					6.43[b]	0.14[c,d]
FTSAs						
6:2 fluorotelomer sulfonic acid*	6:2 FTSA	$C_8H_4F_{13}SO_3H$	428.17	-2.51[b]	4.44[b]	0.36[c]
8:2 fluorotelomer sulfonic acid	8:2 FTSA	$C_{10}H_4F_{17}SO_3H$	528.18	-3.96[b]	5.66[b]	n.a.
FOSAs						
Perfluorooctane sulfonamide	FOSA	$C_8F_{17}SO_2NH_2$	499.14	-5.05[b]	5.62[b]	6.52[c]
						6.56[d]
n-Ethyl perfluorooctane sulfonamide	Et-FOSA	$C_{10}F_{17}SO_2NC_2H_6$	527.2	-6.97[b]	6.71[b]	7.91[d]

[a] Rayne and Forest (2009)
[b] Wang et al. (2011)
[c] Steinle-Darling and Reinhard (2008)
[d] Ahrens et al. (2012)
[n.a.] not available
[*] PFASs regulated in Naturvårdverkets drinking water guideline

Tab. 2: Comparison of the pretest-, pilot scale- and lab scale setup.

Parameter	Pretest	Pilot scale	Lab scale
Amount water [L]	0.04	50	0.5
Analyzed water type(s)	MilliQ, tap, DOC	tap	MilliQ
Amount catalyst [g]	0.1	10 000	5
Age catalyst	new	1 year old	new
Amount ozone [$g\,h^{-1}$]	-	5	0.3
Amount ozone [$g\,h^{-1}\,L^{-1}$]	-	0.1	0.6
Spike per compound [$ng\,L^{-1}$]	100 - 10 000	1 100	1000
Number of spiked PFASs	18	18	15
Ratio catalyst:water [$g\,L^{-1}$]	2.5	200	10
Ratio Spike per compound:catalyst [$(ng\,L^{-1})\,g^{-1}$]	1 000 - 100 000	0.11	200
System	batch	flow trough	batch
pH stabilization	no, but pH constant	stabilized	no, pH variations depend on experimental conditions
pH	MilliQ, DOC water: 5 tap water: 7	7.5	varied from 7.3 to 2.9

2.3 Pretests on the catalyst material

For a better characterization of the PFASs degradation processes by advanced oxidation with ozone and a special catalyst, two pre-tests were run. The first test was an isotherm study and the second test an experiment to evaluate the adsorption velocity on the catalyst (kinetic study). The result of these studies gave information on the absorption process, like the absorption capacity and adsorption intensity of the PFASs on the catalyst surface.
All used vials were cleaned in LC-MS grade methanol in an ultrasonic bath for 15 min.

2.3.1 Kinetic studies

For receiving information on the adsorption velocity of the different PFASs on the catalyst surface, kinetic studies were performed. For this purpose, 0.1 g of the inorganic iron and oxygen based catalyst material (cf. 2.6) and 40 mL tap water were added into a 50 mL polypropylene (PP) tube. The experiment was conducted as a duplicate. After the addition of 20 µL PFASs stock solution (20 000 $\mu g\,L^{-1}$), the tubes were subsequently put on a horizontal shaking machine at 150 rpm. A list of the analyzed PFASs is presented in Tab. 3. Single 100 µL samples were taken after 1, 2, 5, 10, 15, 30, 75 and 100 min from the same 50 mL tube using an automatic pipette (VWR, maximal pipette volume: 200 µL). Further a positive blank trial (N = 2) was conducted to evaluate the PFASs adsorption to the tube walls. Hereto 40 mL tap-water and 20 µL of the same PFASs mix were added into a 50 mL PP-tube. After shaking the tube for 5 min a 100 µL sample was taken. For the analysis 100 µL sample solution, 80 µL methanol and 20 µL internal standard solution (50 $\mu g\,L^{-1}$) were pipetted into a cleaned 700 µL polypropylene vial and measured by direct injection ultra high performance liquid chromatography tandem mass spectrometry (UHPLC - MS/MS) (see 2.7).

2.3.2 Isotherm studies

A dissolved organic carbon (DOC) water was prepared. For this purpose 1.33 g soil and 150 mL MilliQ water (Millipak® Express 20, 0.22 µm filter, Merck Millipore) each were added in two 250 mL polyethylene bottles. The bottles were shaken for 48 h at 50 rpm and subsequently centrifuged for 30 min at 3 000 rpm. The centrifugated solution was left standing for four more days so that the remaining turbidity could settle to the bottom of the bottle. The supernatant liquid was removed with 10 mL HSW NORM-JECT® syringes, pre-filtered through a quantitative filterpaper (Minktell Ahlstrom, Grade 00H, pore size: 0.45 µm) and filtrated in a second step with syringe filters (VWR International, 0.45µm pore size, nylon membrane). After diluting the DOC water with the double amount of MilliQ water, it had a DOC concentration of 10.0 millig/L. The DOC analysis was conducted with the method described by Lavonen et al. (2013).
The isotherm studies were conducted with MilliQ-, tap-, and DOC water at a time. All samples for the isotherm study were prepared in duplicate as described in the following. 40 mL of the appropriate water type, 0.1 g catalyst material and 20 µL of the particular PFASs-mix stock solution were filled into a 50 mL PP tube. The PFASs-mix contained 18 different PFASs as shown in Tab. 3. Five different PFASs-stock solutions with a content of 200 µg L^{-1}, 1 000 µg L^{-1}, 2 000 µg L^{-1}, 10 000 µg L^{-1} and 20 000 µg L^{-1} in methanol were used resulting in concentrations of 0.1 µg L^{-1}, 0.5 µg L^{-1}, 1 µg L^{-1}, 5 µg L^{-1} and 10 µg L^{-1} for MilliQ- (N = 2), tap- (N = 2), and DOC water (N = 2), respectively. Additional negative blanks were prepared which contained water and catalyst only (N = 2). This was done in order to evaluate possible PFASs contamination of the used equipment. Further, positive blanks under exclusion of catalyst were conducted for the 1 µg L^{-1} PFASs sample (N = 2). On this occasion water and spike were applied to evaluate the PFASs adsorption to the PP tube walls.
All prepared PP-tubes were horizontally shaken for 110 h and 25 min at 150 rpm. On the basis of the shaking, the catalyst was more or less decomposed. In three PP-tubes a complete pulverization occurred (see Fig. A.6). For this reason an additional centrifugation was necessary. Thus, all PP-tubes were centrifuged twice at room temperature for 10 min at 3 000 rpm. Then 100 µL of the sample supernatant from each PP-tube (N = 2), 80 µL methanol and 20 µL methanol based internal standard solution with a content of 50 µg L^{-1} were pipetted into 700 µL PP vials and analyzed using direct injection UHPLC - MS/MS.
Experimental data obtained from the 100 h shaking experiment was evaluated regarding the fit to different adsorption isotherm models (i.e. Freundlich and Langmuir).

2.3.2.1 Freundlich adsorption isotherm

The Freundlich adsorption isotherm is an empirical model which describes the state of equilibrium between adsorbate and adsorbent. It is frequently used to characterize the adsorption process of many compounds on heterogeneous surfaces (Freundlich, 1926; Senevirathna et al.,

Tab. 3: Compounds that were investigated and spiked during the isotherm and kinetic trials

PFCAs		PFSAs	PFAS precursor
PFBA	PFDA	PFBS	6:2 FTSA
PFPeA[a]	PFUnDA[b]	PFHxS	8:2 FTSA
PFHxA	PFDoDA[b]	PFOS	FOSA[b]
PFHpA	PFTeDA[b]		
PFOA	PFHxDA[a]		
PFNA	PFOcDA[a]		

[a] Compounds that were excluded for the evaluation of the adsorption isotherm trials for MilliQ, tap and DOC water because more than two of the measured five concentrations were were below the calculated LOQ. Further PFPeA was excluded as well.

[b] Compounds that were additionally excluded for the adsorption isotherm evaluation of DOC water because more than two of the measured five concentrations were below the calculated LOQ.

2010; Desta, 2013). The Freundlich equation can be expressed as

$$Q_e = K_f \cdot C_e^{\frac{1}{n}} \tag{9}$$

$$\ln(Q_e) = \ln(K_f) + \frac{1}{n} \cdot \ln(C_e) \tag{10}$$

where Q_e represents the equilibrium adsorbate amount (mg g^{-1}) and C_e corresponds to the equilibrium concentration of the analyzed compounds (mg L^{-1}). K_f and n are the Freundlich constants adsorption capacity and adsorption intensity, respectively. K_f ((µg g^{-1})(µg L^{-1})$^{-n}$) describes the loading of adsorbent with adsorbate, whereas n has no unit. They can be determined from a linear plot of $\ln(C_e)$ vs. $\ln(Q_e)$ as presented in (10). Thus K_F corresponds to the y-axis intercept and n to the reciprocal slope of the linear Freundlich isotherm. n has been found to describe the degree of nonlinearity between the concentration of adsorptive and adsorbate. $n = 1$ results in a linear adsorption isotherm. In this case, the compound distribution between the liquid and the solid phase is independent of the respective concentration. In case $n > 1$ the adsorption is a physical process and if $n < 1$ the adsorption is identified as a chemical process (Ochoa-Herrera and Sierra-Alvarez, 2008; Senevirathna et al., 2010; Desta, 2013). Furthermore n^{-1} is a valid parameter for the surface heterogeneity ranging between 0 and 1. With a decreasing value for n^{-1}, the surface heterogeneity increases (Haghseresht and Lu, 1998).

For the evaluation of K_f values a plot with the number of perfluorinated carbon atoms vs the common logarithm of K_f ($\lg(K_f)$) was created. This type of plot was previously used by Hansen et al. (2010), however the total chain length instead of the perfluorinated carbon atom number was applied. This means that a number of eight carbon atoms was taken into account for PFOA instead of seven, since the carbon atom of the carboxylic group was added.

2.3.2.2 Langmuir adsorption isotherm

The Langmuir adsorption isotherm model assumes a finite number of sites on the adsorbent surface. Since it further assumes monolayer adsorption and the absence of sorbat-sorbat interactions, no further adsorption can take place at a once occupied site. For this reason, the surface theoretically reaches a point of saturation (Ochoa-Herrera and Sierra-Alvarez, 2008; Desta, 2013). The Langmuir isotherm is represented by

$$q_e = \frac{b \cdot q_{max} \cdot C_e}{1 + b \cdot C_e} \tag{11}$$

where q_e is the equilibrium adsorbate amount (mg g^{-1}), b refers to the adsorption energy, q_{max} describes the maximum adsorption capacity (mg g^{-1}) and C_e is the equilibrium concentration of the analyzed compounds (mg L^{-1}) (Hameed et al., 2007; Yu et al., 2009; Desta, 2013).

2.3.2.3 Calculations

First, the detection and quantification limits LOD and LOQ were calculated according to equation (19) and (20). Solely the values exceeding the LOQ were used for further calculations e.g. the adsorption isotherms. Q_e and C_e were determined from the raw data according to:

$$c_{corr} = \frac{2 \cdot c_m \cdot m_{cat,ideal}}{m_{cat,is}} \tag{12}$$

$$C_e = \frac{c_{corr}}{1000} \tag{13}$$

$$Q_e = \frac{(c_t - c_{corr}) \cdot V}{m_{cat,ideal}} \tag{14}$$

where c_m is the measured concentration (µg L^{-1}), c_{corr} represents the, according to the weighed in mass of catalyst, corrected concentration (µg L^{-1}). $m_{cat,ideal}$ refers to the target amount of catalyst material which is 100 mg and $m_{cat,is}$ describes the actually weighed in amount of catalyst (mg). The factor 2 is needed since the water samples were diluted with the same amount of methanol for the UHPLC-MS/MS measurement (cf. section 2.3.2). c_t refers to the initially spiked target concentration and V describes water volume and thus is constant at 0.04 L. With the exception of PFPeA, PFTeDA, PFHxDA and PFOcDA for MilliQ- and tap-water as well as PFPeA, PFUnDA, PFDoDA, PFTeDA, PFHxDA, PFOcDA and FOSA for DOC-water, all spiked compounds listed in Tab. 3 were fitted according to the mentioned adsorption isotherm models. A behavior according to either Freundlich or Langmuir was found the most reasonable.

2.4 Pilot scale trials

Further experiments with the specific catalyst material were conducted at the facilities of the company Ozonetech in a 50 L pilot scale system as shown in Fig. A.1. A scheme of the setup is presented in Fig. 2. The water circulates in the system and passes from the bottom to the top through a catalytic bed containing of 12 L (~10 kg) granulated catalyst material. An average amount of 5 g h^{-1} ozone is introduced in the system via a venturi injector. The venturi injector works as follows: by a pressure drop between the inlet and the outlet of the injector a vacuum is created inside. The vacuum causes a suction into the injector, whereby ozone is yield into the system (Leusink, 2013). Excess ozone is removed in the contact tank and the water containing dissolved ozone is pumped through the catalytic bed. Further the spike was introduced into the system via the venturi injector.

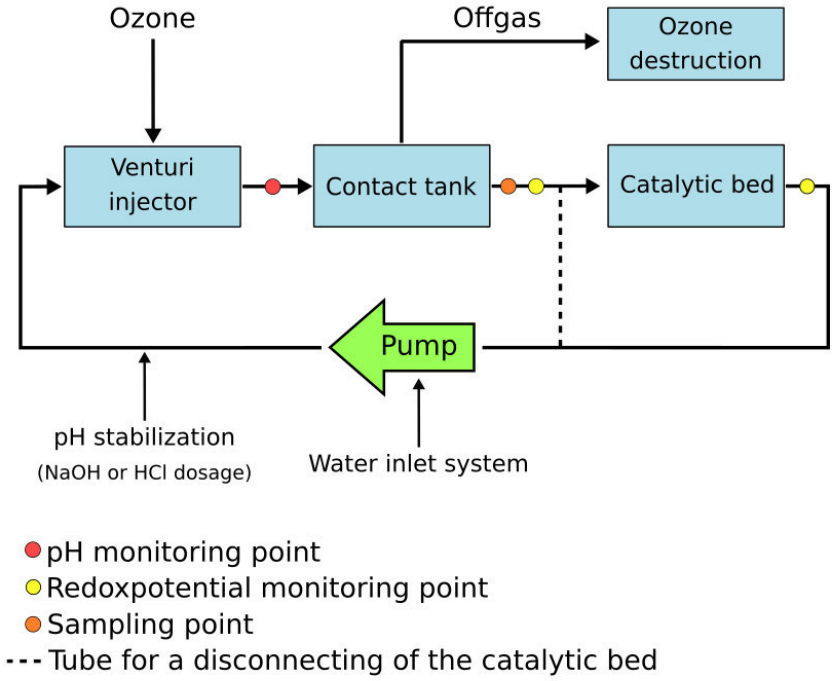

Fig. 2: Experimental set up pf the pilot scale trials.

It was not possible to apply fresh catalyst material for the conducted experiment. According to Ozonetech, the used catalyst was approximately one year old and the system was run for a few days per week to treat organic solvents, effluent of different pharmaceutical companies and tap water which was spiked with an amount of 5 mg L^{-1} PFOS. After each treatment experiment the system was rinsed with water and/or organic solvent (e.g. methanol). To ascertain whether the previous use of the catalyst could affect the conducted experiment, the pilot scale system was filled with tap water which circulated for 8 h. Samples taken after 8 h were compared to fresh tap water samples taken at the Ozonetech facility. Since the detected PFOS concentration increased about the factor 3.4 (13.6 ng L^{-1}) in the 8 h sample compared to fresh tap water (4.0 ng L^{-1}), a cleaning step was necessary. For this purpose, the system was flushed for four hours with a 20 % methanol 80 % water mixture. The pilot scale experiment was conducted as

shown in Tab. 4 and described in the following steps.
On day one, the tap water was spiked with 0.1 mL of a mix, containing the same 18 PFASs as used during the pretests (Tab. 3), with a concentration of 50 000 ng mL^{-1} absolute per compound. An originally planned injection of 1 mL PFASs-mix was due to complications not possible. During the first test section, the catalytic bed was excluded and the water circulated with a flow of 850 L h^{-1} through the tubes only. This trial was conducted to evaluate the losses of PFASs due to adsorption to the tube walls. After the injection, the system was equilibrated for 23.5 h and sample S6 was taken. Since the catalytic bed did not contain water, it was necessary to add the corresponding amount of 5 - 10 L into the pilot scale system on day two. Subsequent to this, the catalytic bed was opened and the system was adjusted to the new conditions with a circulation flow of 400. A reduced flow of 400 L h^{-1} was applied. The whole modification process including time for a pressure stabilization took 15 min. The water was spiked again (at 00:23:30) with 1.0 mL of the same PFASs mix containing 18 PFASs with a concentration of 50 000 ng absolute per compound. Thus in total 1.1 mL of the PFASs mixture was spiked, resulting in a theoretical concentration of 1 100 ng L^{-1} in the pilot plant. This was necessary to achieve the desired PFASs concentration in the system. The sampling was continued 30 min after the second injection (S8 sample at 01:00:46). At day six, a last sample (S14 (0h) at 04:23:25) was taken before the ozone flow was turned on. Subsequent to the sampling, the ozonation started. The starting and accompanying adjustments of the ozone flow took 5 min. All parameters were set at 04:23:30. 30 min later the next sample (S15 (0.5h) at 05:00:00) was taken.
During the whole experiment, the redox potential before (RI-A) and after the catalytic bed (RI-B) as well as the pH value were measured every ten seconds. However, problems with the automated data logging led to a lack of information for day 3 and 4. For the same reason no data are available for the last hour of the ozonation trial on day six. According to detected changes, the pH was automatically adjusted by the addition of 5 % hydrochloric acid or 5 % sodium hydroxide solution to a value of pH = 7.5. The redox potential functions as a unit for the amount of dissolved ozone.
At each sampling time (see Tab. 4) duplicate samples were taken. For each sampling 4.98 mL water were filled directly into 10 mL graduated polystyrene vials. Then 20 µL internal standard mix c = 50 ng mL^{-1} (cf. Tab. A.2) were added into the polystyrene vial and the samples were measured by online SPE UHPLC-MS/MS. Additionally two 0.5 L samples were taken in duplicates before (at 04:23:25) and after the ozonation experiment (at 05:07:30) to evaluate potentially occurring changes in fluorine concentration. The analysis was conducted by the geochemical laboratory, Swedish University of Agricultural Sciences making use of the SS-EN ISO 10304-1:2009 (modified) method (Geochemical laboratory, Department of Aquatic Sciences and Assessment, Swedish University of Agricultural Sciences, 2017).

2.4.1 Calculations

The PFASs concentrations received from the pilot scale trial were standardized to the PFASs concentration measured at day six S14 (0h) (04:23:25) before the ozonation was turned on.

Tab. 4: Chronological procedure of the pilot scale trials.

Day	Experiment	Description	Modifications on the system	Time[a]	Sampling
				DD:HH:MM	[h]
1	Positive blank walls	Determination of the PFASs adsorption to the walls		00:00:00	S1
			+spike PFASs-mix 1	00:00:00	
				00:00:30	S2
				00:01:07	S3
				00:04:00	S4
				00:09:30	S5
2-5	Positive blank catalyst	Determination of the PFASs adsorption to the catalyst and time for an establishment of equilibrium		00:23:30	S6
			+ 5-10 L water catalytic bed was opened		
			+ spike PFASs-mix 2	00:23:45	
				01:00:15	S7
				01:00:46	S8
				01:03:45	S9
				01:07:45	S10
				03:23:47	S11
				04:01:47	S12
				04:03:46	S13
6	Degradation trial	Evaluation of the degradation by ozone		04:23:25	S14 (0h)
			Ozone flow was turned on	04:23:30	
				05:00:00	S15 (0.5)
				05:00:30	S16 (1h)
				05:01:30	S17 (2h)
				05:02:30	S18 (3h)
				05:03:30	S19 (4h)
				05:04:30	S20 (5h)
				05:05:30	S21 (6h)
				05:06:30	S22 (7h)
				05:07:30	S23 (8h)

[a] The time measurement was started with the spike of 0.1 mL of the standard mix and continued until the end of the trial.

First of all, the mean of this duplicate is computed and set as 100 %. The deviation of the mean from one sample of the standardized duplicate was used as the standard deviation. The standard deviation of the 0 h sample is yield as the deviation of the absolute mean from one sample of the duplicate with a subsequent conversion into a relative value.
Furthermore an investigation of the received data regarding a reaction kinetic of first and second order was conducted. The respective integrated and linear forms of the first order (equations 15 and 16) and second order (equations 17 and 18) rate law are given as (Atkins and de Paula, 2006):

$$-\frac{dc}{dt} = k \cdot c \tag{15}$$

$$\ln(c) = -k \cdot t + \ln(c_0) \tag{16}$$

$$-\frac{dc}{dt} = k \cdot c^2 \tag{17}$$

$$\frac{1}{c} = k \cdot t + \frac{1}{(c_0)} \tag{18}$$

where k is the rate constant with (s^{-1}) for first order reactions and ($L\,mol^{-1}\,s^{-1}$) for second order reactions. t is the time (s). To this purpose time was plotted against the natural logarithm ($\ln(c)$) for first (cf. 16) and c^{-1} for the second order (cf. 18) reaction kinetic. Hereby c refers to the standardized data mentioned above. The plots of t vs. $\ln(c)$ or c^{-1} were applied for all data points. Not all data points of the ozonation trial were affected by removal since adsorption and desorption processes on the catalyst surface took place. For the calculation of rate constant solely data points were used which are within the time interval of a compound in which the detected amount decreases. From the point of time where a slightly increase in amount was visible the following data were excluded from this evaluation since balance reactions cover potentially continuing degradation reactions. The absolute value of slope corresponds to the particular rate constant.
The redox potential was monitored during the whole pilot scale experiment and a graph showing the data from day five and six is presented in Fig. A.12. An excerpt for day 6 is presented in Fig. A.11. Within the first hour of ozonation, RI-A increased around 170 mV and RI-B around 110 mV. At this time, the maximal redox potential was attained. During the following six hours of ozonation, the redox potential degreased constantly around 6 mV for RI-A and 7 mV for RI-B. A fluorine concentration of 0.173 mg L^{-1} was detected for both samples taken after the ozonation experiment (at 04:23:25). The detected concentration of sample taken before the ozonation trial at (at 05:07:30) showed low accordance in concentration with values of 0.160 mg L^{-1} and 0.381 mg L^{-1}. A repeated measurement of the latter sample resulted in 0.188 mg L^{-1}.

2.5 Laboratory scale trial

Further laboratory (lab) scale trials were conducted to evaluate the improvement potential of during the pilot scale experiments applied AOP treatment conditions by a combination with

persulfate. Persulfate is a strong oxidant which creates radicals by a homolytical bond cleavage with an even increased redox potential after activation (Kolthoff and Miller, 1951; Yang et al., 2016). A broad approach was chosen for the experiment and various combinations of the presence of catalyst, ozone and persulfate were evaluated with the custom-made set-up, which differs strongly from the previously tested pilot scale. The water : catalyst ratio is 20 times smaller and the spike per compound : catalyst ratio is about a factor 1818 bigger in the lab scale trials than in the pilot scale experiment (cf. Tab. 2).

An overview over the performed experiments is shown in Tab. 5. The use of three necked flasks (500 mL) has big advantages over e.g. gas washing bottles, since it allows a simultaneous pH- and temperature monitoring. Further it is not necessary to stop the ozone flow for sampling. To ensure an effective mixing in the system, glass coated stirring bars (1.9 cm long) and a magnetic stirrer were applied. The broadly used polytetrafluoroethylene coated stirring bars were resigned since the coating material contains fluorine. As presented in Fig. A.6 a permanent shaking of the catalyst material led to a clear damage of the inorganic catalyst during the performance of the isotherm study. Therefore, and in consideration of the high iron content (cf. Tab. 7), it was essential to fix the catalyst material in the flask. For this purpose, perforated 50 mL PP centrifuge tubes were prepared. Four holes (4 mm Ø) were drilled per cm^2 and the burr on the inner tube wall was removed with the help of tweezers. PP tubes as an inert material were chosen over metallic sieves, as radical reactions taking part during the trial could be influenced by metal. As found in the isotherm study (cf. 3.1.2), PFASs adsorption to the tube walls had negligible influence on the applied spike-concentration. Ozone resistant chloropene rubber stopper were applied to fix the gas-inlet and outlet tubes. The application of a gas diffuser was essential to enlarge the water-gas contact area and to thereby enhance the dissolution of ozone gas in the water. A consideration of the high surface tension of water is important, since no gas bubbles are created at a diffuser pore size of 25 - 50 µm.

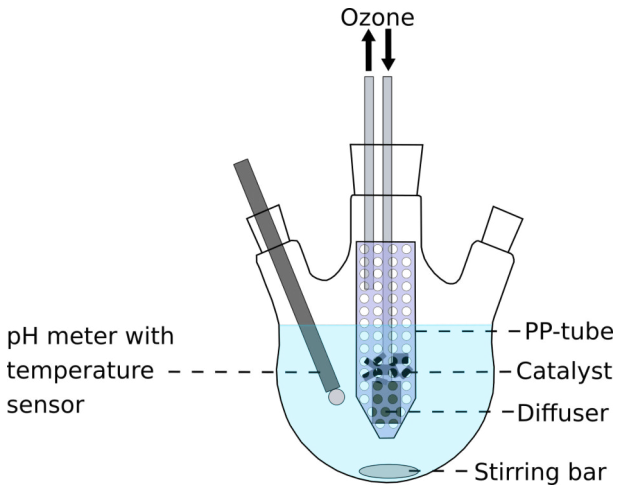

Fig. 3: Experimental set up of the lab scale trials.

The trials were proceeded as follows: A perforated PP-tube was placed in the middle of the three-necked flask. Then the diffuser and/or an amount of 5 g catalyst were placed in the tube if needed. Diffuser and ozone generator were connected via a 115 cm long tube (inner diameter: 5 mm). A volume of 500 mL MilliQ water was filled in the flask and it was spiked with 50 µL of

Tab. 5: Overview over the conducted lab scale trials with the applied combinations of persulfate, ozone and catalyst.

Sample ID	Persulfate	Ozone	Catalyst	Spike[a]	Description
Negative blank					
1	-	-	-	-	Test for contaminations in the water or the trial setup
Positive blanks					*Adsorption to :*
2a	-	-	Yes	Yes	the walls and the catalyst
2b	-	-		Yes	the walls
Degradation trials					*Treatment of PFASs trough:*
T1	-	Yes	-	Yes	ozone
T2	-	Yes	Yes	Yes	ozone and catalyst
T3	Yes	-	-	Yes	persulfate
T4	Yes	Yes	-	Yes	persulfate and ozone
T5	Yes	-	Yes	Yes	persulfate and catalyst
T6	Yes	Yes	Yes	Yes	persulfate, ozone and catalyst

[a] The stock solution contained 10 000 ng mL^{-1} per compound and a concentration of 1 000 ng L^{-1} per compound was achieved in the flask. A list of all spiked compounds is presented in Tab. 6.

a PFASs-mix containing 15 PFASs with 10 000 ng mL^{-1} per compound resulting in a theoretical initial concentration of 1 000 ng L^{-1} in the flask. A list of all spiked compounds is shown in Tab. 6. For the lab scale trials compounds with an even carbon atom number were spiked only. Nevertheless PFPeA, PFHpA, PFNA and PFUnDA were still analyzed. Through this it was evaluated whether they could be generated as the degradation products of longer chain compounds. The solution was stirred at 500 rpm. After ten minutes of balance adjustment, the first sample was taken and the ozone flow was turned on if needed. An ozone amount of 300 mg h^{-1} was produced. Because of this small quantity no ozone degradation step was needed. The off gas was piped to the outlet of the fume hood. In case persulfate was involved in the trial, 187 mg (mole ratio PFASs/ammonium persulfate 1:50) of the salt were added after the ten minutes of PFASs balance adjustment. The stirring was increased briefly to achieve the best possible mixing.

Further 1 mL samples were taken after 5, 15, 30, 60, 90 and 120 min. 1 mL samples were collected and pipetted into a 1.5 mL PP vial. Thereupon, the samples were purged with nitrogen gas for five seconds to remove dissolved ozone and to stop ongoing reactions. Since the catalyst material is magnetic, the vial was placed on a magnet for 5 - 10 s to attract possibly dispersed catalyst material to the bottom of the vial. Then 350 µL of the liquid supernatant sample was transferred into a 700 µL PP vial. Subsequently 280 µl methanol and 70 µl internal standard mixture (c = 50 µg L^{-1}) were added into the vial. Samples of trial T1, T2 and T3 (cf. Tab. 5) as well as the positive blank samples were analyzed via direct injection using UHPLC-MS/MS (see 2.7.1). Due to complications with the measuring instrument samples of the trials T4, T5 and T6 (cf. Tab. 5) were analyzed with direct injection using HPLC-MS/MS (Agilent) (cf. 2.7.2). All trials were run in duplicates and during the trial pH and temperature were measured every five minutes. After the experiment, the whole equipment was rinsed three times with

methanol (LC-MS grade). Additionally, PP-tube and stirring bars were each time sonicated for 15 min.

Tab. 6: Compounds that were spiked during the lab scale trial.

PFCAs	PFSAs	PFAS precursosr
PFBA	PFBS	6:2 FTSA
PFHxA	PFHxS	8:2 FTSA
PFOA	PFOS	FOSA
PFDA		Et-FOSA[a]
PFDoDA		
PFTeDA[a]		
PFHxDA[a]		
PFOcDA[a]		

[a] No quantification possible since the sample repipetting into new vials caused a worsening of R^2 to a value < 0.99 for the calibration curve.

2.5.1 Calculations

As with the pilot scale data, no absolute values were used for the result evaluation. At first the raw data were corrected by multiplication with a positive blank correction factor and if needed mass correction factors for different initial weights of catalyst and persulfate. The positive blank correction factor was computed as the mean concentration at the time 0 min (N = 2) divided by the mean of all mean concentrations (N = 2) from further samples. Mass correction factors were the result of the target weight of catalyst or persulfate divided by the actual used amount. Then the PFASs concentrations obtained for the duplicates were standardized separately on the 0 h sample of each experiment, which was taken before the degradation process was started. As a next step, the mean of the computed relative values was calculated per duplicated. The deviation of the mean from one sample of the duplicate was used as the according standard deviation.

2.6 Catalyst characteristics

To gain more insights about the catalyst material, it was sent to the industrial research institute Swerea|IVF for a detailed characterization. The conducted analysis comprised mercury intrusion porosimetry (Hg-porosimetry), surface area determination (BET) and low vacuum scanning electron microscopy with energy-dispersive X-ray spectroscopy (SEM-EDS). A picture of the catalyst material is shown in Fig. A.3. It is a predominantly black colored granulate with an approximate particle size of 0.5 - 1.0 cm. Some pieces show a white discoloring. Hg-porosimetry (Micromeritics AutoPore III 9410) was carried out to determine parameters like pore volume and median pore diameter. The surface area was analyzed via a BET measurement (Micromeritics, Gemini VII). Results of this analysis are summarized in Tab. 7.

Tab. 7: Results of the catalyst characterization.

Parameter	Result	Error	Unit
Hg-porosimetry			
Pore volume	0.3		$cm^3\,g^{-1}$
Pore diameter	0.2		µm
Median pore diameter	0.2 - 0.3		µm
Pore area	6		$m^2\,g^{-1}$
Porosity	54		vol%
BET			
Specific surface area	26.4	±0.3	$m^2\,g^{-1}$
Water content	1.9		%
Density	4.3		$g\,cm^{-3}$
SEM-EDS[a]			
High concentration (> 10 wt%)	Fe		
	O		
Low concentration (> 1 wt%)	Si		
	Zn		
Also detectable (< 1 wt%)	Mn		

[a] In particles with white discoloring, higher concentrations of silicon and oxygen, lower concentrations of iron and additionally manganese and aluminum were found.

The elemental composition was determined via SEM-EDS (JEOL JSM-6610LV with an EDS detector from Bruker, model XFlash 5010). An acceleration voltage of 15 kV and a working distance of 10 mm were applied. The test results are displayed in Tab. 7 and a spectra is exemplary shown for one piece of catalyst in Fig. A.4. Oxigen, iron and zinc are homogeneously distributed in the catalyst material and no difference in composition was observed comparing core and surface. An uneven distribution was solely found for silicon. Further exemplary microscopy pictures for a 30x enlargement are displayed in Fig. A.5.

2.7 Sample preparation and instrumental analysis

Pretest samples and the samples of the lab-scale experiments T1 (ozone), T2 (ozone, catalyst), T3 (persulfate) as well as the positive blanks adsorption to the walls and adsorption to the catalyst (cf.Tab. 5) were analyzed by direct injection UHPLC-MS/MS. The analysis was carried out by a TSQ Quantiva (Thermo Scientific, Waltham, MA, USA). Due to problems with the instrument, further samples of the lab-scale experiments T4 (persulfate, ozone), T5 (persulfate, catalyst) and T6 (persulfate, catalyst, ozone) (cf.Tab. 5) were measured via direct injection HPLC-MS/MS (HPLC, Agilent Technologies 1200 Series, Palo Alto, CA, USA). Samples taken during the pilot scale experiment at the facility of Ozonetech were analyzed by online SPE using UHPLC-MS/MS (TSQ Quantiva by Thermo Scientific, Waltham, MA, USA).

2.7.1 Direct injection using UHPLC-MS/MS

A reverse-phase Waters Acquity UPLC BEH C18 (2.1 x 50 mm, 1.7 µm particle size, Waters) column, at a temparature of 40 °C was used for PFASs separation. In order to prevent interferences cause by solvent contaminations, an UPLC BEH C18 column (2.1 x 5 mm, 1.7 µm particle size, VanGuard) is preconnected to the analytical column. A gradient with 98 % eluent A (MilliQ water with 0.5mM ammonium acetate) and 2 % eluent B (acetonitrile) as initial conditions, at a constant flow rate of 0.5 mL h^{-1}, was run. Between 30 s and 8 min the mixing ratio of the mobile phase was slowly inverted with a constant rate. The new conditions of 2 % A and 98 % B were kept for two minutes. Then, without a gradient, the mixing ratio was switched back again to initial conditions. A sample volume of 10 µL was injected for direct injection.
The PFASs were introduced in the MS-part via an electron ionization (ESI) interface in the negative mode. The ion source had a voltage of 1 000 V, the ion transfer tube had a temperature of 325 °C and the vaporizer of 450 °C. The mass spectrometer is a triple quadrupol.

2.7.2 Direct injection using HPLC-MS/MS

The analysis via direct injection HPLC-MS/MS was carried out with a HPLC, Agilent Technologies 1200 Series, Palo Alto, CA, USA. The analysis was conducted with the method described by Ahrens et al. (2016).

2.7.3 Online SPE using UHPLC-MS/MS

A reversed-pased Accucore C18 trapping column (30x2.1 mm, Waters) was used for online SPE and an analytical Acquity UPLC BEH C18 (2.1 x 50 mm, 1.7 µm particle size, Waters) for PFASs separation. An UPLC BEH C18 column (2.1 x 5 mm, 1.7 µm particle size, VanGuard) is in each case preconnected to the online SPE and the analytical column in order to delay backgroud peaks caused by solvent contaminations and thereby prevent interferences. For the preconcentration and the analytical separation of PFASs different ratios of eluent A (MilliQ water with 0.5mM ammonium acetate) and eluent B (acetonitrile) were used.
1 mL sample volume was first injected into a high volume loop and then transferred into the trapping column by the loading pump (flow rate 1.2 mL, eluent ratio 98 % A, 2 % B) for PFASs enrichment. This conditions were kept constant for 3.3 min. After a swith-over of a six-way valve, the trapping column was backflushed by the elution gradient (flow rate: 0.5 mL min^{-1}; eluent ratio 98 % A : 2 % B). At the same time, the high volume loop was rinsed with 5 % A and 95 % B at a flow rate of 0.2 mL min^{-1} by the loading pump. Between 3.3 min and 9.15 min the mixing ratio of the elution gradient was slowly inverted to 5 % A and 95 % B was adjusted. The new conditions were kept constant for further 2 min. Then, the mixing ratio of the elution gradient was switched back immediately to the initial conditions of 98 % A and 2 % B. At the same time, the flow rate of the loading pump was increased to 1.2 mL and an eluent ratio of 98 % A, and 2 % B. The analytical column had a temperature of 40 °C.
The PFASs were introduced in the MS-part via an electron ionization (ESI) interface in the

negative mode. The ion source had a voltage of 1 000 V, the ion transfer tube had a temperature of 325 °C and the vaporizer of 450 °C. The mass spectrometer is a triple quadrupol.

2.8 Quality control and quality assurance

2.8.1 Negative blanks

Negative blanks are samples from experiments that were conducted with the same procedure as the real trials with the only difference, that the water was not spiked with PFASs. A list with the detected PFASs contaminations in negative blank samples is presented in Tab. A.7.

2.8.2 Method detection limit

Tab. 8 presents the limits of detection in the unit ng L^{-1} for all analyzed PFASs and all conducted experiments. The LODs were calculated according to equation (19). c_{ng} refers to the mean of a detected PFAS concentrations in a negative blank replicate sample (ng L^{-1}) and σ represents the relative standard deviation (ng L^{-1}). Further the LOQ is calculated similarly as shown in equation 20

$$LOD = c_{nb} + 3 \cdot \sigma \tag{19}$$

$$LOQ = c_{nb} + 10 \cdot \sigma \tag{20}$$

If no PFASs contamination was detected in the negative blank, the mean of all lowest calibration point at the same concentration with a signal to noise ratio > 3 was set as the LOD.

2.8.3 Positive blanks

An overview of the recovery of spike in the conducted positive blank samples is shown for the pretests and the lab scale trials (Tab. 9). The variations in concentration during the equilibrium adjustment of the pilot scale trials were large and noticeably for different PFASs wherefore no recovery of spike is calculated (cf. Fig. A.13).

2.8.4 Standard deviation of duplicates

In this study, the standard deviation of duplicates was calculated as a quality parameter of the repeatability of replicate samples. For this purpose, the percentage deviation of a single duplicate sample from the mean of the duplicate, which was set as 100 %, was calculated. Then the calculated values were averaged per PFAS for all samples of an experiment. Further, the standard deviation was computed, respectively. The results are displayed in Tab. 10.

Tab. 8: Overview of the limits of detection for all analyzed PFASs in all conducted experiments. σ refers to the from the replicate samples calculated standard deviation. If the LODs were calculated from the negative blank, the value is marked with [b]. If the LOD value is not marked, it is calculated from the lowest calibration standard with a S/N > 3. All values have the unit ng L^{-1}.

	Pretests						Pilot scale		Lab scale[a]			
	MilliQ		Tap		DOC				2a, 2b, T1, T2, T3		T4, T5, T6	
Compound	**LOD**	**σ**	**LOD**	**σ**	**LOD**	**σ**	**LOD**	**σ**	**Mean**	**σ**	**LOD**	**σ**
PFCAs												
PFBA	200.0	0.0	200.0	0.0	200.0	0.0			60.0	40.0	21.3	20.3
PFPeA	100.0	0.0	100.0	0.0	100.0	0.0	2.0	0	100.0	0.0	5.0	4.7
PFHxA	52.0	39.2	52.0	19.6	52.0	39.2	0.2	0.0	51.4[b]	13.0[b]	51.4[b]	13.0[b]
PFHpA	68.0	39.2	52.0	19.6	52.0	39.2	1.1	0.9	5.8[b]	1.8[b]	5.8[b]	1.8[b]
PFOA	68.0	39.2	52.0	19.6	8.7[b]	2.3[b]	9.3[b]	0.4[b]			1.0	1.9
PFNA	36.0	32.0	20.0	0.0	20.0	0.0	0.2	0.0	3.3[b]	0.9[b]	3.3[b]	0.9[b]
PFDA	20.0	0.0	20.0	0.0	73.0[b]	18.9[b]	1.1	0.9	20.0	0.0	16.5	0.7
PFUnDA	66.6[b]	11.5[b]	20.0	0.0	217.6[b]	41.5[b]	2.4[b]	0.7[b]	20.0	0.0	87.0	9.9
PFDoDA	25.4[b]	6.8[b]	20.0	0.0	95.3[b]	25.7[b]	0.8[b]	0.2[b]	20.0	0.0	177.1	24.2
PFTeDA	1163.4[b]	88.8[b]	20.0	0.0	2604.0[b]	702.4[b]	2.6[b]	0.7[b]				
PFHxDA	20.0	0.0	20.0	0.0	622.6[b]	22.8[b]	1.1	0.9				
PFOcDA	84.0	32.0	68.0	19.6	5844.9[b]	1576.7[b]	5.1	4.9				
PFSAs												
PFBS	36.0	32.0	20.0	0.0	16.0	8.0	7.1[b]	0.4[b]	33.4[b]	6.2[b]	33.4[b]	6.2[b]
PFHxS	20.0	0.0	20.0	0.0	16.0	8.0	3.1[b]	0.2[b]	13.6[b]	3.6[b]	13.6[b]	3.6[b]
PFOS	12.7[b]	3.4[b]	0.0[b]	0.0[b]	26.0[b]	7.0[b]	5.9[b]	0.6[b]	115.7[b]	28.8[b]	115.7[b]	28.8[b]
PFAS precursor												
6:2 FTSA	20.0	0.0	20.0	0.0	16.0	8.0	0.2	0.0	60.0	40.0	31.0	12.7
8:2 FTSA	20.0	0.0	36.0	16.0	60.7[b]	16.4[b]	0.6[b]	0.1[b]	56.4[b]	11.1[b]	56.4[b]	11.1[b]
FOSA	33.8[b]	9.1[b]	52.0	19.6	148.9[b]	36.8[b]	1.1[b]	0.2[b]	110.0	90.0	188.0	0.0

[a] It was not possible to quanitfy PFTeDA, PFHxDA and PFOcDA since the repipetting into new vials caused a deterioration of the calibration curve and thus the repipetting also caused changes in concentration for these compounds in the affected samples.
[b] LODs and σ were calculated from the negative blank.

Tab. 9: Overview of the recovery of spike in positive blanks for the conducted pretests and the lab scale trials. σ is the calculated standard deviation.

	Adsorption Isotherms						Kinetics		Lab scale			
	MilliQ		Tap		DOC		Tap		Adsorption to the			
									catalyst		walls	
Compound	**Recovery**	σ	**Recovery**	σ	**Recovery**	σ	**Recovery**	σ	**Recovery**	σ	**Recovery**	σ
PFCAs												
PFBA	26.5	0.5	39.4	5.4	48.6	9.8	25.8	0.5	98.7	0.04	102.5	1.2
PFPeA	87.7	4.3	87.1	3.1	102	3.8						
PFHxA	26.3	3.5	47.0	1.6	46.6	7.2			99.8	2.2	116.2	1.1
PFHpA	36.9	1.3	57.3	7.3	35.3	1.5						
PFOA	70.8	11.0	63.6	1.0	76.3	2.5	54.3	0.0	90.4	3.9	111.3	5.6
PFNA	39.8	1.0	37.4	7.2	46.9	1.5	25.6	1.3				
PFDA	38.4	1.2	20.2	3.4	40.0	1.4	26.9	0.9	114.0	8.0	116.3	5.6
PFUnDA	27.4	2.0	13.6	2.2	24.4	2.0	19.5	0.02				
PFDoDA	17.4	1.6	3.1	0.7	21.0	0.0	21.7	1.1	119.5	1.5	125.0	14.3
PFTeDA	137.2	0.6	59.1	59.1	158.9	5.5	47.4	0.2				
PFHxDA	35.5	35.5	0.0	0.0	79.6	1.4	11.4	1.4				
PFOcDA	0.0	0.0	0.0	0.0	270.0	0.6	68.2	0.2				
PFSAs												
PFBS	75.2	4.4	78.0	7.0	102.4	3.0			97.4	4.7	99.7	4.1
PFHxS	91.0	10.6	89.6	2.4	95.0	12.2	81.7	3.3	98.3	0.9	100.5	1.3
PFHxS br									91.1	11.4	99.2	7.9
PFOS	85.2	0.4	75.9	0.3	77.8	3.4	103.5	2.6	92.8	2.0	102.4	1.6
PFOS br									80.9	13.3	113.4	18.9
PFAS precursor												
6:2 FTSA	79.9	10.9	67.8	0.2	112.3	6.7	54.7	54.7	98.2	0.6	106.1	3.4
8:2 FTSA	66.6	3.8	17.8	0.6	79.0	2.2	88.4	0.7	96.7	4.8	104.8	1.7
FOSA	53.5	4.3	60.3	4.5	51.4	1.4	76.9	2.9	84.4	5.3	80.8	3.1

Tab. 10: Overview of the percentage deviation between two samples of a duplicate. Here, the mean deviations of all samples taken during an experiment is presented. σ is the calculated standard deviation.

	Adsorption isotherms						Kinetic study		Pilot scale		Lab scale	
	MilliQ		tap		DOC							
Compound	**Mean**	σ	**Mean**	σ	**Mean**	σ	**Mean**	σ	**Mean**	σ	**Mittelwert**	σ
PFCAs												
PFBA	13.3	6.4	10.5	14.8	10.0	7.5			-	-	6.6	3.6
PFPeA	5.2	5.6	3.4	2.7	5.5	5.2			8.1	8.2		
PFHxA	16.2	11.1	3.9	3.7	23.1	20.3			4.9	2.9	6.1	3.5
PFHpA	9.0	7.9	7.4	3.6	17.3	15.2			5.1	2.3		
PFOA	9.8	3.7	8.3	4.3	7.3	2.0			5.6	2.0	6.4	3.4
PFNA	12.8	12.7	8.8	6.5	20.7	20.5			6.1	3.6		
PFDA	12.3	12.0	8.6	7.2	11.2	14.3			8.6	3.7	15.0	5.1
PFUnDA	2.7	2.6	13.3	7.7	8.1	11.5			7.3	5.7		
PFDoDA	13.8	11.5	22.3	15.9	47.4	35.2			9.4	7.4	15.9	5.9
PFTeDA							6.5	8.5	11.1	9.4		
PFHxDA	4.6	5.5	1.7	0.4			15.1	15.2	14.8	10.9		
PFOcDA	0.7	0.4					1.4	2.2	18.0	16.6		
PFSAs												
PFBS	14.9	14.3	5.2	2.0	6.4	5.5			3.8	2.5	12.3	9.7
PFHxS	6.1	4.2	8.3	5.1	8.5	6.2	4.8	2.5	4.9	2.2	8.1	4.8
PFHxS br									5.3	2.0	10.9	6.0
PFOS	8.6	8.6	14.0	16.1	2.6	2.8	5.3	3.9	11.6	12.1	13.4	5.2
PFOS br									11.9	12.2	18.5	13.5
PFAS precursor												
6:2 FTSA	17.7	18.3	10.7	7.9	10.8	10.6			5.8	3.0	17.6	14.8
8:2 FTSA	7.0	7.8	10.9	9.8	11.7	3.0	4.4	3.7	8.3	3.3	18.4	3.6
FOSA	8.6	9.2	10.2	5.4	32.9	27.5	4.6	3.2	7.7	7.8	30.9	22.3
FOSA br									7.5	6.9		

2.8.5 Recovery of internal standards

The recovery of the internal standard is a parameter which is accounting for losses and matrix effects during sample preparation and analysis. The area of internal standard peaks of the calibration curve was averaged and set as 100 %. Then the area of internal standard peaks in samples was calculated relative to 100 %. Finally, the mean of all recovery values was calculated per PFAS and experiment. In Tab. 11 a list of the recoveries is presented for the pretests, the pilot and the lab scale experiment.

Tab. 11: Recovery of analyzed internal standards for the Pretests, the pilot scale and the lab scale experiments.

Internal Standard	Pretest Recovery [%]	Pilot Scale Recovery [%]	Lab scale Recovery [%]
PFCAs			
$^{13}C_4$-PFBA	72.8		102.9
$^{13}C_2$-PFHxA	118.8	88.3	179.4
$^{13}C_4$-PFOA	122.0	53.7	161.9
$^{13}C_5$-PFNA	110.3	48.8	94.75
$^{13}C_2$-PFDA	101.1	59.0	86.1
$^{13}C_2$-PFUnDA	86.5	83.1	79.5
$^{13}C_2$-PFDoDA	76.9	175.3	80.2
PFSAs			
$^{18}O_2$-PFHxS	117.4	70.8	114.9
$^{13}C_4$-PFOS	99.4	65.5	93.2
Precursor			
$^{13}C_8$-FOSA	91.7	439.3	89.1
d_5-*N*-EtFOSA	70.7		125.7

3 Results

3.1 Pretests on the catalyst material

3.1.1 Kinetic studies

Kinetic studies were conducted to evaluate the velocity of PFASs adsorption on the catalyst material. No reliable results were obtained for many PFASs since the detected concentrations for the 0 min samples (adsorption to the walls) were lower than the detected amount of samples taken after 1 min and later (adsorption to the walls and the catalyst). An increase in concentration due to PFASs desorption from the catalyst is very unlikely since new catalyst material was applied (cf. Tab. 2) and further PFASs adsorption on the catalyst is favored over desorption (cf. 3.1.2). Thus uncertainties caused by pipetting of spike and samples as well as uncertainties by the measuring instrument predominate. For this reason, is was solely possible to evaluate the compounds with a higher initial concentration in the 0 min sample. These PFASs were PFTeDA, PFHxDA, PFOcDA, PFHxS, PFOS, 8:2 FTSA and FOSA (Fig. A.8). With the exception of PFTeDA and PFOcDA, a fast decrease in concentration within 10 min is apparent for all PFASs. Small changes in concentration during the remaining time of the experiment were observed for PFHxS, PFOS, and FOSA. However, for PFOS and 8:2 FTSA, an increase in concentration between 10 min and 75 min with a subsequent decrease in concentration until the end of the trial (5436 min, which is 3 d, 18 h and 36 min) was found. Compared to this, the long chain PFASs PFTeDA, PFHxDA and PFOcDA behave differently. Whereby a slow decrease in concentration of PFTeDA was found during the whole time of the experiment, the concentration of PFHxDA and PFOcDA remains constant between the 1 min and 100 min sample. However, a decrease between the 100 min and the 5436 min sample was observed for PFHxDA and PFOcDA.

3.1.2 Adsorption isotherms

The evaluation of the data acquired though the shaking experiments was conducted by means of the Freundlich and the Langmuir model for adsorption isotherms. As exemplarily shown for PFOA in Fig. 4 a), the Freundlich model is suitable for the three analysed water types since a linear relationship, demonstrated by high coefficients of determination, was found. The Freundlich parameters, adsorption intensity n and adsorption capacity K_f are calculated form the slope and the intercept of the lane (see equation (10)), respectively (Desta, 2013). In general K_f varied between $3.75 \cdot 10^{-6}$ (PFOS, DOC water) and $1.36 \cdot 10^{-3}$ (PFDoDA, tap water) as can be seen in Tab. 12 . The Langumir model does not fit to the data since no linear relationship resulted (see Fig. 4 b).
Adsorption isotherms were further calculated for each individual component. With the resulting Freundlich constants different plots were created. The correlation of the PFASs perfluorinated chain length vs. the n and $\lg(K_f)$ values are most reasonable. Fig. 5 a) and Fig. 5 b) show plots

a)

b)

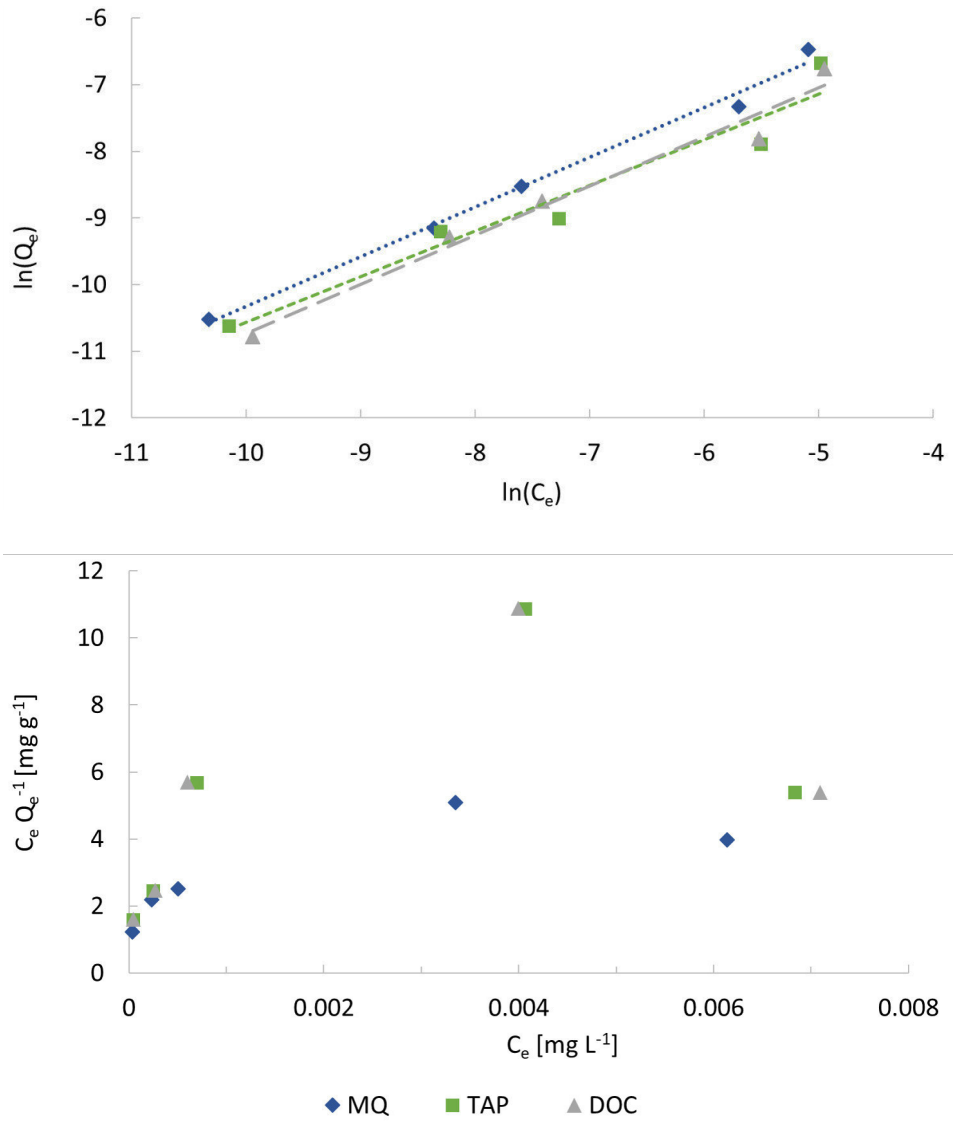

Fig. 4: a) Freudlich and b) Langmuir adsorption isotherm exemplarily shown for PFOA in the three water types MilliQ, tap and DOC water.

Tab. 12: Freundlich isotherm parameters n and K_f for all analyzed PFASs in MilliQ, tap and DOC water. R^2 functions as a quality parameter for the Freundlich fit.

	MilliQ water			Tap water			DOC water		
Compound	n	K_f	R^2	n	K_f	R^2	n	K_f	R^2
PFCAs									
PFBA	1.06	6.64E-04	0.995	0.97	8.52E-04	0.950	0.93	1.21E-03	0.997
PFHxA	1.32	1.41E-04	0.996	1.89	2.23E-05	0.927	1.37	9.14E-05	0.964
PFHpA	1.39	1.09E-04	0.992	1.44	4.30E-05	0.950	1.35	7.16E-05	0.997
PFOA	1.34	5.67E-05	0.992	1.46	2.41E-05	0.941	1.35	3.50E-05	0.990
PFNA	1.61	3.69E-05	0.964	1.48	3.91E-05	0.945	1.89	2.17E-05	0.973
PFDA	1.87	1.92E-05	0.926	1.58	4.25E-05	0.957	1.23	1.61E-04	0.931
PFUnDA	1.21	1.92E-04	0.981	1.24	4.36E-04	0.972			
PFDoDA	1.28	1.64E-04	0.986	1.27	1.36E-03	0.981			
PFSAs									
PFBS	1.39	3.36E-05	0.969	1.15	1.40E-04	0.982	0.97	2.16E-04	0.976
PFHxS	1.39	3.26E-05	0.972	1.53	1.15E-05	0.961	1.66	9.19E-06	0.975
PFOS	1.60	1.27E-05	0.909	1.59	1.73E-05	0.961	2.13	3.75E-06	0.787
PFAS-precursor									
6:2 FTSA	1.47	3.03E-05	0.969	1.98	5.33E-06	0.869	1.92	4.45E-06	0.911
8:2 FTSA	1.95	1.05E-05	0.893	1.37	7.85E-05	0.985	1.37	2.48E-05	0.960
FOSA	1.02	2.16E-04	0.983	1.78	9.36E-06	0.922			

[a] PFPeA, PFTeDA, PFHxDA and PFOcDA were excluded from the calculation of Freundlich isotherm parameters.

a)

b)

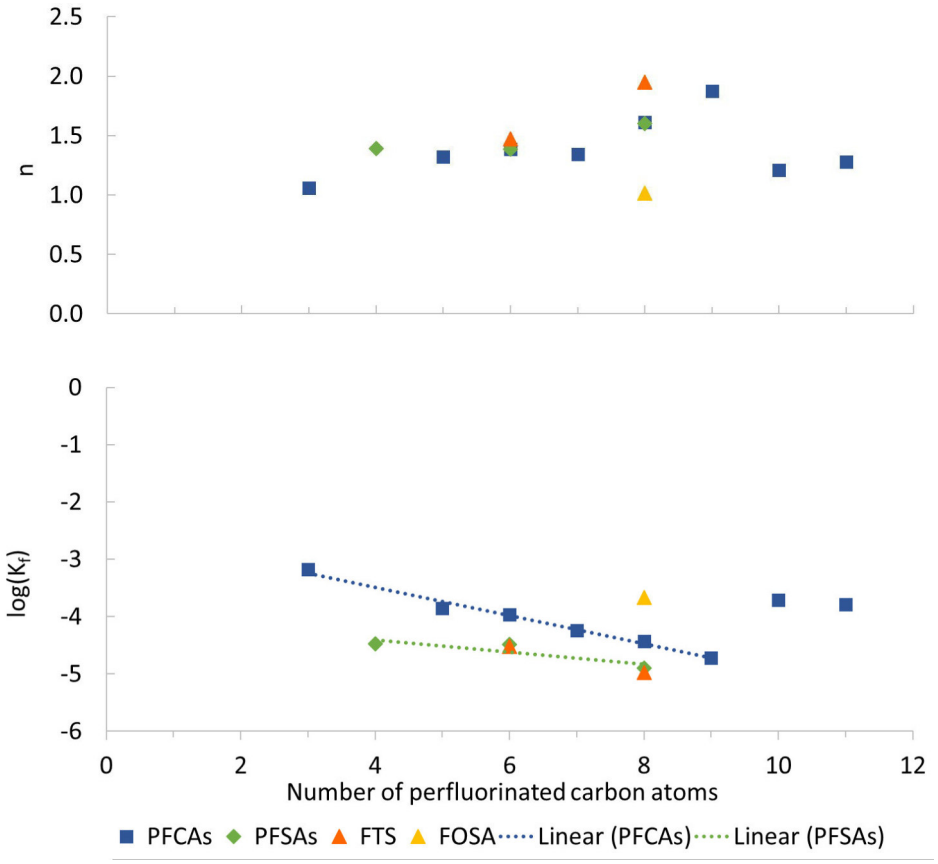

Fig. 5: Estimated Freundlich isotherm parameters of MilliQ water for all fitted compounds a) adsorption intensity (n) and b) adsorption capacity (K_f).

for MilliQ water. The respective graphs for tap and DOC water can be found in the appendix Fig. A.7 and Fig. A.9.
As can be seen in Fig. 5 (a), Fig. A.7 (a) and Fig. A.9 (a) 90 % of all values for the adsorption intensity n range between 1 and 2 for all water types. However, the distribution of n values differs in this range. For MilliQ water a trend is visible: the values of the compounds with 4 to 9 perfluorocarbon atoms (except for FOSA) fit on a common curve, with the minimal n-value for PFHxA. From PFHxA, the n-value increases with increasing number of perfluorocarbon atoms. The values for PFSAs and the corresponding PFCAs are nearly equal. PFBA, FOSA, PFUnDA and PFDoDA have smaller n-values. Nevertheless, the value still increases with an increasing number of perfluorocarbon atoms. This behavior was characteristic for these compounds when compared to the others and it was also observed for the K_f values.
The K_f values for all PFASs consisting out of a hydrophobic chain with four to nine perfluorocarbon atoms are less than $1.5 \cdot 10^{-4}$ $(mg\,g^{-1})(\mu g\,L^{-1})^{-n}$. The value for PFBA as well as the values for FOSA, PFUnDA and PFDoDA are much larger ($1.6 \cdot 10^{-4}$ - $6.6 \cdot 10^{-4}$ $(mg\,g^{-1})(\mu g\,L^{-1})^{-n}$), whereas the calculated values for PFHxS and PFOS are nearly equal to 6:2 FTSA and 8:2 FTSA ($1.1 \cdot 10^{-5}$ - $3.4 \cdot 10^{-5}$ $(mg\,g^{-1})(\mu g\,L^{-1})^{-n}$). The values for the PFCAs from PFHxA to PFDA show a linear relationship. A regression line through these points has a determination coefficient of 0.960. The described distribution of K_f values was similar for the other water types (see data in appendix).

3.2 Pilote scale trials

Fig. 6 shows an overview over the whole six days of the pilot scale trials for PFPeA, PFOA, PFUnDA and PFOcDA as well as for PFNA, PFOS, 8:2 FTSA and FOSA as examples for the analyzed PFASs. Fig. A.13 presents an overview over the whole period of the pilot scale trial for all analyzed PFASs. The water was spiked twice and for the corresponding 30 min samples (S2 after PFASs spike 1 and S7 after PFASs spike 2) an increase in concentration was visible. Between the sample S7 on day 2 (01:00:15) and the start of the degradation trial (04:23:30) diverse adsorption and desorption reactions were visible. On this occasion no consistent trend was apparent, besides the fact, that the increase in concentration of PFDoDA, PFTeDA, PFHxDA and PFOcDA after a spike was more pronounced than the increase of all other analyzed compounds (cf. Fig. A.13). A significant decrease in concentration (two sample t-test, one sided, $p < 0.05$ for PFPeA and $p < 0.01$ for all other analyzed PFASs) is visible from the moment when the ozonation was started.
The influence of the ozone and catalyst treatment on the amount of each single compound during the eight hours ozonation trial is shown in Fig. 7. It can be seen - that a reduction of the initially present amount, set as 100 %, by approximately 65 % for $\sum$PFASs took place during the first three hours of the trial. Throughout the next five hours of the trial, the measured amount remained constant. The increase in concentration between 3 h and 5 h followed by a slightly decrease until the end of the trial is located within the overall standard deviation. Interestingly, this increase in concentration was found for almost all compounds. Even the PFAS precursors (i.e.

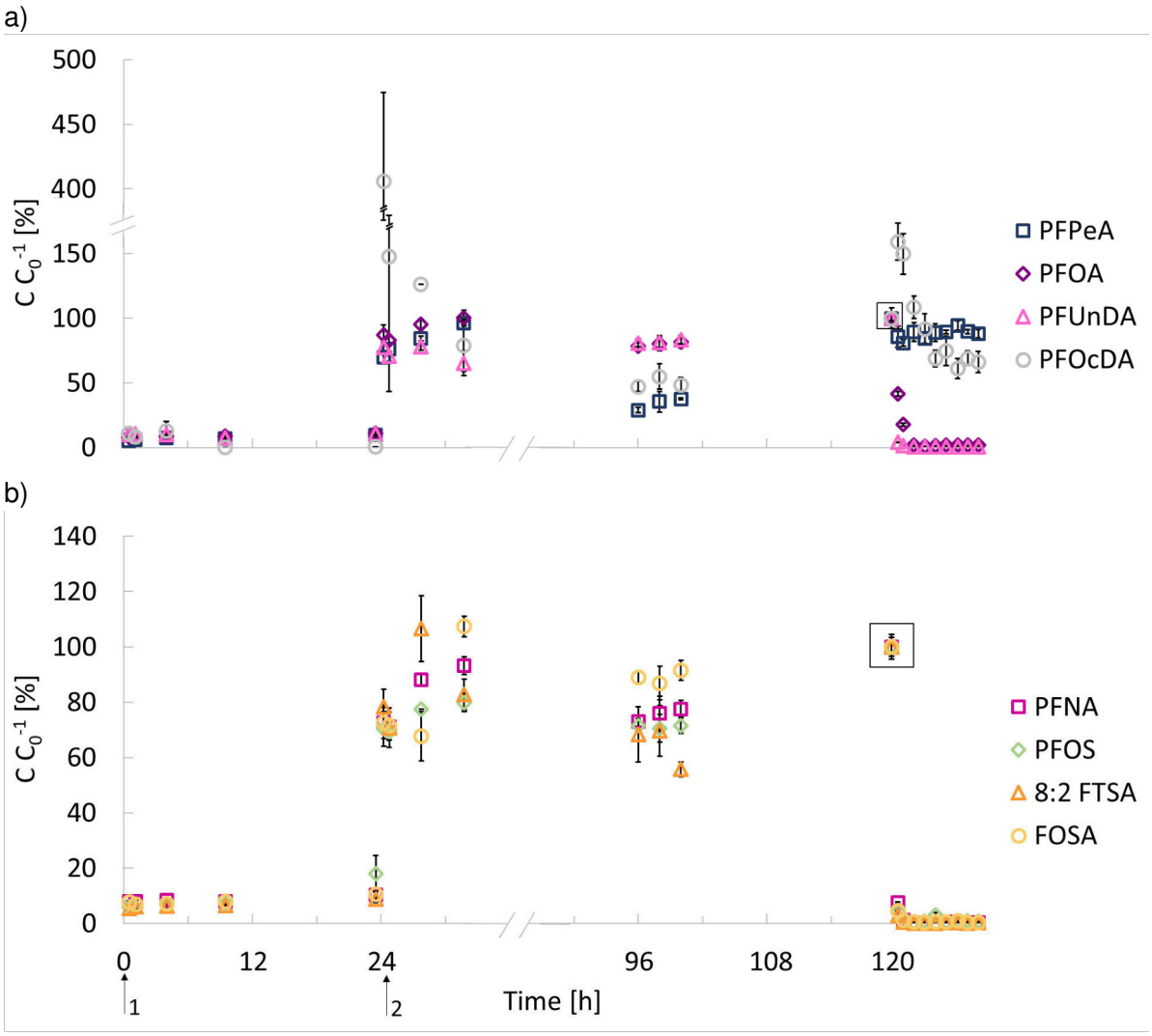

Fig. 6: Overview over the whole period of the pilot scale experiment exemplary shown for a) PFPeA, PFOA, PFUnDA and PFOcDA and b) PFNA, PFOS, 8:2 FTSA and FOSA. Arrow 1 marks the first spike of 0.1 mL PFASs-mix and arrow 2 marks the second spike of 1 mL PFASs-mix (c.f. Tab. 4). All samples are standardized to S 14 (0h) which is marked with the black square. The shown values are the mean of relative duplicate samples, the errors are calculated as the deviation between the mean and a duplicate sample. Please note different y-axis labelings.

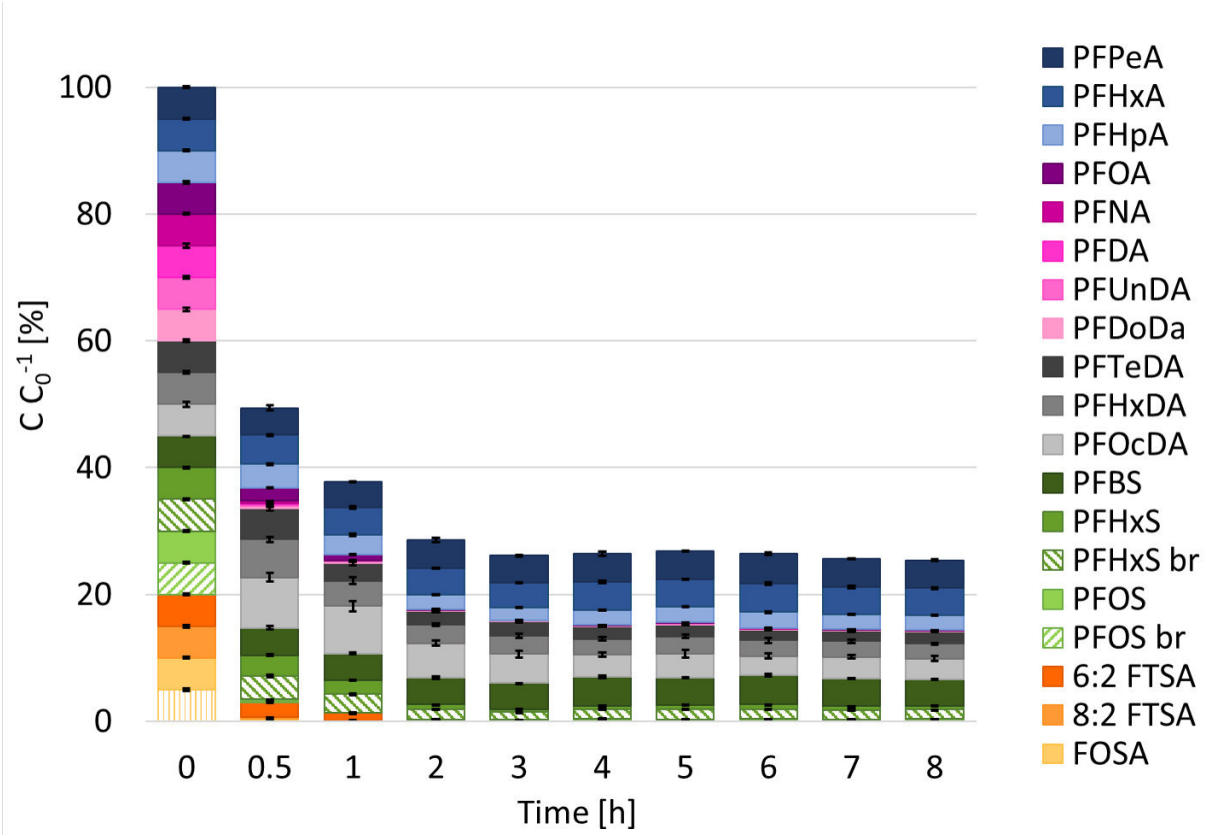

Fig. 7: Effect of ozone treatment on each single compound. The shown values are the mean of relative duplicate samples and the errors are calculated as the deviation between the mean and a duplicate sample. The sum of all relative values at the time of the 0 h sample is set as 100 %. Following values are calculated corresponding to this.

6:2 FTSA, 8:2 FTSA, FOSA, see Fig. 11) and PFCAs (i.e. PFOA, PFNA, PFDA,PFUnDA and PFDoDA, see Fig. 9 c) which were removed almost completely showed this behavior. Though, the difference between the lowest detected concentration and the concentrations of the following samples is not significant (two sample t-test, 95% significance interval, one sided, $p > 0.05$). Since the PFCAs behave differently in relation to degradability, a classification into three groups, according to the chain length, could be observed. Group 1 (i.e. PFPeA, PFHxA, PFHpA) was characterized by the highest remaining concentration compared to group 2 (i.e. PFOA, PFNA, PFDA, PFUnDA, PFDoDA, cf. Fig. 9 c) and group 3 (i.e. PFTeDA, PFHxDA and PFOcDA, cf. Fig. 9 d). Group 3 also differentiated from group 2 regarding the remaining concentration. Whereas for group 2 98 % of $\sum$Group 2 PFCAs, solely 47 % of $\sum$Group 3 PFCAs were removed. The group differentiation regarding the removal rate becomes even more clear under respect of Fig. 8 which shows the removal per compound. A clear difference, not only for the

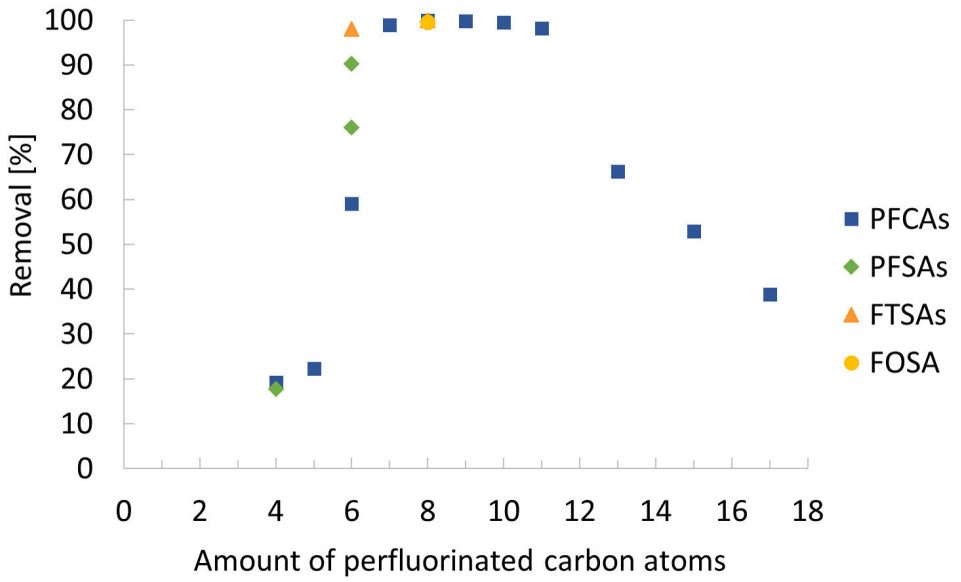

Fig. 8: Maximal removal of each compound during the ozone and catalyst treatment at the pilot scale system. The initial amount of each PFASs is set as 100 %. The removal is calculated as the difference between the initial concentration and the minimal concentration per individual PFAS.

sum of PFCAs per group, but also for the individual PFCAs is visible. Moreover, to group 2 comparable high removals were found for all PFAS precursors and PFOS. A further difference relating the group classification (cf. Fig. 9) is the needed time to reach the minimal concentration. Whereas the minimal concentration for group 1 and group 2 PFASs is reached after 3 h ozone treatment, three additional hours of ozonation are required for group 3. The main degradation of $\sum$PFCAs is though completed within three hours Fig. 9. However, Fig. 9 b) shows a ten percent increase for group 1 (i.e. PFPeA, PFHxA and PFHpA) between hour three and six, followed by a five percent decrease until the end of the trial. The anew increase in concentration of group 1 was significant (two sample t-test, 95 % confidence interval, one sided). A reverse behavior could be noticed for group 3 (i.e. PFTeDA, PFHxDA and PFOcDA) displayed in Fig. 9 d). As a consequence the outlined variation between three hours and eight hours of group 1 and group 3 cancel each other out. That is why the total amount for PFCAs shown

a)

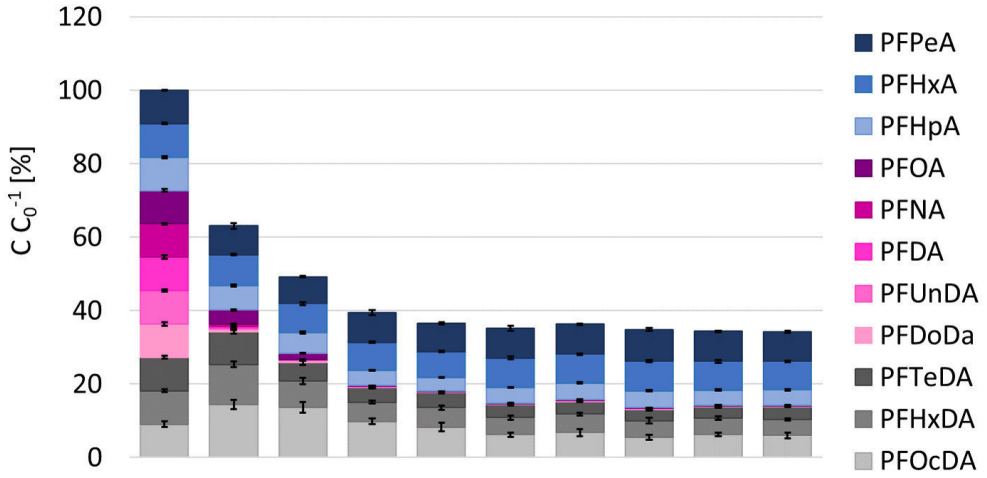
120
100
80
60
40
20
0
C C0-1 [%]
PFPeA
PFHxA
PFHpA
PFOA
PFNA
PFDA
PFUnDA
PFDoDa
PFTeDA
PFHxDA
PFOcDA

b)

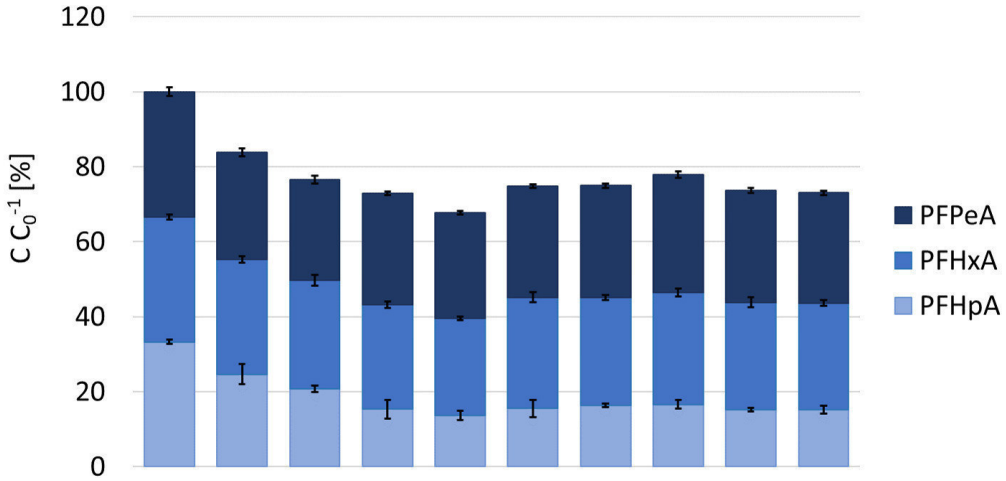
120
100
80
60
40
20
0
C C0-1 [%]
PFPeA
PFHxA
PFHpA

c)

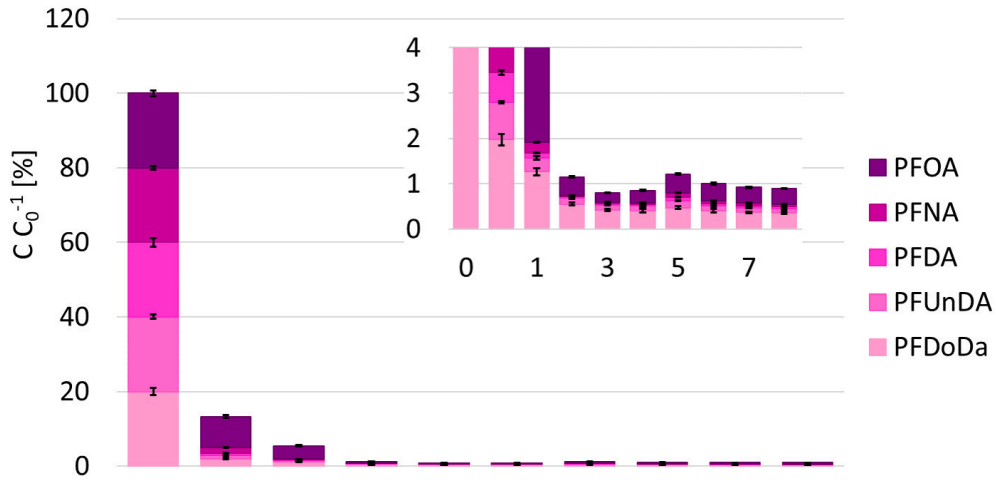
120
100
80
60
40
20
0
C C0-1 [%]
4
3
2
1
0
0
1
3
5
7
PFOA
PFNA
PFDA
PFUnDA
PFDoDa

d)

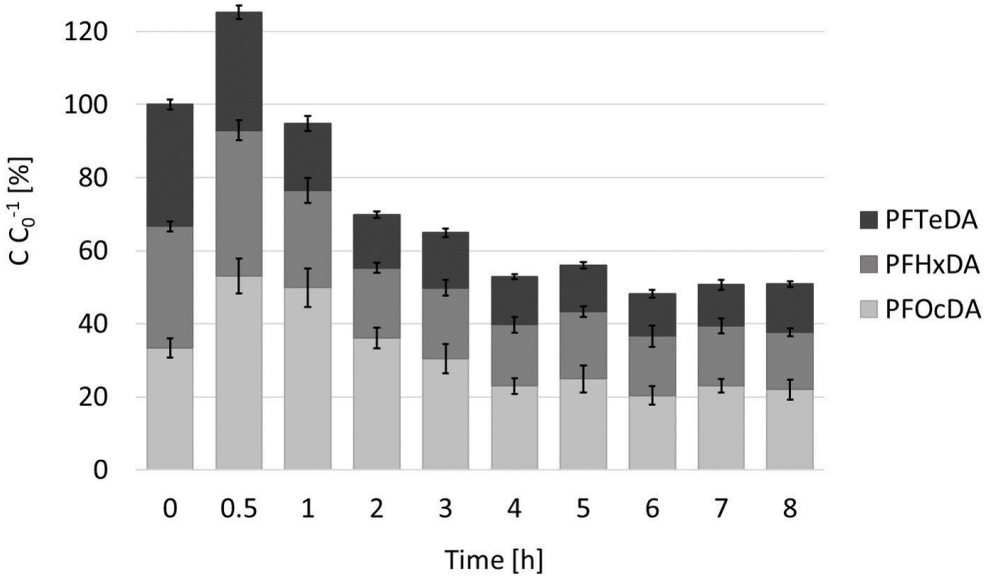

Fig. 9: Residual concentration of PFCAs during 8 h of ozone treatment: a) sum of all PFCAs b) group 1, c) group 2, d) group 3. Graph c) includes an enlargement of the low values. The shown values are the mean of relative duplicate samples. The errors are calculated as the deviation between the mean and a single duplicate sample. The sum of all relative values at the time of the 0 h sample is set as 100 %. Following values are calculated corresponding to this.

in Fig. 9 a) remains steady for the last five hours. In contrast to all analyzed PFASs and thus another reason for the group classification is the observed significant increase in concentration of PFOcDA during the first 30 min of the experiment (two sample t-test, 95 % confidence interval, one sided, $p < 0.05$). Although the appropriate increase for PFHxDA was not found to be significant (two sample t-test, 95 % confidence interval, one sided,$p > 0.05$) a trend could be observed for group 3 compounds, since the concentration of PFTeDA remained constant during the first 30 min of ozonation whereas in this time a removal of over 90 % was found for PFDoDA.

The main degradation of all analyzed shorter chain PFASs, besides branched PFHxS, took place during the first 30 min of treatmentIn comparison to this, the main decrease in concentration of PFTeDA occurred between 30 min and 60 min. In this regard group 3 behaves differently than all other analyzed compounds.

The degradation of group 2 (i.e. PFOA, PFNA, PFDA, PFUnDA, PFDoDA) presented in Fig. 9 c) proceeded very rapidly. Only 5.4 % of the initial quantity was left after one hour of treatment. In the period of concern between three and eight hours approximately one percent remained in the analyzed water. PFOA and PFDoDA are degraded more slowly and the remaining amount is slightly higher than one of the other compounds belonging to this group.

In case of the PFSAs, as presented in Fig. 10, the shorter compounds PFBS and PFHxS (branched and linear) were degraded more slowly than PFOS. This behavior is in a line with the observations for PFCAs. Further, branched and linear PFOS behave very similar, whereas a difference between the linear and branched form of PFHxS was visible. After three hours, when the degradation process was finished, more than twice the amount of branched PFHxS

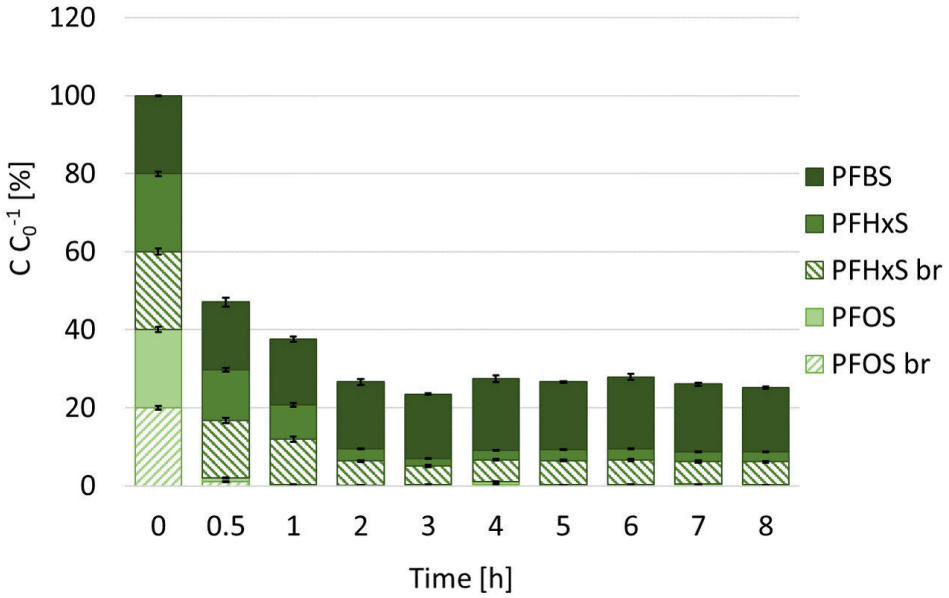

Fig. 10: Residual concentration of sulfonic acids during 8 h of ozone treatment. The sum of all relative values at the time of the 0 h sample is set as 100 %. Further, the shown values are the mean of relative duplicate samples and the errors are calculated as the deviation between the mean and a single duplicate sample.

(residual amount 24 %) as compared to linear PFHxS (residual amount 10 %) remained in the water. In the remaining five hours, a significant increase in the amount of both PFHxS forms occurred (two-sample t-test, 95 % confidence interval, one sided, $p < 0.05$). PFBS, on the contrary, increased at first and then decreased again to the concentration measured after three hours. For PFOS no significant change was observed (two-sample t-test, 95 % confidence interval, one sided, $p > 0.05$). This behavior is in accordance with the PFCAs. For the $\sum$PFAS precursors the removal was > 99 % after three hours (cf.Fig. 11). Moreover, the shorter chain compound 6:2 FTSA was removed more slowly and less good (53 % removal after 0.5 h of ozonation for 6:2 FTSA compared to > 95 % reomoval of 8:2 FTSA, FOSA and FOSA br; 98 % removal after 3 h of ozonation for 6:2 FTSA compared to > 99.5 % removal of 8:2 FTSA, FOSA and FOSA br). In addition, the increase in concentration of 1.5 % for 6:2 FTSA was observed after the first three hours of the trial, whereas 8:2 FTSA, FOSA and FOSA branched, showed an increase of less than 0.5 %.

A comparison between all compounds with eight perfluorocarbon atoms shows an accordance in relation to their degradability as illustrated in Fig. 12. In particular it was visible, contrary to Fig. 9, Fig. 10 and Fig. 11, that the degradation process was already finished after two hours instead of three. Although the residual amount, with less then one percent, was extremely low, the formerly observed increase in concentration for the remaining time of the trial was still visible.

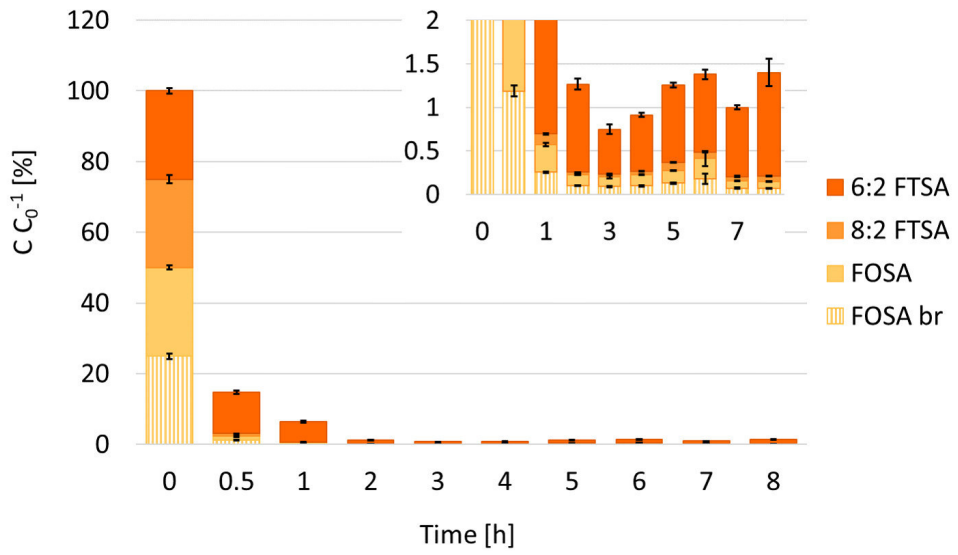

Fig. 11: Residual concentration of PFAS precursors during the ozone-catalyst treatment at the pilot scale. An enlargement of the low values is included in the graph. The shown values are the mean of relative duplicate samples. The errors are calculated as the deviation between the mean and a single duplicate sample. The sum of all relative values at the time of the 0 h sample is set as 100 %. Following values are calculated corresponding to this.

6:2 FTSA, PFHxS and PFHpA comprise, as a common feature, a six carbon atom long perfluorocarbon chain (Fig. 12 b). The comparison of these PFASs shows explicit differences in degradability regarding the influence of the functional group. 6:2 FTSA is degraded best (98 % removal), followed by PFHxS (90 % removal), PFHxS br (76 % removal) and with the worst removal of this selection PFHpA (59 % removal). The minimal concentration of all four PFASs is consistently reached after 3 h of ozonation. The at this time detected remaining amount of 6:2 FTSA is five times lower than the residue of PFHxS and 12 or 20 times lower than the amount of PFHxS br and PFHpA, respectively. PFPeA and PFBS, both consist five perfluorocarbon atoms, showed a removal of 81 % and 82 %, respectively. Thus, no difference in degradability was visible Fig. A.10.

A comparison of the residual concentrations after 3 h ozone treatment for the three analyzed compound classes PFCAs, PFSAs and PFAS precursors shows, that the degradation of the PFAS precursors was by far the best (> 99 % of $\sum$PFAS precursor), Fig. 9, Fig. 10 and Fig. 11. In case of the $\sum$PFSAs 23 % and 37 % of the $\sum$PFCAs remained in the water. Though it needs to be considered, that the groups contain different amounts of compounds and compounds with different perfluorocarbon chain length.

Based on equations (16) and (18) reaction order and rate constant were calculated (Fig. 13, Fig. 14). A list of the calculated values is shown in Tab. A.8. From Fig. 14 it becomes apparent, that removal rate increases with a rising rate constant until both reach a maximum for PFNA. This effect is primarily depending from the perfluorocarbon chain length, since for PFASs with an over nine perfluorocarbon atoms increasing chain length, removal and rate constant start to decrease simultaneously. The type of functional group is a subordinate issue. An increase in rate constant by two orders of magnitude corresponds to a significant increase in removal

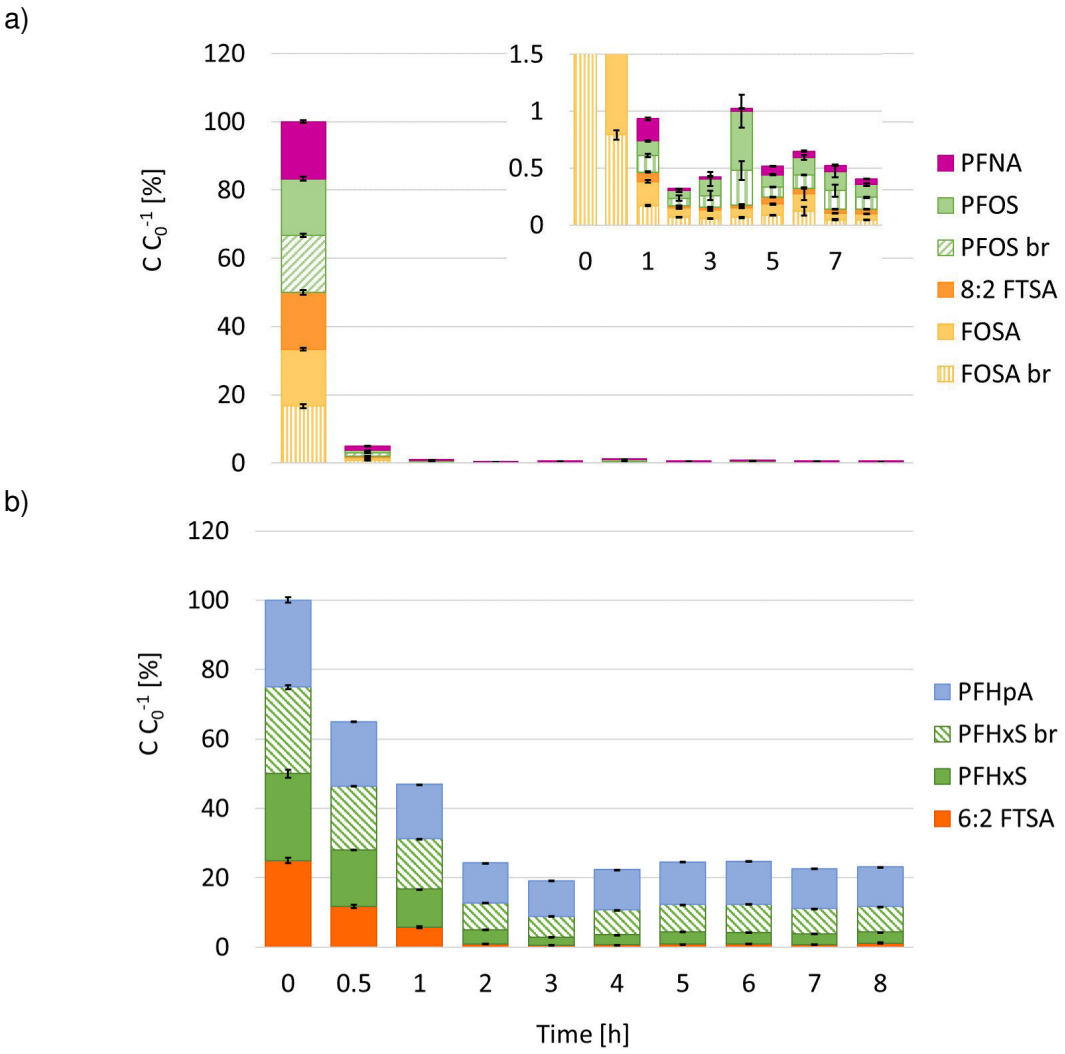

Fig. 12: Residual concentration of compounds with a) eight and b) six perfluorocarbon atoms during 8 h of ozonation. For clarification low values are presented in a magnification. The shown values are the mean of relative duplicate samples. The errors are calculated as the deviation between the mean and a duplicate sample. The sum of all relative values at the time of the 0 h sample is set as 100 %. Following values are calculated corresponding to this.

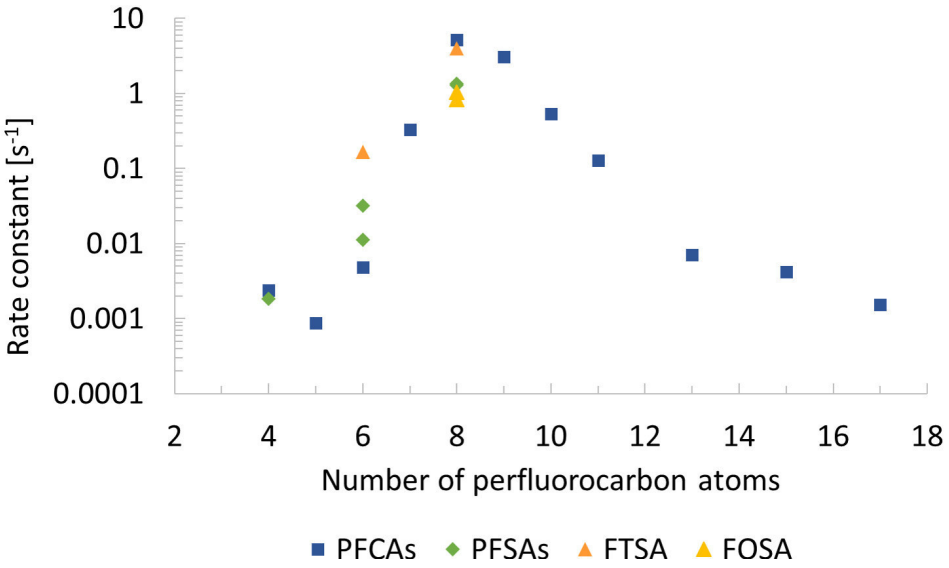

Fig. 13: Second reaction order rate constants for all analyzed compounds of the pilot scale ozone treatment. The rate constants were calculated according to equations (17) and (18).

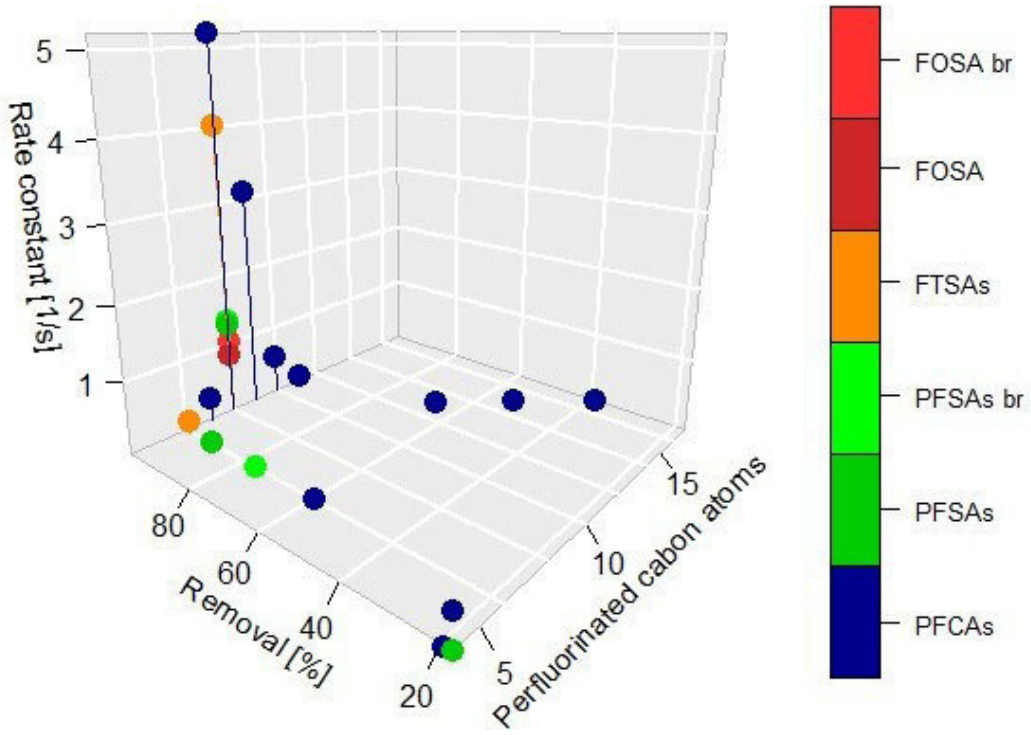

Fig. 14: 3D plot describing the relationship between perfluorinated chain length, rate constant and maximal achieved removal rate during the ozonation trial.

rate for PFASs with six perfluorocarbon atoms (PFASs, rate constant, ramoval rate: PFHpA, 0.0048 s^{-1}, 59 %; PFHxS br, 0.011 s^{-1}, 76 %; PFHxS, 0.032 s^{-1}, 90 %; 6:2 FTSA, 0.017 s^{-1}, 98 %; $p < 0.01$, two-sample t-test, one sided). Further rate constant and removal rate increase slower for PFOA and all analyzed PFASs with eight perfluorocarbon carbon atoms (PFASs, rate constant, ramoval rate: PFOA, 0.32 s^{-1}, 98.9 %; FOSA, 0.84 s^{-1}, 99.6 %; FOSA br, 1.0 s^{-1}, 99.6 %; 8:2 FTSA, 4.0 s^{-1}, 99.9 %; PFNA, 5.2 s^{-1}, 99.9 %). This trend continues in reverse order for an onward increasing chain length.
Despite a removal rate of > 98 %, for PFDA, PFUnDA and PFDoDA, the rate constant decreases for PFCAs with 9, 10 and 11 perfluorocarbon atoms from 3.1 s^{-1} (PFDA) to 0.2 s^{-1} (PFDoDA). As can be seen in Fig. A.11, the longer chain PFASs, PFTeDA, PFHxDA and PFOcDA, are located in isolation from all other analyzed PFASs. Regarding all three dimensions, the data points lie on a line with $R^2 > 0.999$. The decrease in rate constant and removal rate in relation to an increasing chain length applies for PFTeDA, PFHxDA and PFOcDa as well.

3.3 Laboratory scale trials

Laboratory scale experiments were carried out, to evaluate the possibility of an improvement of the reaction conditions in the previously conducted pilot scale experiments using persulfate, catalyst and ozone. Significant removal was mainly observed for the experiments using ozone (i.e. PFBA, PFHxA, PFOA, PFDA, PFDoDA, PFBS and FOSA) and ozone, catalyst and persulfate (i.e. PFBA, PFHxA, PFOA, PFDA, PFDoDA, PFHxS, PFHxS br, PFOS br, 6:2 FTSA, 8:2 FTSA and FOSA) (cf. Tab. 13, $p < 0.05$, two-sample t-test, one-sided). The relationship between perfluorocarbon chain length vs. removal rate is shown in Fig. 15. A negative removal rate is associated with an increase in concentration relative to the respective point of standardization (sample taken before the degradation experiment started). No significant removal was found for the treatment with persulfate and catalyst as well as persulfate only (cf. Tab. 13). In general, in the results of experiment T6 (persulfate, catalyst, ozone), T4 (persulfate, ozone), T2 (catalyst, ozone) and T1 (ozone) showed i) FOSA was the PFASs with the highest removal rate in all experiments, ii) Removal increases with a growing perfluorocarbon chain length, iii) The influence of different functional groups on the removal rate for PFASs with an equal perfluorocarbon atom number is more pronounced for PFASs with eight than for PFASs with six perfluorocarbon atoms. However, in case of the PFCAs, the removal increases with a growing perfluorocarbon chain length for PFHxA, PFOA, PFDA and PFDoDA but PFBA (12 % - 30 %) was in experiment T2 (catalyst, ozone), T4 (persulfate, ozone) and T6 (persulfate, catalyst, ozone) slightly better removed than PFHxA (8 % - 16 %). A further exception of the observed increase is PFDoDA (72 %) in experiment T6 (persulfate, catalyst, ozone) which is removed inferior to PFDA (82 %). An increase in removal with a rising perfluorocarbon chain length was also found for linear and branched PFSAs. However, in experiment T1 (ozone) and T2 (catalyst, ozone) branched isomers were less well removed than the according linear molecule form whereas in experiment T6 (persulfate, ozone, catalyst) higher removals were observed for the branched isomers. Solely in experiment T4 (persulfate ozone) PFHxS br was less well

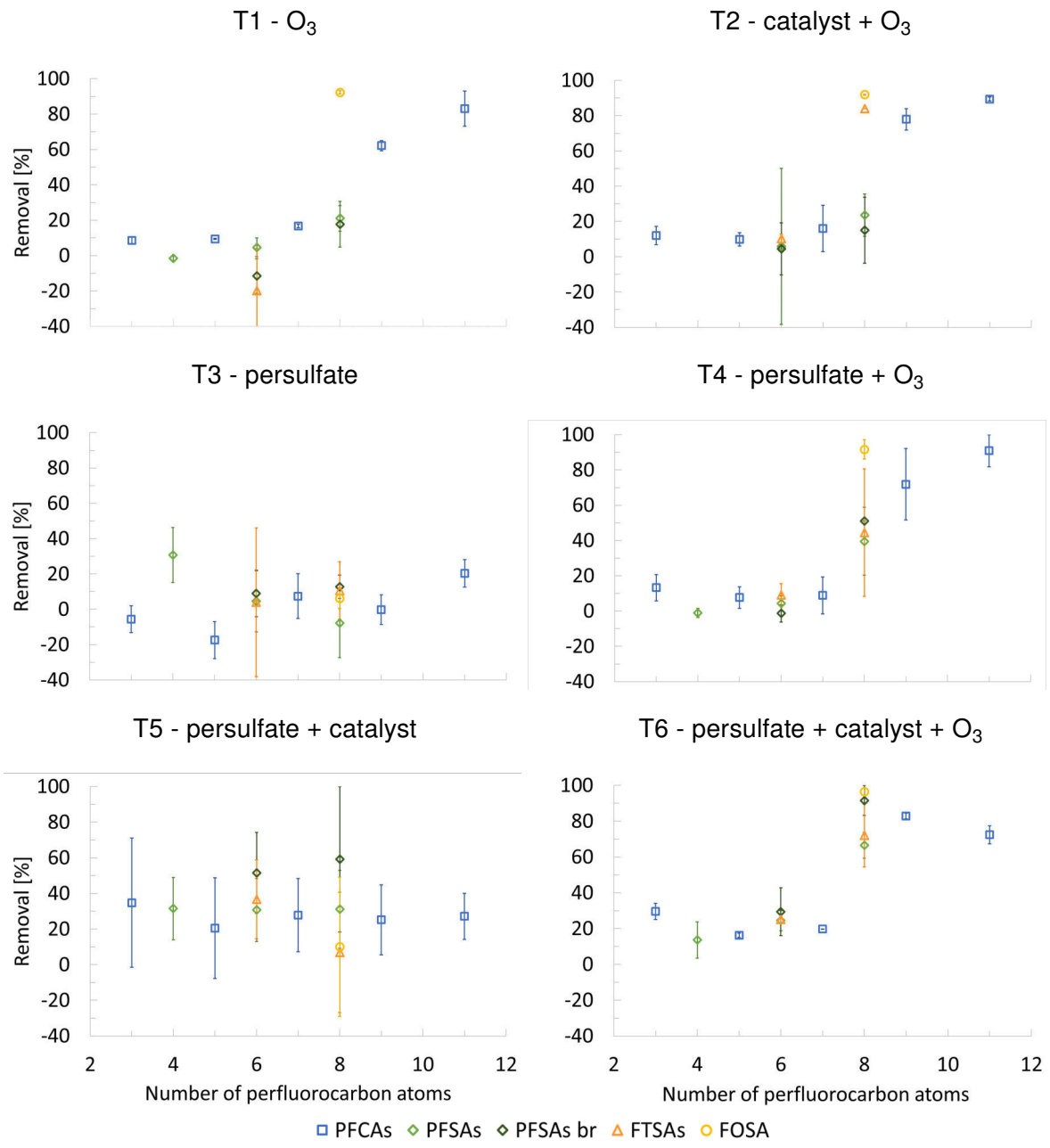

Fig. 15: Removal of all analyzed PFASs after 120 min treatment. The initial concentration is set as 100 % and the removal is calculated as the difference between the remaining concentration after 120 min treatment and the initial concentration. The shown values are the mean of relative duplicate samples and the errors are calculated as the deviation between the mean and a single duplicate sample.

Tab. 13: Results of a two-sample t-test (95 % confidence interval, one sided) for the removal of all quantifiable PFASs during the different degradation approaches in the lab scale trials. A • symbolizes a significant difference ($p < 0.05$) between the relative residual concentrations after 120 min treatment compared to the relative initial concentration (100 %) at 0 min. However, a - shows that no significant difference was found ($p > 0.05$).

	Ozone	**Ozone, catalyst**	**Persulfate**	**Persulfate, ozone**	**Persulfate, catalyst**	**Persulfate, catalyst, ozone**
PFCAs						
PFBA	•	-	-	-	-	•
PFHxA	•	-	-	-	-	•
PFOA	•	-	-	-	-	•
PFDA	•	•	-	•	-	•
PFDoDA	•	•	-	•	-	•
PFSAs						
PFBS	•	-	-	-	-	-
PFHxS	-	-	-	-	-	•
PFHxS br	-	-	-	-	-	•
PFOS	-	-	-	-	-	-
PFOS br	-	-	-	-	-	•
PFAS precursors						
6:2 FTSA	-	-	-	-	-	•
8:2 FTSA	-	•	-	-	-	•
FOSA	•	•	-	•	-	•

and PFOS br was better removed than PFHxS and PFOS respectively. Thus no clear trend was found for the difference between linear and branched isomers. Even though no measuring point was available for 8:2 FTSA in trial T1 (O_3), a clear increase in removal rate was furthermore observed for FTSAs with increasing perfluorocarbon chain length in experiment T6 (persulfate, catalyst, ozone), experiment T4 (persulfate, ozone) and experiment T2 (catalyst, ozone).

A comparison of all PFASs containing six perfluorocarbon atoms (i.e. PFHxS, 6:2 FTSA) showed either corresponding or only slightly varying removal rates. In contrast, for PFASs with eight perfluorocarbon atoms (i.e. PFOS, 8:2 FTSA and FOSA) with up to 75 % different (i.e. 8:2 FTSA vs. FOSA in experiment T1; 8:2 FTSA was not removed in experiment T1). Besides the fact, that in all experiments the highest removal was detected for FOSA (92 % - 96 %) while the second best removal had PFOS (21 % - 67 %), PFOS br (15 % - 92 %) and 8:2 FTSA (72 % - 84 %; not removed in experiment T1) depending on the experiments.

Generally high uncertainties were found for the present set of data Fig. 16. However the following trends were observed within the calculated deviation of the mean. Nevertheless single values were compared. An increase or a decrease in removal of about ≥ 10 % compared to T2 was considered as an improvement or deterioration respectively. All calculated values in between the ± 10 % range are considered as equal. With the exception of PFDoDA and PFOS, the highest removal rate was found for the treatment with persulfate, catalyst and ozone. For PFBA, all PFSAs and 6:2 FTSA an improvement in removal was found by 18 % (PFBA), 14 % (PFBS), 19 % (PFHxS), 77 % (PFHxS br), 43 % (PFOS), 15 % (PFOS br) and 15 % (6:2 FTSA)

in comparison to the removal by a catalyst, ozone treatment. A good accordance in removal was found for T2 (catalyst, ozone) and T4 (persulfate, ozone) with a difference of less than ± 10 % in removal rate for 10 out of 13 PFASs (except PFOS, PFOS br and 8:2 FTSA). The removal of PFOS and PFOS br was even higher in T4 (40 % and 51 % respectively) than in T2 (24 % and 15 % respectively). Solely 8:2 FTSA was explicitly better removed in experiment T2 (catalyst, ozone). The treatment with ozone alone was in comparison to the other three treatment approaches the worst with removals of 62 %, 21 %, -12 %, 18 %, -20 % and 0 % for PFDA, PFOS, PFHxS, PFHxS br, PFOS br and 8:2 FTSA respectively. A comparison of experiment T1 (ozone) with experiment T2 (catalyst ozone) shows that similar removal rates were found for PFBA (12 % and 9 %), PFHxA (10 % and 9 %), PFOA (16 % and 17 %), PFDoDA (89 % and 83 %), PFBS (-1 % and 0 %), PFHxS (6 % and 5 %) and FOSA (92 % for T1 and T2).
In general, a decrease of the initial pH which varied between 6.8 (catalyst, ozone) and 5.1 (ozone) to pH = 3 after 120 min treatment was observed for all trials in which ozone was applied. As presented in Fig. A.15 a comparable decrease in pH from pH = 7.3 to pH = 3.0 was also observed for the positive blank adsorption to the catalyst (2a) though no ozone was applied. During the treatment with persulfate and catalyst as well as the treatment with persulfate only, pH decreased slightly from pH = 6.2 and 5.1 respectively (t = -10 min) to pH = 5.6 and 4.7 respectively, but the observed changes were less than one pH unit (cf. Fig. 17).

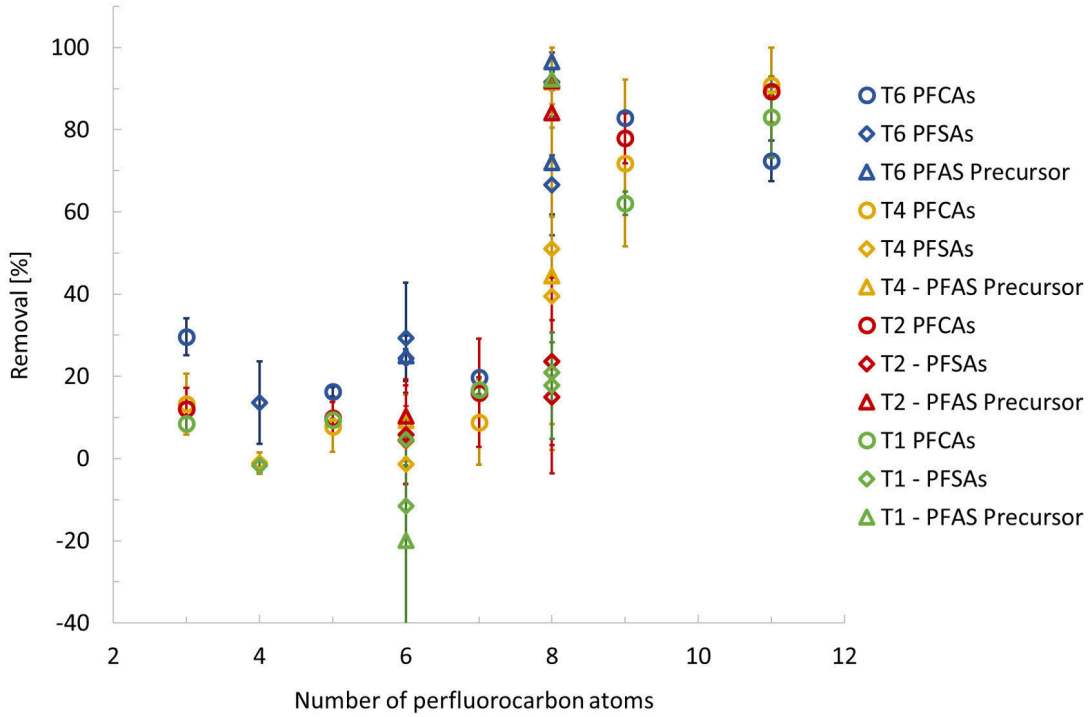

Fig. 16: Comparison of the PFASs removals achieved after 120 min treatment with T1 (ozone), T2 (ozone, catalyst), T4 (ozone, persulfate) and T6 (ozone, persulfate, catalyst). The presented values are the mean of relative duplicate samples. The errors are calculated as the deviation between the mean and a single duplicate sample.

T1 - O_3
T2 - catalyst + O_3
T3 - persulfate

T4 - persulfate + O_3
T5 - perssulfate + catalyst
T6 - perssulfate + catalyst + O_3

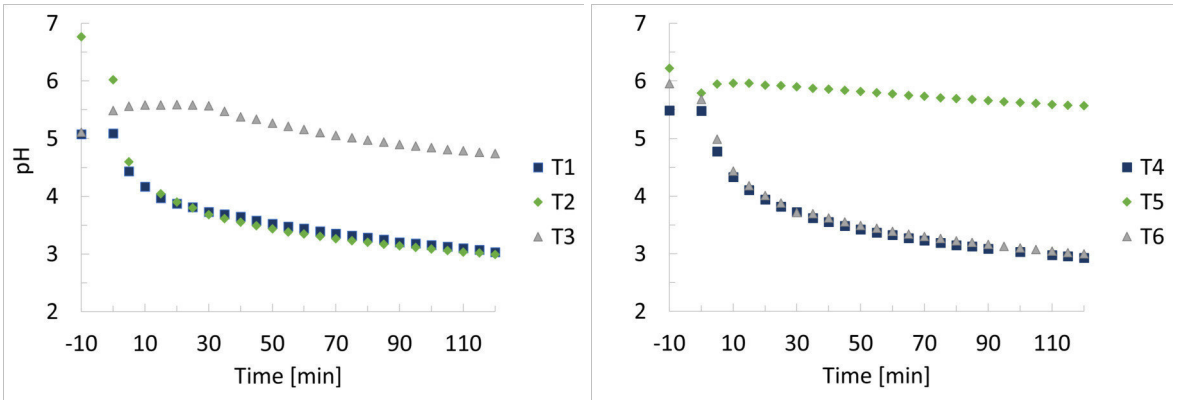

Fig. 17: Detected pH during the whole time of the six lab-scale experiments.

4 Discussion

4.1 Sorption and kinetic of PFASs to the catalyst

The individual PFASs fit to the Freundlich adsorption isotherm model (Fig. 4 a) but not to the Langmuir adsorption isotherm model (Fig. 4 b). This observation was found also in previous studies investigating the adsorption of PFOA and PFOS on diverse types of GAC, powdered activated carbon (PAC) and three activated carbon fibers (Zhi and Liu, 2015) and for different PFASs on GAC (Qiu et al., 2007) even though different adsorption materials were used compared to this study. Other researchers reported the applicability of Freundlich and Langmuir adsorption isotherm models for PFASs adsorption on activated carbon (Ochoa-Herrera and Sierra-Alvarez, 2008; Yu et al., 2009; Hansen et al., 2010). This is not surprising, since for moderate concentration ranges fits according to the Freundlich model show a good accordance with the fit according to the Langmuir model, whereas no linear fit according to the Freundlich model can be expected for very low concentrations (Weber and Borchardt, 1972). This affirms the results of the present study with a concentration rage of 0.1 µg L^{-1} to 10 µg L^{-1} for individual PFASs, which were about three orders of magnitude lower compared to studies conducted by Ochoa-Herrera and Sierra-Alvarez (2008); Yu et al. (2009) and Senevirathna et al. (2010) with a range of The applied catalyst is, an inorganic material consisting mainly of iron and oxygen (> 10 wt%) with smaller proportions of silicon and zinc (> 1 wt%) see hereto Tab. 7. Furthermore, the surface area of the catalyst is 26.4 m^2 g^{-1} whereas the surface area of activated carbon for example of GAC (Filtersorb 400, coal based) comprises 900 - 1 100 m^2 g^{-1} (Senevirathna et al., 2010). A linear relationship between the logarithm of the adsorption capacity K_f and the number of perfluorocarbon atoms was found for PFSAs and most PFCAs (cf.Fig. 5 and Fig. A.9). A similar linear relationship was found by Hansen et al. (2010) for PFASs adsorption on GAC and PAC. The authors analyzed the adsorption of the same PFSAs as in the present study and a homologous series of PFCAs from PFHxA to PFDA and found that $\lg(K_f)$ increased with a rising total chain length of the analyzed PFCAs and PFSAs.
In contrast to the study by Hansen et al. (2010), the present study found a decrease in $\lg(K_f)$ with an increasing perfluorocarbon chain length for the same compounds in MilliQ water and with the exception of PFDA also in DOC water (see Fig. 5 b) and Fig. A.9 b)). This behavior can be explained with the interactions between the different PFASs and the catalyst material. A conceptual model for the adsorption of anionic charged PFASs onto mineral surfaces and the occurring types of interactions is presented by Tang et al. (2010). The researchers discuss three types of interactions:

i) Electrostatic interactions between the anionic charged PFASs molecule and the mineral surface,

ii) Columbic repulsion between the charged PFASs molecule part,

iii) Non-electrostatic interactions, for example hydrophobic interactions, between the perfluoroalkyl chains itself as well as hydrophobic parts of the minerals surface.

While i) and ii) strongly depend on pH and ionic strength, iii) is nearly unaffected by the solution chemistry. The decreasing K_f value could be explained with the presence of electrostatic interactions, as the ratio of charged molecule part to the uncharged, hydrophobic perfluorinated chain decrease with an increasing chain length for the concerning compounds. Therefore it can be hypothesized that interactions between positive charged catalyst surface sites and the negatively charged functional PFASs groups also decrease with an increasing hydrophic perfluorinated tail. This would result in a increasing adsorption and consequently rising $\lg(K_f)$ values for shorter chain PFASs due to stronger interactions between the concerning compounds and the catalyst.

At the same time an increase in $\lg(K_f)$ was observed for PFCAs with a longer perfluorocarbon chain length (Fig. 5, Fig. A.9). Tang et al. (2010) came to the conclusion that non-electrostatic interactions dominate the electrostatic interactions. As a consequence, a strong adsorption of PFOS on the investigated mineral surfaces geothite and silica can be expected if the required hydrophobic interactions between them are present (Tang et al., 2010). Despite a corresponding element composition between the catalyst material examined in this study and geothite, no direct comparison of both materials is possible since no information about the functional groups at the catalyst surface and accompanying surface charge are available. Nevertheless, the model helps to understand the observed results of the present experiment. According to the results of Tang et al. (2010) it can be assumed that the observed increase in $\lg(K_f)$ for longer chain PFCAs is an indication for occurring hydrophobic interactions on the catalyst surface. This theory is further strengthened by the absence of adsorption isotherm data for PFTeDA, PFHxDA and PFOcDA since the detected residual concentrations of those compounds were below the LOQ. This can be interpreted as a hint for the increasing hydrophobic interactions on the catalyst surface with increasing chain length. Moreover, the decreasing water solubility for PFASs with an increasing chain length (cf. Tab. 1) might enhance this effect.

When it comes to the influence of different functional group types, Hansen et al. (2010) found that PFSAs adsorb stronger to GAC and PAC compared to PFCAs, and the increase of the K_f is more pronounced with a higher perfluorocarbon chain length. The reason for the stronger adsorption of the PFSAs compared to PFCAs with an equal perfluorocarbon chain is most likely due to the slightly larger size of the functional sulfonic acid group compared to a functional carboxylic acid group (Higgins and Luthy, 2007). This explanation counts for organic materials such as GAC or PAC (Higgins and Luthy, 2007; Ochoa-Herrera and Sierra-Alvarez, 2008). In contrast, this study found lower $\lg(K_f)$ values for PFSAs compared to PFCAs with the same perfluorinated chain length (Fig. 5, Fig. A.9), which means that the PFSAs adsorption is weaker than the adsorption of PFCAs. However, compared to the GAC evaluated by Ochoa-Herrera and Sierra-Alvarez (2008), the catalyst material used in this study is an inorganic material (cf. Tab. 7). Thus an inverted behavior of the functional groups is assumedly led back to the weak ligand properties of PFSAs compared to PFCAs (Higgins and Luthy, 2007). Even tough no information of functional groups on the catalyst surface are available, the presence of positively charged functional groups can be assumed, since geothite, which consists also of iron and oxygen, is positively charged at $pH < pH_{pzc}$ which is 9.4 (Tang et al., 2010) and the pH was ranging from 3 - 9 during the adsorption of PFOS on geothite in this study. Therefore a weaker

adsorption of PFSAs to the catalyst can be explained.
However, these observations do not apply for the adsorption isotherm data for tap water since the $\lg(K_f)$ values of all compounds seem to depend on the perfluorocarbon chain length only. No differences regarding the behavior of PFSAs and PFCAs as observed for MilliQ and DOC water were visible. The clear differences between the K_f values of MilliQ, DOC and tap (**??**, Fig. A.7, Fig. A.9) water regarding the influence of functional groups or the perfluoroccarbon chain length might be caused by different water compositions such as differences in salt or organic matter content. Furthermore, MilliQ and DOC water correspond in pH (pH = 5) whereas tap water showed a pH value of pH = 7. As reviewed by Du et al. (2014) a significant influence of the solution pH on the adsorption of PFASs to various adsorbents has been observed in many studies. Usually an increase in pH leads to a decrease in PFASs adsorption, though in some cases, under influence of divalent cations, divergent observations were made (Du et al., 2014). For the PFAS precursors it was not possible to find a trend that the calculated $\lg(K_f)$ values followed a perfluorocarbon chain dependency as the number of analyzed precursors was too small (Fig. 5, Fig. A.7, Fig. A.9). Moreover, FTSA and FOSA showed different behaviors according to their functional group which is why they could not be considered as one unit.
The adsorption intensity, represented by n, varied between 1 and 2 for all three water types (Fig. 5, Fig. A.7, Fig. A.9). Solely 10 % of the detected values lie beyond this range but are still close to this range. A deviation of $n = 1$ and accompanying non-linearity can be caused by heterogeneous sorption sites and sorbate-sorbate interactions (Cheung et al., 2001).
A kinetic study was performed in the laboratory to gain information on the adsorption velocity and to allow a rough estimation of the needed time for adsorption processes and the establishment of an equilibrium at the pilot scale trial (Fig. A.8 and **??**). A state of equilibrium was aimed to enable a differentiation between to the ozone treatment related removal and ongoing equilibrium adjustment processes. The pilot scale systems and the lab scale set-up differed i.a. in treated water volume, amount of catalyst and ozone as presented in Tab. 2. Compared to the pilot scale setup, mixing under pretest conditions can be assumed to be much higher due to permanent shaking (batch process) instead of a flow though process. Therefore a faster adsorption to the catalyst material and an adjustment of equilibrium was expected in the conducted laboratory pretests compared to the pilot scale system (cf. **??** and Fig. A.8). However, the deviation was assumed to be small, thus four days of mixing was chosen for the ozonation trial at the pilot scale as the decrease in concentration was expected to exceed potentially remaining balance adjustment processes by far.

4.2 Removal of PFASs with the combination of ozone and catalyst

Within the eight-hour of ozone treatment, a significant removal (two sample t-test, 99 % confidence interval, one sided) was found for all PFASs with the exception of PFPeA for which the removal was solely significant at 95 % confidence interval.
Since no equilibrium seemed to be reached for most compounds in the four days prior to the ozonation trial in the pilot scale system, equilibrium adjustment processes were assumed to be sufficiently slow compared to the concentration changes expected to happen during the experiment. However, the observed decrease in PFASs concentration is no explicit proof for degradation, because no increase in concentration for shorter chain PFASs was found. Whereas the detected increase in fluoride concentration of approximately 8 % during the eight-hour ozone treatment is an indication for occurred degradation processes. This observations corresponds with results found by Park et al. (2016) and Yang et al. (2014b) in diverse AOP experiments. A direct comparison of the increased fluoride percentage with the literature is not possible due to different initial concentrations and different tested water types. However it needs to be considered, that exceedingly high fluoride concentrations were detected for one of the samples taken before the ozonation. Since replicate measurements have given the similar high results for the pertinent sample, a fluoride contamination of the regarding sampling bottle is surmised and the sample was excluded.
It is unambiguous, that ozonation and the decrease of PFASs concentration are directly linked, as no other parameter of the system was changed at the concerning time and pH as well as temperature were kept constant. Still it has to be considered that the ozone itself modified the system in a manner that caused the decrease in concentration. This may include chemical reactions through which PFASs were transformed. An equally conceivable ozone caused mechanical damage to the catalyst and accompanying increase in surface area could theoretically enable an enhanced PFASs adsorption to the catalyst. Whereby this would contradict observations of the shaking experiment, as an outright pulverization of the catalyst (cf. Fig. A.6) did not lead to an increased PFASs adsorption. According to Ozonetech, the increase in redox potential during the ozonation was unusually low. In routine trials values of 800 - 900 mV are reached instead of approximately 210 - 240 mV. The responsible engineers at Ozonetech assumed that changes at the catalyst caused these unexpected low values. A possible system error during th data logging has to be considered as well since the on day six after midnight detected hydrochloric acid and sodium hydroxide dosages start to clearly deviate from dosages of the previous days. Thus, the increases in acid and base addition started independent of the ozonation, at a time with constant experimental reaction conditions. Moreover, the accuracy of the respective flow rates has to be questioned as even more the simultaneous addition of acid and base is not reasonable (Fig. A.14). The following discussion is based on the assumption, that an actual degradation of PFASs has taken place during the ozoation experiment.
As presented in Fig. 14 and Fig. 7 an optimum in degradation is reached for compounds with a perfluoroalkyl tail consisting out of six to eleven carbon atoms, depending on the functional group. Since no information on the functional groups of the catalyst surface are available, speculations on adsorption and reaction mechanism are resigned. However, it can be hypothesized

that a special ratio of electrostatic and hydrophobic interactions between catalyst and PFASs is responsible for the outstanding degradability of several PFASs. As previously discussed by means of the $\lg(K_f)$ values, the binding strength increases for shorter as well as for longer chain PFASs which does not match to the observed extraordinary high removals of PFASs with six to eleven perfluorocarbon atoms. Therefore it can be suggested, that the degradability determining parameter is rather the type of interactions than the binding strength itself. As shown previously by Torn et al. (2003) for sodium dodecylbenzenesulfonate hydrophobic and electrostatic interaction contribute to the adsorption on kaolinite. Therefore it might be a special ratio of hydrophobic and electrostatic interactions between PFASs and catalyst that could make some PFASs highly prone for degradation.

It is found in the present study, that PFTeDA, PFHxDA and PFOcDA show a linear relationship with a coefficient of determination of over 0.999 regarding the relation of removal, rate constant and perfluorinated chain length (cf. Fig. 14). The average pore size of the catalyst, as shown in Tab. 7, is a factor 10^2 larger than the approximately molecular length of PFOcDA with 2.1 nm (Zhang et al., 2013). Because all further analyzed PFASs are smaller, steric hindances to diffusion of PFASs into the catalyst can generally be excluded as an influencing factor for the adsorption process. Though, it can be assumed that in the case of PFTeDA, PFHxDA and PFOcDA both rate constant and removal rate strongly depend on the chain length.

Under consideration of the functional group, a general trend was observed. Precursors are degraded best, followed by PFSAs and PFCAs as can be seen Fig. 12 b) as well as in Fig. 8. Regarding the precursor compounds only, it is conspicuous that 6:2 FTSA is degraded worst. This is in that respect surprising, since 6:2 FTSA is solely a polyfluorinated PFASs as illustrated in Tab. 1 and thus a reduced stability regarding degradation, compared to perfluorinated PFASs, would be expected. As found by Park et al. (2016) the 6:2 FTSA molecule is much more receptively according to degradation by oxidation because of the non-fluorinated ethyl-group between the sulfonate and the perfluorinated molecule part. This was previously confirmed by Yang et al. (2014b) since the the degradability of 6:2 FTSA compared to PFOS is generally much better in various AOPs. FOSA, which is the only perfluorinated PFASs in the group of precursors, decomposed as good as 8:2 FTSA (cf. Fig. 12 a)). Consequently this can be explained by the identical number of perfluorocarbon atoms. A further proof for the connection of degradability and perfluorinated chain length, could be the fact that, though PFOS, 6:2 FTSA and PFOA have an equal total number of carbon atoms, considerably differences concerning their removals are observable (cf. Fig. 8). At the same time an outstanding accordance in removal was found for all investigated PFASs with a number of eight perfluorocarbon atoms as displayed in Fig. 12 a). Moreover a comparison of all analyzed PFASs containing six perfluorocarbon atoms confirms the generally observed trend regarding differences in removal caused by disparate functional groups (cf. Fig. 12 b)). Regarding a difference in degradability of linear and branched isomers the study by Ochoa-Herrera et al. (2008) showed an enhanced vulnerability of branched PFOS in comparison to linear PFOS to a chemical reductive dehalogenation treatment with vitamin B_{12}. An increased stability of tertiary radicals as well as steric hindrances of adjacent trifluoromethyl groups and a thereby decreased C-C bond strength are suggested as possible causes for the observed behavior (Ochoa-Herrera et al., 2008). In contrast the authors results,

the present study found a less well (PFHxS br) or sightly slower (PFOS br, FOSA br) degradability for branched isomers (cf. Fig. 12 a) and b)). This observation is surprising since the applied AOP is also based on radical reactions. A linear perfluorinated chain consisting out of eight carbon atoms was found to be the degradation optimum. Therefore, it can be assumed that in the case of PFOS br and FOSA br, a branched chain has a proportional low impact on the degradability since PFASs with a number of six or seven linearly arranged perfluorocarbon atoms show high removal as well. Consequently a branching of a trifluoromethyl or pentafluorethyl group has a proportionally low impact since the remaining linear molecule part still remains in range of high removal rates.
Furthermore, it can be supposed, that the decreased degradability of PFHxS br is also related to the shorter molecular length and a slightly more spherical form. The single difference of PFHxS br to PFOS br and FOSA br is that the by the branching caused difference in linear chain length from the optimum condition is even bigger. Therefore it can be hypothesized that the impact on degradability increases as well. As moreover a deterioration in decomposability was also found for the analyzed PFCAs and PFSAs, it can generally be assumed that the impact of a from the optimum departing perfluorinated chain length rises with a rising degree of deviation Fig. 13.
There is no clear explanation for the observed increase in concentration of group 3 PFCAs after 30 min of ozonation (cf. Fig. 9 d)). Since it is assumed that the adsorption to the catalyst becomes stronger for PFASs with an increasing hydrophobic tail, a desorption of PFHxDA or PFOcDA from the catalyst surface seems very unlikely. Nevertheless, a significant increase in concentration was found for PFOcDA after 0.5 h of ozonation. Although the equilibrium processes were still not finished at that time and an increase in concentration between the samples taken on day 5 and the 0 h sample on day 6 is significant as well, the velocity of these reactions would be too slow to explain the changes after 30 min ozonation. For this reason it is suggested, that the observed exceptional degradation of e.g. group 2 PFCAs led to the generation of huge amounts of degradation products which might adsorb faster but less strong at the catalyst surface. This could cause - purely hypothetical - a temporary release of PFHxDA and PFOcDA.
Moreover the visible PFASs removal stagnated after 3 h of treatment (cf. Fig. 7). It is therefore clear, that the total concentration of all detected PFASs remains constant. At the same time still changes in concentration for diverse PFASs were observed between 3 h and 8 h as can be seen in Fig. 9, Fig. 10 and Fig. 11. The theory, that the degradation of PFASs with high rate constants is finished and the further occurring degradation processes of the remaining PFASs, for example group 1 and group 3 PFCAs is, according to their low rate constants (cf. Fig. 13), too slow to have a visible effect, needs to be resigned since even for the regarding PFASs a significant removal was observed in the initial three hours. On the one hand it is possible that the described alterations between 3 h and 8 h (cf. 3.2) were caused by degradation of longer chain PFASs to shorter chain PFASs whereby the total PFASs concentrations would not be changed. On the other hand it is alike possible that the variations are solely a result of de novo adsorption and desorption processes. There is no explicit explanation for the observed processes.

4.3 Removal of PFASs with the previous tested combination of ozone and catalyst and the addition of persulfate

Compared to the pilot scale, similar results were obtained for the lab scale experiments T1 (ozone), T2 (catalyst, ozone), T4 (persulfate ozone) and T6 (persulfate, catalyst, ozone).
In comparison to the samples taken during the pilot scale trials, the samples of the lab-scale experiments were analyzed via direct injection and thus the LOD is a factor ten higher than in the online SPE (Tab. 8). Because of problems with the analysis on the instrument previously used for data aquisition and analysis samples of T4 (persulfate, ozone), T5 (Persulfate, catalyst) and T6 (persulfate, catalyst, ozone) as well as the negative blanks were measured on a different instrument. This was additionally connected to long storage periods of the samples (approximately eight weeks) as well as an indispensable transfer of the affected samples into new vials. Thus, it has to be noted, that the observed trends are matter to high uncertainties and often not significant at the 95 % confidence interval level. Further, high deviations from the mean can also be caused by high uncertainties in the experimental setup or the low amount of replicate experiments. However, a correction of errors caused by differences in spiking was achieved by the conducted data standardization, since differences in spiking are a systematical error and thus constant for all samples per experiment (cf. 2.5). A direct comparison of the pilot scale and the lab scale set-up shows that both set-ups vary widely (cf. Tab. 2). Moreover, the pilot scale was according to the responsible engineers of Ozonetech previously used for the treatment of wastewater and organic solvents. Therefore parameters like flow rate, amount of ozone or the catalyst-water ratio for example have already been optimized to obtain best possible results at least for those water types and containing contaminations like pharmacutical residues. On the contrary the lab-scale trials are solely a first approach to test if similar conditions would lead to a removal at all.
Despite all differences and uncertainties, a similar trend for PFASs removal efficiency was observed for the laboratory scale trial T2 (ozone, catalyst) aiming to simulate the conditions of the pilot scale and furthermore for T4 (persulfate, ozone), T6 (persulfate, catalyst, ozone) and T1 (ozone). For these experiments, an increase in removal rate was observed for PFASs with a chain length of seven and more perfluorocarbon atoms. Interestingly, this was not only observed for T2 (cat, O_3) and T6 (PS, cat, O_3), but also for T1 (O_3) and T4 (PS, O_3) although no catalyst was applied in the regarding experiment. The only common parameter between the pilot scale experiment and T1 and T4 is the use of ozone. As a consequence it can be hypothesized, that the described effect is, contrary to previous assumptions in this discussion, based on interactions between ozone or ozone related radicals and PFASs instead of reactions happening between ozone and PFASs with the help of the catalyst. This theory is strengthened by the fact, that no such increase in removal rate with an increasing perfluorocarbon chain length was found for the trials T3 (persulfate) and T5 (persulfate, catalyst) where no ozone was applied. Since ozone concentrations per treated water volume were higher in the lab scale trial it is also possible, that occurring reactions followed different mechanisms. Thus reactions with ozone directly might be favored or higher amounts of hydroxyl radicals were generated in the lab scale trials. In contrast to this, the pilot scale trials were characterized by a considerable

higher amount of catalyst. Therefore, high amounts of catalyst might on the one hand lead to the generation of certain radical species that are generated in too small quantities to have a notable influence in the lab scale trials. On the other hand PFASs adsorption might be more pronounces whereby ongoing reactions might be less affected by limitations arising from mass transport. Thus, it might be that the catalyst simply favors the transformation of ozone into hydroxyl radicals which then are more abundant in the system as compared to the system with ozone only. The influence of PFASs adsorption processes on the catalyst surface in relation to the actual degradation reactions is thus not clear. However, it is apparent, that the application of ozone alone (T1) resulted in the lowest removal rates and nearly no removal of PFSAs and FTSAs (cf. Fig. 15 a) and Fig. 16). Hence, a catalytic ozone destruction, either heterogeneous or homogeneous seems to be needed to enhance the PFASs elimination. As found by Sotelo et al. (1987) the ozone self-decomposition in water proceeds via the following mechanism at a pH ranging between pH = 3 - 7:

$$O_3 + HO_2\cdot \longrightarrow 2\,O_2 + HO\cdot \tag{21}$$

$$O_3 + H_2O \longrightarrow 2\,HO\cdot + O_2 \tag{22}$$

Generated $OH\cdot$ radicals lead to an autocatalytic decomposition of further ozone molecules (equation (8)). The generation of hydroxyl radicals in absence of the tested catalyst material explains the observed removal of PFASs in T1 (O_3). Nonetheless it is most surprising that a PFASs removal, for at least PFCAs and FOSA, was found for a treatment with ozone at all. As reviewed by Rahman et al. (2014) diverse studies investigated the degradability of PFAAs via ozone based oxidation treatments, but no degradation was detected. Even for multiple ozonation stages with an ozone amount of $5\,mg\,L^{-1}$ at a water reclamation plant in Australia no PFASs transformation was found (Thompson et al., 2011). An improved oxidizing ability for the combination of ozone and persulfate was found in the present study and previously by Abu Amr et al. (2014) and Yang et al. (2016) since $OH\cdot$ leads to the generation of $SO_4^{-}\cdot$ as follows:

$$S_2O_8^{2} + \cdot OH \longrightarrow HSO_4\cdot^{-} + SO_4\cdot^{-} + \frac{1}{2}\,O_2 \tag{23}$$

In this context, it can be assumed that an additional application of catalyst material further increases the amount of radicals and thereby leads to an even higher PFASs removal as observed in T6 (PS, cat, O_3, cf. Fig. 16). However, it needs to be considered, that an excess amount of ozone or persulfate leads to a consumption of radicals and thereby to an inhibition of degradation reactions Yang et al. (2016). Excess ozone would lead to high hydroxyl radical concentrations and thereby a promoted generation of HSO_4^- as follows:

$$SO_4\cdot^{-} + \cdot OH \longrightarrow HSO_4^- + \frac{1}{2}\,O_2 \tag{24}$$

Yang et al. (2016) reported an inhibited degradation of BPA at high persulfate dosages since excess sulfate radicals on the one hand recombine to persulfate and on the other hand radicals

with a lower redox potential:

$$SO_4 \cdot^- + SO_4 \cdot^- \longrightarrow S_2O_8^{2-} \quad (25)$$

$$SO_4 \cdot^- + S_2O_8^{2-} \longrightarrow SO_4^{2-} + S_2O_8 \cdot^- \quad (26)$$

$$SO_4 \cdot^- + HO_2 \cdot \longrightarrow SO_4^{2-} - H^+ + O_2 \quad (27)$$

Accordingly it is quite possible, that the ratio of persulfate, ozone and catalyst was not adjusted to the optimal conditions, yet. The lab scale study was conducted to determine if the adjustment on the system led to with the pilot scale comparable results. Since the received results are similar to the ones of the simulated pilot scale system (T2), further research is needed to optimize the applied system and to test it in larger scales or at constant pH levels.
As can be seen in Fig. 17 pH was not constant during the conducted trials. A declination to pH = 3 was observed for all ozone treatment related experiments (T1- O_3, T2 - cat, O_3, T4 - PS, O_3 and T6 - PS, cat, O_3) and experiment 2b - the adsorption to the catalyst. No such decrease in pH was found for T5 (PS, cat). The decrease in pH in presence of catalyst is thus not consistent and might be explained by problems with the pH-meter during this trial. Observed changes in pH were therefore only considered as a qualitative parameter Low pH vlaues on the one hand caused a reduced generation of hydroxyl radicals but also an increased generation of sulfate radicals in previous studies (de Laat and Le, 2005; Yang et al., 2016). As found by Kolthoff and Miller (1951) the activation energy for an asymmetric bond cleavage of the peroxide group in persulfate decreases from 33.5 kcal in an uncatalyzed reaction to 26.0 kcal under acid-catalysis. The asymmetric bond break generates a hydrogensulfate ion and a sulfate radical (Kolthoff and Miller, 1951). The increased generation of sulfate radicals might explain the increased removal rate of T6 (PS, cat, O_3)

$$S_2O_8^{2-} + H^+ \longrightarrow HSO_4^- + SO_4 \cdot^- \quad (28)$$

5 Conclusion

The present study has shown that PFASs with a perfluorocarbon chain length of six to eleven perfluorinated carbon atoms can efficiently be removed by an advanced oxidation process (AOP) making use of ozone and an inorganic catalyst at a pilot scale setup. Further it was shown, that there is a potential for optimization by combining the existing approach with persulfate. The present thesis work consists of three parts that are based on each other. In the first part, the adsorption to the material in questions Ia and Ib (2.5) were evaluated, and it was found that all evaluable PFASs adsorbed within 10 min to the catalyst surface. This fast process was followed by a slow adjustment of equilibrium which was characterized by alternating adsorption and desorption processes.
Regarding the adsorption behavior, a fit according to the Freundlich model was found. The calculated values for the adsorption intensity n were slightly larger than one which indicated for the presence of heterogeneous surface sites. An initial decrease in adsorption capacity (K_f) followed by a repeated increase in K_f with a rising number of perfluorocarbon atoms per PFASs was caused by strong electrostatic interactions of short chain PFASs and high hydrophobic interactions of long chain PFASs with the catalyst material. This assumes the presence of different active sites on the catalyst surface. For all PFASs with low K_f values probably the formation of strong electrostatic strong hydrophobic interactions was most likely not possible. The catalyst is an inorganic material which mainly consists of iron and oxygen. The porous are characterized a macro porous and it has a surface area of 26.4 $m^2\,g^{-1}$.
The results of part I were essential for planning part II - the pilot scale trials - and later the evaluation and understanding of gained data. With the applied ozone-catalyst treatment all PFASs were removed significantly. A clear statement about PFASs degradation was not possible as no increase in concentration of shorter chain PFASs was found. Though, an increase in fluoride ion concentration was found which however indicates to occurred degradation processes. PFASs with a chain length of six to eleven carbon atoms were degraded best while the number of nine perfluorinated carbon atoms was the optimum. It was found that the size of the hydrophobic molecular part determined the removal primarily and the type of functional group was subordinate. A comparison of PFASs with six perfluorinated carbon atoms showed that precursors are degraded best followed by PFSAs and PFCAs. The removal followed a second order reaction kinetic. High removals of PFASs with six to eleven perfluorinated carbon atoms were traced back to a particular ratio of hydrophobic and electrostatic interactions with the catalyst. However, the results of the lab scale trials (part III), which were conducted to evaluate the potential for a method optimization using persulfate as a further adjustment, suggested a connection between removal and ozone instead of interactions with the catalyst. This was explained by the absence of a perfluorinated chain length dependency in trial T5 (persulfate, catalyst) and an occurrence of this connection at T1 (O_3) and T4 (persulfate, O_3). In total six experiments were conducted during the lab scale trial to test all possible combinations of catalyst, ozone and persulfate. No or little removal was found for the combination of persulfate only (T3) as well as persulfate and catalyst (T5). High removal was found for T2 (catalyst, ozone) which was

the lab scale experiment of the pilot scale treatment conditions and T1 (O_3), T4 (persulfate, O_3) as well as T6 (persulfate, catalyst, O_3). In contrast to many studies it was possible to remove PFCAs with the treatment of ozone only. According to high deviations of the mean it was not possible to clearly determine the best out of the last four listed treatment methods. However, not quantitatively but qualitatively a trend could be observed. For all spiked compounds under exception of PFDoDA, T6 (persulfate, catalyst, O_3) showed the highest removal.
For a significant validation of the results further experiments are necessary, which though would have exceeded the scope of the present master thesis. Part III trials were solely conducted to test if a removal can be achieved at all under changed experimental conditions. Since this is possible, further research in terms of triplicate experiments or an even higher number of replicates is needed. Moreover it would be important to test different ratios of persulfate, catalyst and ozone since either excess ozone as well as excess persulfate would lead to a reduced redox potential or decreasing amounts of radicals. A further big influencing factor is the pH. Low pH-values promote the generation of sulfate radicals whereas high pH-values increase the generation of hydroxyl radicals. Since pH was not stable during the conducted trials, experiments at a stabilized pH level for example at pH = 3, 7 and 11 would be useful. A reduction of spike to one ore two compounds at high concentrations (maybe even mg L^{-1} range) would also be an alternative approach aiming for high concentrations of degradation products that do not adsorb to the catalyst surface completely. Furthermore it would be interesting to additionally evaluate the redox potential during the lab scale trials i.a. as an parameter for the applied ozone concentration.
After the conduction of these further lab scale studies, it would be important to scale up the treated water volume and to evaluate the most efficient treatment conditions in a pilot scale size. Of course this has to be done under respect of actual in a water treatment plant feasible reaction conditions. Furthermore it would be important to test the setup with real waste water which contains on the one hand diverse ions or dissolved organic carbon that will probably affect the efficiency and on the other hand other micropollutants like pharmacutical and personal care product residues as well as pesticides or polychlorinated biphenyls for example. Apart from method optimization and upscaling it is absolutely necessary to receive more information about the reaction mechanism and degradation products. For this purpose the conduction of radical scavenger experiments with tert-butanolfor example would be useful. Therefore, it might be possible to confirm the 'unzipping' mechanism whereby CF_2 units are removed from the PFASs chain or the generation of fluoride ions and carbon dioxide for example. A non-target screening of treated water might be helpful as well to evaluate if so far unknown degradation products are generated. The application of gas chromatography for the identification of volatile degradation products would be an additional estimate.

Bibliography

3M (1999). The science or organic fluorochemistry. Available online at URL: https://www.fluoridealert.org/wp-content/pesticides/pfos.fr.final.docket.0006.pdf. Last accessed on 27.09.2017.

Abu Amr, S. S., Aziz, H. A., Adlan, M. N., and Alkasseh, J. M. (2014). Effect of ozone and ozone/persulfate processes on biodegradable and soluble characteristics of semiaerobic stabilized leachate. *Environmental Progress & Sustainable Energy*, 33(1):184–191.

Ahrens, L. (2011). Polyfluoroalkyl compounds in the aquatic environment: A review of their occurrence and fate. *Journal of environmental monitoring : JEM*, 13(1):20–31.

Ahrens, L., Gashaw, H., Sjöholm, M., Gebrehiwot, S. G., Getahun, A., Derbe, E., Bishop, K., and Åkerblom, S. (2016). Poly- and perfluoroalkylated substances (PFASs) in water, sediment and fish muscle tissue from Lake Tana, Ethiopia and implications for human exposure. *Chemosphere*, 165:352–357.

Ahrens, L., Harner, T., Shoeib, M., Lane, D. A., and Murphy, J. G. (2012). Improved characterization of gas-particle partitioning for per- and polyfluoroalkyl substances in the atmosphere using annular diffusion denuder samplers. *Environmental science & technology*, 46(13):7199–7206.

Andreozzi, R. (1999). Advanced oxidation processes (AOP) for water purification and recovery. *Catalysis Today*, 53(1):51–59.

Anumol, T., Dagnino, S., Vandervort, D. R., and Snyder, S. A. (2016). Transformation of polyfluorinated compounds in natural waters by advanced oxidation processes. *Chemosphere*, 144:1780–1787.

Arias Espana, V. A., Mallavarapu, M., and Naidu, R. (2015). Treatment technologies for aqueous perfluorooctanesulfonate (PFOS) and perfluorooctanoate (PFOA): A critical review with an emphasis on field testing. *Environmental Technology & Innovation*, 4:168–181.

Atkins, P. W. and de Paula, J. (2006). *Atkins' physical chemistry*. Oxford Univ. Press, Oxford, 8. ed. edition.

Buck, R. C., Franklin, J., Berger, U., Conder, J. M., Cousins, I. T., de Voogt, P., Jensen, A. A., Kannan, K., Mabury, S. A., and van Leeuwen, S. P. J. (2011). Perfluoroalkyl and polyfluoroalkyl substances in the environment: Terminology, classification, and origins. *Integrated environmental assessment and management*, 7(4):513–541.

Cheung, C., Porter, J., and Mckay, G. (2001). Sorption kinetic analysis for the removal of cadmium ions from effluents using bone char. *Water research*, 35(3):605–612.

Dalrymple, O. K., Stefanakos, E., Trotz, M. A., and Goswami, D. Y. (2010). A review of the mechanisms and modeling of photocatalytic disinfection. *Applied Catalysis B: Environmental*, 98(1-2):27–38.

de Laat, J. and Le, T. G. (2005). Kinetics and Modeling of the Fe(III)/H 2 O 2 System in the Presence of Sulfate in Acidic Aqueous Solutions. *Environmental Science & Technology*, 39(6):1811–1818.

de Silva, A. O. and Mabury, S. A. (2006). Isomer Distribution of Perfluorocarboxylates in Human Blood: Potential Correlation to Source. *Environmental Science & Technology*, 40(9):2903–2909.

D'eon, J. C. and Mabury, S. A. (2011). Is indirect exposure a significant contributor to the burden of perfluorinated acids observed in humans? *Environmental science & technology*, 45(19):7974–7984.

Desta, M. B. (2013). Batch Sorption Experiments: Langmuir and Freundlich Isotherm Studies for the Adsorption of Textile Metal Ions onto Teff Straw (Eragrostis tef) Agricultural Waste. *Journal of Thermodynamics*, 2013(1):1–6.

Ding, G. and Peijnenburg, W. J. G. M. (2013). Physicochemical Properties and Aquatic Toxicity of Poly- and Perfluorinated Compounds. *Critical Reviews in Environmental Science and Technology*, 43(6):598–678.

Du, Z., Deng, S., Bei, Y., Huang, Q., Wang, B., Huang, J., and Yu, G. (2014). Adsorption behavior and mechanism of perfluorinated compounds on various adsorbents–a review. *Journal of hazardous materials*, 274:443–454.

EFSA (2012). Perfluoroalkylated substances in food: Occurrence and dietary exposure. *EFSA Journal*, 10(6).

Freundlich, H. (1926). *Colloid And Capillary Chemistry*. Methuen And Co. Ltd, London.

Fromme, H., Tittlemier, S. A., Völkel, W., Wilhelm, M., and Twardella, D. (2009). Perfluorinated compounds–exposure assessment for the general population in Western countries. *International journal of hygiene and environmental health*, 212(3):239–270.

Geochemical laboratory, Department of Aquatic Sciences and Assessment, Swedish University of Agricultural Sciences (2017). Water chemical and physical analyses. Available online at URL: http://www.slu.se/en/departments/aquatic-sciences-assessment/laboratories/geochemical-laboratory/water-chemical-analyses/. Last accessed on 20.09.2017.

Giri, R. R., Ozaki, H., Okada, T., Taniguchi, S., and Takanami, R. (2012). Factors influencing UV photodecomposition of perfluorooctanoic acid in water. *Chemical Engineering Journal*, 180:197–203.

Glaze, W. H., Kang, J.-W., and Chapin, D. H. (1987). The Chemistry of Water Treatment Processes Involving Ozone, Hydrogen Peroxide and Ultraviolet Radiation. *Ozone Science & Engineering*, (9):335–352.

Gorrochategui, E., Pérez-Albaladejo, E., Casas, J., Lacorte, S., and Porte, C. (2014). Perfluorinated chemicals: Differential toxicity, inhibition of aromatase activity and alteration of cellular lipids in human placental cells. *Toxicology and applied pharmacology*, 277(2):124–130.

Haghseresht, F. and Lu, G. Q. (1998). Adsorption Characteristics of Phenolic Compounds onto Coal-Reject-Derived Adsorbents. *Energy & Fuels*, 12(6):1100–1107.

Hameed, B. H., Din, A. T. M., and Ahmad, A. L. (2007). Adsorption of methylene blue onto bamboo-based activated carbon: Kinetics and equilibrium studies. *Journal of hazardous materials*, 141(3):819–825.

Hansen, M. C., Børresen, M. H., Schlabach, M., and Cornelissen, G. (2010). Sorption of perfluorinated compounds from contaminated water to activated carbon. *Journal of Soils and Sediments*, 10(2):179–185.

Haug, L. S., Thomsen, C., Brantsæter, A. L., Kvalem, H. E., Haugen, M., Becher, G., Alexander, J., Meltzer, H. M., and Knutsen, H. K. (2010). Diet and particularly seafood are major sources of perfluorinated compounds in humans. *Environment International*, 36(7):772–778.

Higgins, C. P. and Luthy, R. G. (2007). Modeling Sorption of Anionic Surfactants onto Sediment Materials: An a priori Approach for Perfluoroalkyl Surfactants and Linear Alkylbenzene Sulfonates. *Environmental Science & Technology*, 41(9):3254–3261.

Hoigné, J. (1998). Chemistry of aqueous ozone and transformation of pollutants by ozonation and advanced oxidation processes. In Hrubec, J., editor, *The Handbook of Environmental Chemistry*, volume C Quality and Treatment of Drinking water II, pages 83–141. Springer, Berlin, Heidelberg.

Holleman, A. F., Wiberg, E., and Wiberg, N. (2007). *Lehrbuch der anorganischen Chemie*. Walter de Gruyter.

Hori, H., Yamamoto, A., Hayakawa, E., Taniyasu, S., Yamashita, N., Kutsuna, S., Kiatagawa, H., and Arakawa, R. (2005). Efficient Decomposition of Environmentally Persistent Perfluorocarboxylic Acids by Use of Persulfate as a Photochemical Oxidant. *Environmental Science & Technology*, 39(7):2383–2388.

Huling, S. G. and Pivetz, B. E. (2006). In-situ chemical oxidation. Available online at URL: http://www.dtic.mil/get-tr-doc/pdf?AD=ADA507297. Last accessed on 26.08.2017.

Ikehata, K. and El-Din, M. G. (2004). Degradation of Recalcitrant Surfactants in Wastewater by Ozonation and Advanced Oxidation Processes: A Review. *Ozone: Science & Engineering*, 26(4):327–343.

Kasprzyk-Hordern, B. (2003). Catalytic ozonation and methods of enhancing molecular ozone reactions in water treatment. *Applied Catalysis B: Environmental*, 46(4):639–669.

Kolthoff, I. M. and Miller, I. K. (1951). The Chemistry of Persulfate. I. The Kinetics and Mechanism of the Decomposition of the Persulfate Ion in Aqueous Medium1. *Journal of the American Chemical Society*, 73(7):3055–3059.

Krafft, M. P. and Riess, J. G. (2015). Per- and polyfluorinated substances (PFASs): Environmental challenges. *Current Opinion in Colloid & Interface Science*, 20(3):192–212.

Langlais, B., editor (1991). *Ozone in water treatment: Application and engineering ; cooperative research report*. Lewis, Chelsea, Mich., 2. print edition.

Lavonen, E. E., Gonsior, M., Tranvik, L. J., Schmitt-Kopplin, P., and Köhler, S. J. (2013). Selective chlorination of natural organic matter: Identification of previously unknown disinfection byproducts. *Environmental science & technology*, 47(5):2264–2271.

Lee, H. and Mabury, S. A. (2011). A pilot survey of legacy and current commercial fluorinated chemicals in human sera from United States donors in 2009. *Environmental science & technology*, 45(19):8067–8074.

Leusink, J. (2013). Ozone journal: How do ozone venturi injectors work to dissolve ozone into water? Available online at URL: http://www.ozonesolutions.com/journal/tag/ozone-injector/. Last accessed on 25.08.2017.

Lin, A. Y.-C., Panchangam, S. C., Chang, C.-Y., Hong, P. K. A., and Hsueh, H.-F. (2012). Removal of perfluorooctanoic acid and perfluorooctane sulfonate via ozonation under alkaline condition. *Journal of hazardous materials*, 243:272–277.

Loganathan, B. G., Sajwan, K. S., Sinclair, E., Senthil Kumar, K., and Kannan, K. (2007). Perfluoroalkyl sulfonates and perfluorocarboxylates in two wastewater treatment facilities in Kentucky and Georgia. *Water research*, 41(20):4611–4620.

Merino, N., Qu, Y., Deeb, R. A., Hawley, E. L., Hoffmann, M. R., and Mahendra, S. (2016). Degradation and Removal Methods for Perfluoroalkyl and Polyfluoroalkyl Substances in Water. *Environmental Engineering Science*, 33(9):615–649.

Munter, R. (2001). Advanced oxidation processes–current status and prospects. *Proc. Estonian Acad. Sci. Chem*, 50(2):59–80.

Neta, P., Madhavan V., Zemel, H., and and Fessenden R. W. (1977). Rate constants and mechanism of reaction of sulfate radical anion with aromatic compounds. *Journal of the American Chemical Society*, 99(1):163–164.

Ochoa-Herrera, V. and Sierra-Alvarez, R. (2008). Removal of perfluorinated surfactants by sorption onto granular activated carbon, zeolite and sludge. *Chemosphere*, 72(10):1588–1593.

Ochoa-Herrera, V., Sierra-Alvarez, R., Somogyi, A., Jacobsen, N. E., Wysocki, V. H., and Field, J. A. (2008). Reductive Defluorination of Perfluorooctane Sulfonate. *Environmental Science & Technology*, 42(9):3260–3264.

O'Hagan, D. (2008). Understanding organofluorine chemistry. An introduction to the C-F bond. *Chemical Society reviews*, 37(2):308–319.

Organisation for Economic Co-operation and Development (2017). OECD portal on perfluorinated chemicals. Available online at URL: http://www.oecd.org/chemicalsafety/portal-perfluorinated-chemicals/aboutpfass/. Last accessed on 19.08.2017.

Oturan, M. A. and Aaron, J.-J. (2014). Advanced Oxidation Processes in Water/Wastewater Treatment: Principles and Applications. A Review. *Critical Reviews in Environmental Science and Technology*, 44(23):2577–2641.

Ozonetech (2017). Pilot projects. Available online at URL: http://www.ozonetech.com/solutions-

systems/tailored-wastewater-treatment-projects. Last accessed on 15.10.2017.

Park, S., Lee, L. S., Medina, V. F., Zull, A., and Waisner, S. (2016). Heat-activated persulfate oxidation of PFOA, 6:2 fluorotelomer sulfonate, and PFOS under conditions suitable for in-situ groundwater remediation. *Chemosphere*, 145:376–383.

Paul, A. G., Jones, K. C., and Sweetman, A. J. (2009). A First Global Production, Emission, And Environmental Inventory For Perfluorooctane Sulfonate. *Environmental Science & Technology*, 43(2):386–392.

Post, G. B., Cohn, P. D., and Cooper, K. R. (2012). Perfluorooctanoic acid (PFOA), an emerging drinking water contaminant: A critical review of recent literature. *Environmental research*, 116:93–117.

Qiu, Y., Fujii, S., and Tanaka, S. (2007). Removal of perfluorochemicals from wastewater by granular activated carbon adsorption. *Environmental Engineering Research*, 44:185–193.

Rahman, M. F., Peldszus, S., and Anderson, W. B. (2014). Behaviour and fate of perfluoroalkyl and polyfluoroalkyl substances (PFASs) in drinking water treatment: A review. *Water research*, 50:318–340.

Rayne, S. and Forest, K. (2009). Perfluoroalkyl sulfonic and carboxylic acids: A critical review of physicochemical properties, levels and patterns in waters and wastewaters, and treatment methods. *Journal of environmental science and health. Part A, Toxic/hazardous substances & environmental engineering*, 44(12):1145–1199.

Ribeiro, A. R., Nunes, O. C., Pereira, M. F. R., and Silva, A. M. T. (2015). An overview on the advanced oxidation processes applied for the treatment of water pollutants defined in the recently launched Directive 2013/39/EU. *Environment International*, 75:33–51.

Schröder, H. F. and Meesters, R. J. (2005). Stability of fluorinated surfactants in advanced oxidation processes—A follow up of degradation products using flow injection–mass spectrometry, liquid chromatography–mass spectrometry and liquid chromatography–multiple stage mass spectrometry. *Journal of Chromatography A*, 1082(1):110–119.

Schröder, H. F. R., Jose, H. J., Gebhardt, W., Moreira, R. F. P. M., and Pinnekamp, J. (2010). Biological wastewater treatment followed by physicochemical treatment for the removal of fluorinated surfactants. *Water science and technology : a journal of the International Association on Water Pollution Research*, 61(12):3208–3215.

Schröter-Kermani, C., Müller, J., Jürling, H., Conrad, A., and Schulte, C. (2013). Retrospective monitoring of perfluorocarboxylates and perfluorosulfonates in human plasma archived by the German Environmental Specimen Bank. *International journal of hygiene and environmental health*, 216(6):633–640.

Seals, R., Bartell, S. M., and Steenland, K. (2011). Accumulation and clearance of perfluorooctanoic acid (PFOA) in current and former residents of an exposed community. *Environmental health perspectives*, 119(1):119–124.

Senevirathna, S. T. M. L. D., Tanaka, S., Fujii, S., Kunacheva, C., Harada, H., Shivakoti, B. R.,

and Okamoto, R. (2010). A comparative study of adsorption of perfluorooctane sulfonate (PFOS) onto granular activated carbon, ion-exchange polymers and non-ion-exchange polymers. *Chemosphere*, 80(6):647–651.

Sinclair, E. and Kannan, K. (2006). Mass Loading and Fate of Perfluoroalkyl Surfactants in Wastewater Treatment Plants. *Environmental Science & Technology*, 40(5):1408–1414.

Soon, A. N. and Hameed, B. H. (2011). Heterogeneous catalytic treatment of synthetic dyes in aqueous media using Fenton and photo-assisted Fenton process. *Desalination*, 269(1-3):1–16.

Sotelo, J. L., Beltran, F. J., Benitez, F. J., and and Beltran-Heredia, J. (1987). Ozone decomposition in water: kinetic study. *Industrial & engineering chemistry research*, 26(1):39–43.

Steinle-Darling, E. and Reinhard, M. (2008). Nanofiltration for Trace Organic Contaminant Removal: Structure, Solution, and Membrane Fouling Effects on the Rejection of Perfluorochemicals. *Environmental Science & Technology*, 42(14):5292–5297.

Suty, H., de Traversay, C., and Cost, M. (2004). Applications of advanced oxidation processes: Present and future. *Water science and technology : a journal of the International Association on Water Pollution Research*, 49(4):227–233.

Tang, C. Y., Shiang Fu, Q., Gao, D., Criddle, C. S., and Leckie, J. O. (2010). Effect of solution chemistry on the adsorption of perfluorooctane sulfonate onto mineral surfaces. *Water research*, 44(8):2654–2662.

Thompson, J., Eaglesham, G., Reungoat, J., Poussade, Y., Bartkow, M., Lawrence, M., and Mueller, J. F. (2011). Removal of PFOS, PFOA and other perfluoroalkyl acids at water reclamation plants in South East Queensland Australia. *Chemosphere*, 82(1):9–17.

Torn, L., de Keizer, A., Koopal, L., and Lyklema, J. (2003). Mixed adsorption of poly(vinylpyrrolidone) and sodium dodecylbenzenesulfonate on kaolinite. *Journal of Colloid and Interface Science*, 260(1):1–8.

Trudel, D., Horowitz, L., Wormuth, M., Scheringer, M., Cousins, I. T., and Hungerbühler, K. (2008). Estimating consumer exposure to PFOS and PFOA. *Risk analysis : an official publication of the Society for Risk Analysis*, 28(2):251–269.

Tsitonaki, A., Petri, B., Crimi, M., MosbÆK, H., Siegrist, R. L., and Bjerg, P. L. (2010). In Situ Chemical Oxidation of Contaminated Soil and Groundwater Using Persulfate: A Review. *Critical Reviews in Environmental Science and Technology*, 40(1):55–91.

United Nations Environment Programme (2009). Listing of perfluorooctane sulfonic acid, its salts and perfluorooctane sulfonyl fluoride. Available online at URL: http://chm.pops.int/Implementation/IndustrialPOPs/PFOS/Decisions/tabid/5222/Default.aspx. Last accessed on 19.08.2017.

United States Environmental Protection Agency (2009). Long-chain perfluorinated chemicals (pfcs) action plan. Available online at URL: https://www.epa.gov/sites/production/files/2016-01/documents/pfcs_action_plan1230_09.pdf. Last accessed on 27.09.2017.

Vestergren, R. and Cousins, I. T. (2009). Tracking the Pathways of Human Exposure to Perfluorocarboxylates. *Environmental Science & Technology*, 43(15):5565–5575.

von Gunten, U. (2003). Ozonation of drinking water: Part I. Oxidation kinetics and product formation. *Water research*, 37(7):1443–1467.

Wang, B. B., Cao, M. H., Tan, Z. J., Wang, L. L., Yuan, S. H., and Chen, J. (2010). Photochemical decomposition of perfluorodecanoic acid in aqueous solution with VUV light irradiation. *Journal of hazardous materials*, 181(1-3):187–192.

Wang, Z., Cousins, I. T., Scheringer, M., and Hungerbühler, K. (2013). Fluorinated alternatives to long-chain perfluoroalkyl carboxylic acids (PFCAs), perfluoroalkane sulfonic acids (PFSAs) and their potential precursors. *Environment International*, 60:242–248.

Wang, Z., MacLeod, M., Cousins, I. T., Scheringer, M., and Hungerbühler, K. (2011). Using COSMOtherm to predict physicochemical properties of poly- and perfluorinated alkyl substances (PFASs). *Environmental Chemistry*, 8(4):389.

Weber, W. J. and Borchardt, J. A. (1972). *Physicochemical processes for water quality control*. Environmental science and technology. Wiley-Interscience, New York, London, Sydney, Toronto.

Weppner, W. A. (2000). Phase-out Plan for PFOS-Based Products. Available online at URL: https://www.fluoridealert.org/wp-content/pesticides/pfos.fr.final.docket.0009.pdf. Last accessed on 27.09.2017.

Yang, X., Huang, J., Zhang, K., Yu, G., Deng, S., and Wang, B. (2014a). Stability of 6: 2 fluorotelomer sulfonate in advanced oxidation processes: degradation kinetics and pathway. *Environmental science and pollution research international*, 21(6):4634–4642.

Yang, X., Huang, J., Zhang, K., Yu, G., Deng, S., and Wang, B. (2014b). Stability of 6: 2 fluorotelomer sulfonate in advanced oxidation processes: degradation kinetics and pathway. *Environmental science and pollution research international*, 21(6):4634–4642.

Yang, Y., Guo, H., Zhang, Y., Deng, Q., and Zhang, J. (2016). Degradation of Bisphenol A Using Ozone/Persulfate Process: Kinetics and Mechanism. *Water, Air, & Soil Pollution*, 227(2):1434.

Yu, Q., Zhang, R., Deng, S., Huang, J., and Yu, G. (2009). Sorption of perfluorooctane sulfonate and perfluorooctanoate on activated carbons and resin: Kinetic and isotherm study. *Water research*, 43(4):1150–1158.

Zaggia, A., Conte, L., Falletti, L., Fant, M., and Chiorboli, A. (2016). Use of strong anion exchange resins for the removal of perfluoroalkylated substances from contaminated drinking water in batch and continuous pilot plants. *Water research*, 91:137–146.

Zhang, L., Ren, X.-M., and Guo, L.-H. (2013). Structure-based investigation on the interaction of perfluorinated compounds with human liver fatty acid binding protein. *Environmental science & technology*, 47(19):11293–11301.

Zhi, Y. and Liu, J. (2015). Adsorption of perfluoroalkyl acids by carbonaceous adsorbents: Ef-

fect of carbon surface chemistry. *Environmental pollution (Barking, Essex : 1987)*, 202:168–176.

6 Appendix

Tab. A.1: Used analytical standard.

Compound	Abbrevation	Manufacturer	Purity
Perfluorobutyric acid	PFBA	Sigma-Aldrich Sweden AB	98 %
Perfluoropentanoic acid	PFPA	Sigma-Aldrich Sweden AB	97 %
Perfluorohexanoic acid	PFHxA	Sigma-Aldrich Sweden AB	97 %
Perfluoroheptanoic acid	PFHpA	Sigma-Aldrich Sweden AB	99 %
Perfluorooctanoic acid	PFOA	Sigma-Aldrich Sweden AB	96 %
Perfluorononanoic acid	PFNA	Sigma-Aldrich Sweden AB	97 %
Perfluorodecanoic acid	PFDA	Sigma-Aldrich Sweden AB	98 %
Perfluoroundecanoic acid	PFUnDA	Sigma-Aldrich Sweden AB	95 %
Perfluorododecanoic acid	PFDoDA	Sigma-Aldrich Sweden AB	95 %
Perfluorotetradecanoic acid	PFTeDA	Sigma-Aldrich Sweden AB	97 %
Perfluohexadecanoic acid	PFHxDA	Alfa Aesar GmbH & Co.KG	95 %
Perfluorooctadecanoic acid	PFOcDA	Alfa Aesar GmbH & Co.KG	97 %
Potassium nonafluoro-1-butanesulfonate	PFBS-K	Sigma-Aldrich Sweden AB	98 %
Potassium tridecafluorohexane-1-sulfonate	PFHxS-K	Sigma-Aldrich Sweden AB	98 %
Potassium heptadecafluorooctanesulfonate	PFOS-K	Sigma-Aldrich Sweden AB	98 %
1H,1H,2H,2H-Tridecafluorooctane-1-sulfonic acid	6:2 FTSA	Apollo Scientific Ltd	98 %
1H,1H,2H,2H-Perfluorodecanesulfonic acid	8:2 FTSA	Apollo Scientific Ltd	$\leq$ 100 %
Perfluorooctanesulfonamide	FOSA	Sigma-Aldrich Sweden AB	$\leq$ 100 %
n-Ethyl perfluorooctan sulfonamide	Et-FOSA	Apollo Scientific Ltd	95 %

Tab. A.2: Compounds contained in the internal standard mix and PFASs for which they are applied.

Internal standard[a]	Calibrated PFASs
$^{13}C_4$-PFBA	PFBA
$^{13}C_2$-PFHxA	PFBS, PFPeA, PFHxA
$^{13}C_4$-PFOA	PFHpA, PFOA
$^{13}C_5$-PFNA	PFNA
$^{13}C_2$-PFDA	PFDA
$^{13}C_2$-PFUnDA	PFUnDA
$^{13}C_2$-PFDoDA	PFDoDA, PFTeDA, PFHxDA, PFOcDA
$^{18}O_2$-PFHxS	PFHxS, 6:2 FTSA
$^{13}C_4$-PFOS	PFOS, 8:2 FTSA
$^{13}C_8$-FOSA	FOSA
d_5-*N*-EtFOSA	*N*-EtFOSA

[a] Further contained internal standards for compounds that were not investigated in this thesis: d_3-*N*-MeFOSAA, d_5-*N*-EtFOSAA, d_3-*N*-MeFOSA, d_7-*N*-MeFOSE, d_9-*N*-EtFOSE

Fig. A.1: By the company Ozonetech applied pilot scale system (Ozonetech, 2017).

Tab. A.3: Used laboratory equipment.

Material	Company
Pretests on the catalyst material	
250 mL bottle	Thermo Fischer Scientific, Nalgene™ Narrow-Mouth HDPE bottle
Filterpaper	Munktell Ahlstrom, quantitative filterpaper, Grade 00H
Syringe filter	VWR International, VWR®syringe filters, 0.45 µm pore size, Nylon membrane, USA
Syringe	HENKE SASS WOLF, 10 mL HSW NORM-JECT®
Shaking machine	Gerhardt
Pilot scale trials	
Ozone generator	Ozonetech, Sweden
Pilot scale treatment system	Ozonetech, Sweden
Online SPE vials	Thermo scientific, Autoselect™ Polyvial™, 10 mL, Polystyrene
Lab scale trials	
Ozone generator, tubes, Gas diffuser	Green Air
500 mL three necked flask	Lenz
500 mL volumetric flask	Witeg, Germany
Chloroprene rubber stopper	DEUTSCH & NEUMANN
Y-tubing connector	Ismatec, Polyoxymethylen
Magnetic stirrer no. 1	JP Selecta, Agimatic-E
Magnetic stirrer no. 2	IKA®Werke, IKAMAG®RCT basic
Glass coated stirring bars	Cowie®, Stirring magnet, length: 19 mm, diameter: 6 mm
pH-meter	VWR International, pHenomenal®1000H, Germany
Conductometer	VWR International, EC 300
Standing drill	AB Arboga, Type: B 2512, Sweden
Plastic coated wires	Davu Cables, Great Britain
General Equipment	
2 mL glass vials	Agilent Technologies, Poland
1.5 mL PP vial	Scantec Nordic
Vial -Caps	Agilent Technologies, USA
700 µL PP vials	Thermo Scientific, USA
Vial -Caps	Thermo Scientific, USA
50 mL centrifuge tube (PP)	Corning
pH indicator stripes	Merck, MColorpHast™ pH 0-14
Vortexer	Heidolph, REAX 2000
Centrifuge	Eppendorf, Centrifuge 5810
Pipette	VWR International
Precision Balance	Mettler Toledo, Switzerland
Ultrasonic Bath	Branson
Parafilm	Bemis, Parafilm M®, USA

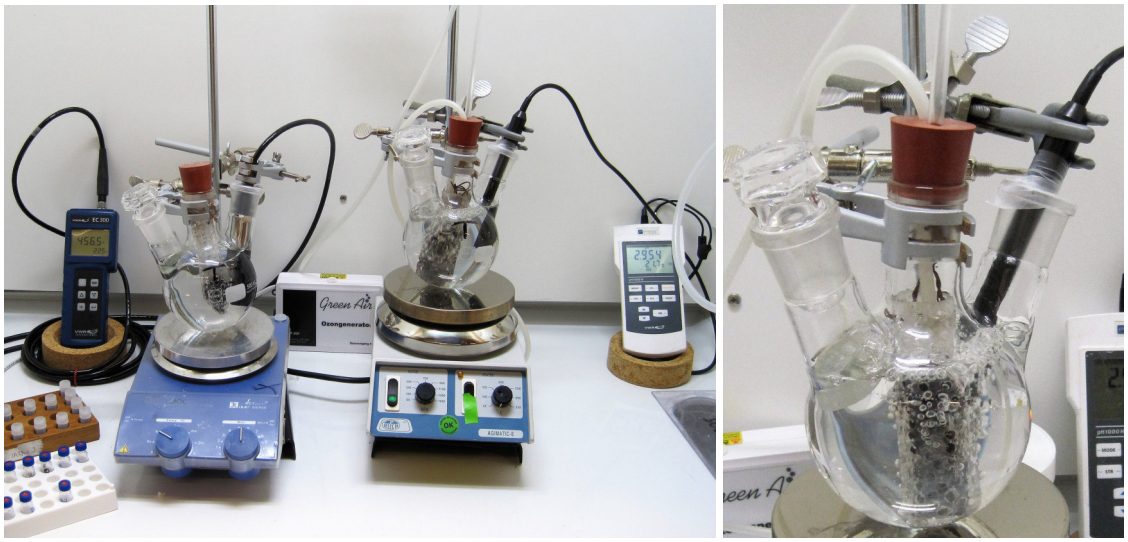

Fig. A.2: Experimental set up of the lab scale trials.

Fig. A.3: Applied catalyst material.

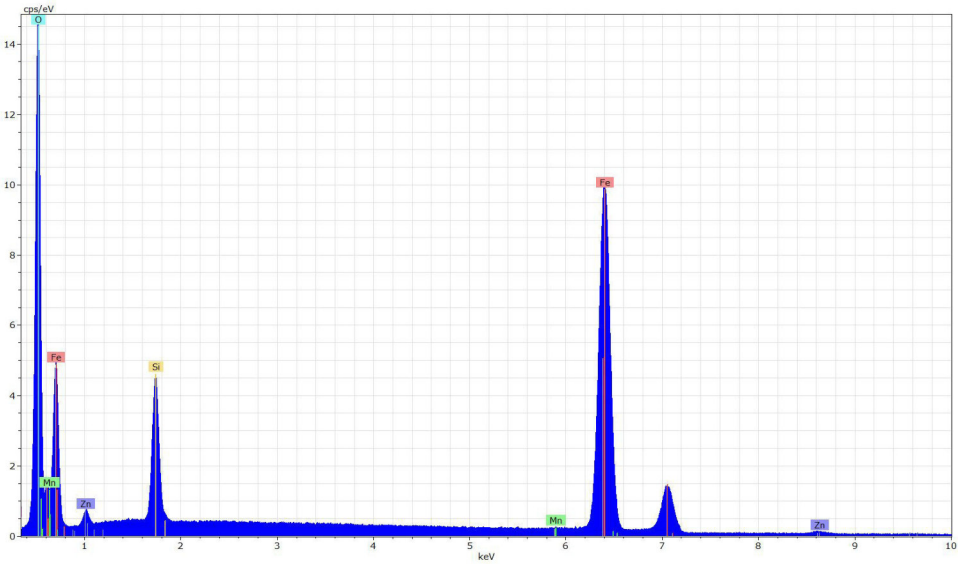

Fig. A.4: EDS spectrum acquired from a 50 fold enlargement of the catalyst. The spectrum presents the element distribution in the catalyst material.

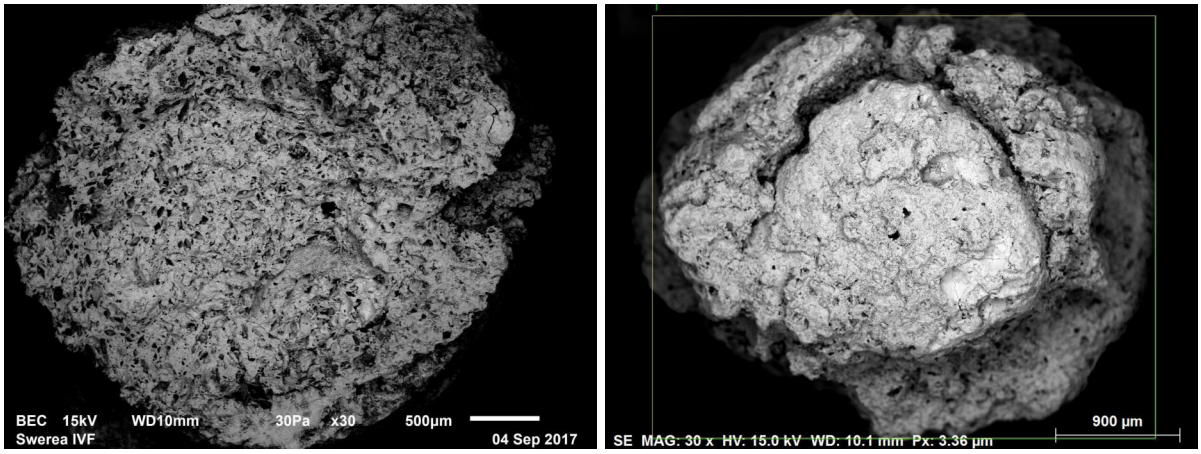

a) b)

Fig. A.5: Cross section a) and top view b) SEM/EDS pictures of the catalyst material at a 30x magnification. For picture a) imaging with backscattered electrons (BEC) was applied to show the atomic contrast (a brighter contrast refers to a heavier material) and for picture b) imaging via secondary electrons was used to show the topographic contrast.

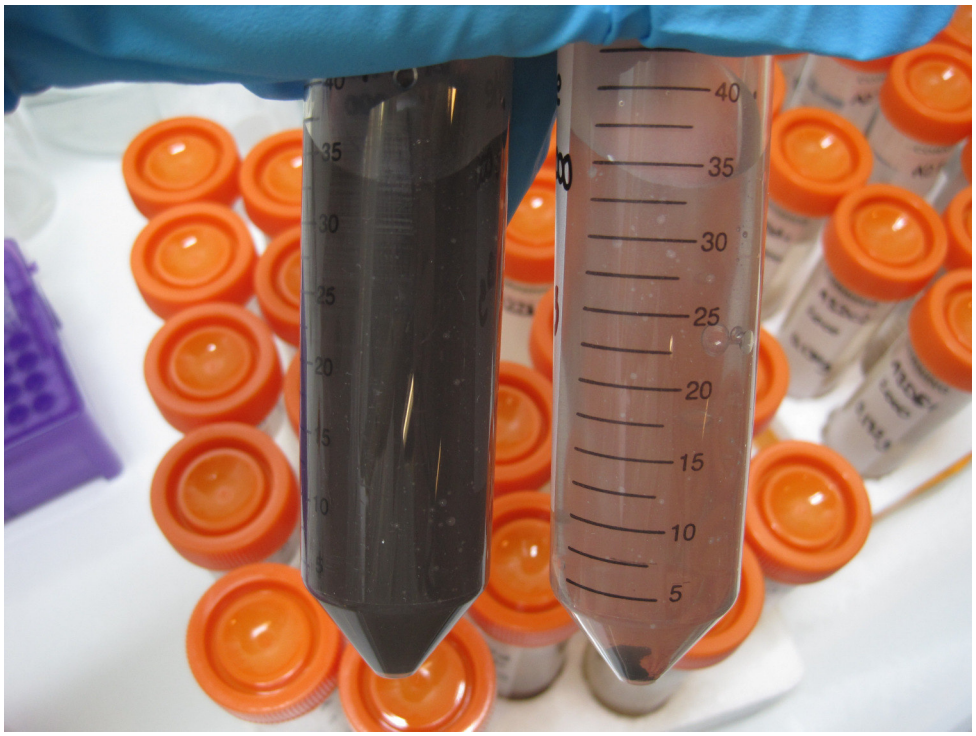

Fig. A.6: Isotherm study - after a shaking time of > 100 h (partly) pulverized catalyst material

Tab. A.4: LC-MS/MS parameter for target analysis by HPLC, Agilent Technologies 1200 Series, Palo Alto, CA, USA containing precursor and product ion and collision energy.

Compound	Precursor ion [m/z]	Product ion [m/z]	Collision energy V
PFCAs			
PFBA	213.0	168.9	5
PFBA IS	217.1	172.1	5
PFPeA	263.0	219.0	5
PFHxA	313.0	313.1	5
		269.0	5
PFHxA IS	315.0	270.0	5
PFHpA	363.0	319.1	5
		168.9	10
PFOA	413.0	369.0	5
		168.9	10
PFOA IS	417.0	372.1	5
PFNA	463.0	419.0	5
		219.0	10
PFNA IS	468.0	423.1	5
PFDA	513.0	469.0	5
		169.0	5
PFDA IS	515.0	470.0	5
PFUnDA	563.0	518.9	10
		169.0	20
PFUnDA IS	565.0	520.0	5
PFDoDA	613.0	568.9	5
PFDoDA IS	615.0	570.0	5
PFTeDA	713.0	669.0	5
PFHxDA	813.0	769.0	5
PFOcDA	913.0	868.9	5
PFSAs			
PFBS	299.0	99.0	40
		80.0	40.0
PFHxS	399.0	99.0	40
		80.0	40.0
PFHxS IS	403.0	103.0	40
PFOS	499.0	99.0	40
		80.0	40
PFOS IS	503.0	80.0	40
PFAS Precursor			
6:2 FTSA	426.8	406.8	20
		80.9	30
FOSA	498.0	498.0	5
		77.9	40
FOSA IS	506.0	77.9	40

Tab. A.5: LC-MS/MS parameter for target analysis by TSQ Quantiva (Thermo Scientific, Waltham, MA, USA) containing precursor and product ion and collision energy.

Compound	Precursor ion [m/z]	Product ion [m/z]	Collision energy V
PFCAs			
PFBA	213.0	168.9	10.25
PFBA IS	217.1	172.1	10.25
PFPeA	262.9	218.9	10.25
PFHxA	313.0	118.9	21.17
		268.9	10.25
PFHxA IS	315.0	270.0	10.25
PFHpA	362.9	318.9	10.25
		169.0	16.62
		318.9	10.25
PFOA	413.0	369.1	10.25
		169.1	18.8
		218.9	16.67
PFOA IS	417.0	372.1	10.25
PFNA	463.0	419.0	10.25
		219.0	17.13
		168.9	19.76
PFNA IS	468.0	423.1	10.25
PFDA	513.0	469.0	10.25
		169.0	21.53
		218.9	18.14
		268.9	17.64
PFDA IS	515.0	470.0	10.25
PFUnDA	563.0	519.0	12.93
		268.9	19.81
		319.0	19.1
PFUnDA IS	565.0	520.0	12.93
PFDoDA	613.0	569.0	10.25
PFDoDA IS	613.0	268.9	19.51
		318.9	19.15
		569.0	10.25
		570.0	10.25
PFTeDA	713.0	668.9	11.47
		319	21.38
		368.8	20.72
PFHxDA	812.9	768.9	13.03
		319	24.11
		369	22.54
		419.1	20.21
PFOcDA	912.9	869	14.1
		419	22.39
		369	24.21
PFSAs			
PFBS	299.0	99.0	30.78
		80.0	34.73
	299.0	168.9	23.65
PFHxS	399.0	99.0	37.25
		79.9	41.9
		168.9	31.14
PFHxS IS	403.0	103.0	37.25

Tab. A.6: UHPLC-MS/MS parameter for target analysis by TSQ Quantiva (Thermo Scientific, Waltham, MA, USA) containing precursor and product ion and collision energy - continued.

Compound	Precursor ion [m/z]	Product ion [m/z]	Collision energy V
PFOS	499.2	98.9	42.41
		80.0	48.07
		229.9	39.98
PFOS IS	503.0	80.0	48.07
PFAS Precursor			
6:2 FTSA	427.0	406.9	23.85
		81.0	34.27
		406.9	23.85
8:2 FTSA	527.2	392.8	51.8
		486.9	40.4
		506.9	35.3
FOSA	498.0	478.0	24.66
		78.0	34.07
FOSA IS	506.0	77.9	34.07
Et-FOSA	526.0	168.9	29.11
		219.0	26.64
		269.0	27.04
		419.0	18.24
Et-FOSA IS	531.0	169	29.11

a)

b)

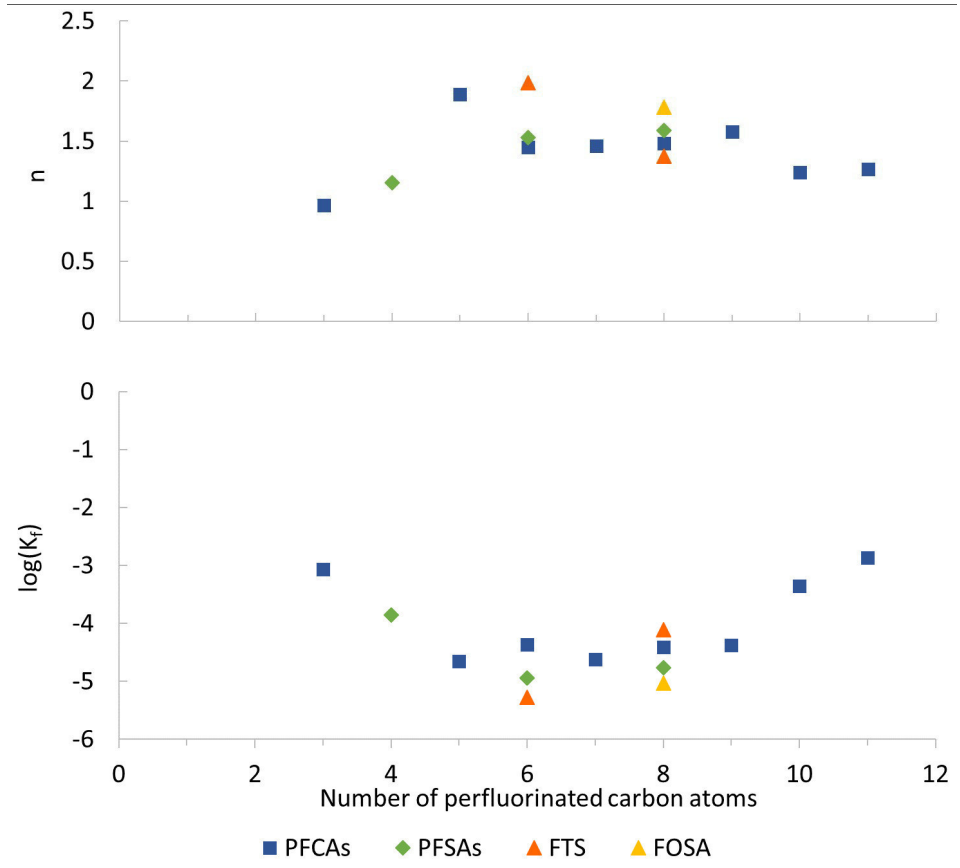

Fig. A.7: Estimated Freundlich isotherm parameters for all fitted compounds in tap water a) adsorption intensity (n) and b) adsorption capacity (K_f)

Tab. A.7: Overview over detected PFASs concentrations in negative blank samples. For the Pretest the mean is calculated from duplicate samples. For the Pilot scale, the mean is calculated from triplicate and for the lab scale trials the mean is calculated for quadruplicate samples. σ refers to the with Excel calculated standard deviation for these samples.

	Pretests									
	MilliQ		tap		DOC		Pilot scale		Lab scale	
Compound	**mean**	σ	**mean**	σ	**mean**	σ	**mean**	σ	**mean**	σ
PFCAs										
PFBA	0.0	0.0	0.0	0.0	0.0	0.0	-	-	0.0	0.0
PFPeA	0.0	0.0	0.0	0.0	0.0	0.0	0.0	0.0	0.0	0.0
PFHxA	0.0	0.0	0.0	0.0	0.0	0.0	0.0	0.0	12.5	13.0
PFHpA	0.0	0.0	0.0	0.0	0.0	0.0	0.0	0.0	0.4	0.9
PFOA	0.0	0.0	0.0	0.0	1.7	2.3	8.1	0.4	0.0	0.0
PFNA	0.0	0.0	0.0	0.0	0.0	0.0	0.0	0.0	0.5	0.9
PFDA	0.0	0.0	0.0	0.0	16.4	18.8	0.0	0.0	0.0	0.0
PFUnDA	32.2	11.5	0.0	0.0	92.9	41.5	0.4	0.7	0.0	0.0
PFDoDA	4.8	6.8	0.0	0.0	18.2	25.7	0.1	0.2	0.0	0.0
PFTeDA	896.9	88.8	0.0	0.0	496.7	702.4	0.4	0.7	0.0	0.0
PFHxDA	0.0	0.0	0.0	0.0	554.1	22.8	0.0	0.0	0.0	0.0
PFOcDA	0.0	0.0	0.0	0.0	1114.9	1576.7	0.0	0.0	0.0	0.0
PFSAs										
PFBS	0.0	0.0	0.0	0.0	0.0	0.0	5.8	0.4	14.9	6.2
PFHxS	0.0	0.0	0.0	0.0	0.0	0.0	2.5	0.2	2.2	3.3
PFHxS br	0.0	0.0	0.0	0.0	0.0	0.0	0.0	0.0	0.0	0.0
PFOS	2.4	3.4	0.0	0.0	5.0	7.0	4.0	0.6	22.1	27.7
PFOS br	0.0	0.0	0.0	0.0	0.0	0.0	0.0	0.0	0.0	0.0
PFAS precursor										
6:2 FTSA	0.0	0.0	0.0	0.0	0.0	0.0	0.0	0.0	0.0	0.0
8:2 FTSA	0.0	0.0	0.0	0.0	11.6	16.4	0.3	0.1	23.2	11.1
FOSA	6.5	9.1	0.0	0.0	38.4	36.8	0.5	0.2	0.0	0.0

Tab. A.8: Second order rate constants for the PFASs removal during the ozone and catalyst treatment in the pilot scale set-up. R^2 functions as a quality parameter for the fit according to a second order rate law.

Compound	Recovery [%]	R^2
PFCAs		
PFPeA	2.4E-03	0.948
PFHxA	8.8E-04	0.943
PFHpA	4.8E-03	0.977
PFOA	3.3E-01	0.925
PFNA	5.2E+00	0.828
PFDA	3.1E+00	0.938
PFUnDA	5.3E-01	0.931
PFDoDa	1.3E-01	0.942
PFTeDA	7.0E-03	0.913
PFHxDA	4.2E-03	0.839
PFOcDA	1.5E-03	0.614
PFSAs		
PFBS	1.8E-03	0.877
PFHxS	3.2E-02	0.963
PFHxS br	1.1E-02	0.985
PFOS	1.3E+00	0.967
PFOS br	1.3E+00	0.967
PFAS precursor		
6:2 FTSA	1.7E-01	0.931
8:2 FTSA	4.0E+00	0.925
FOSA	8.4E-01	0.940
FOSA br	1.0E+00	0.954

a)

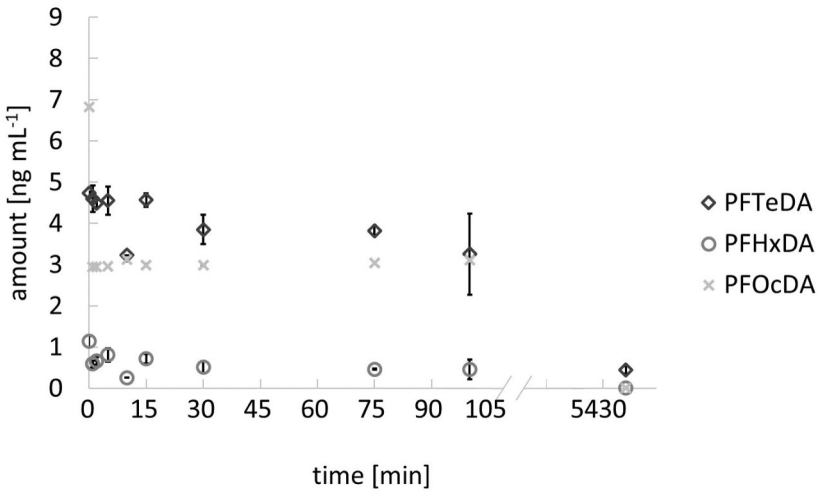

b)

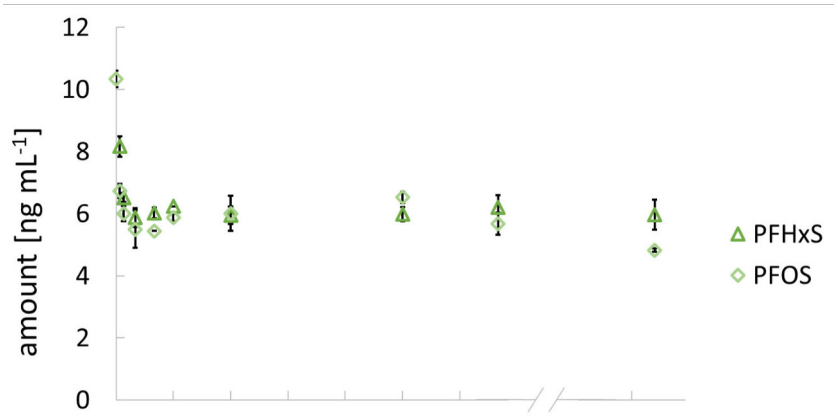

c)

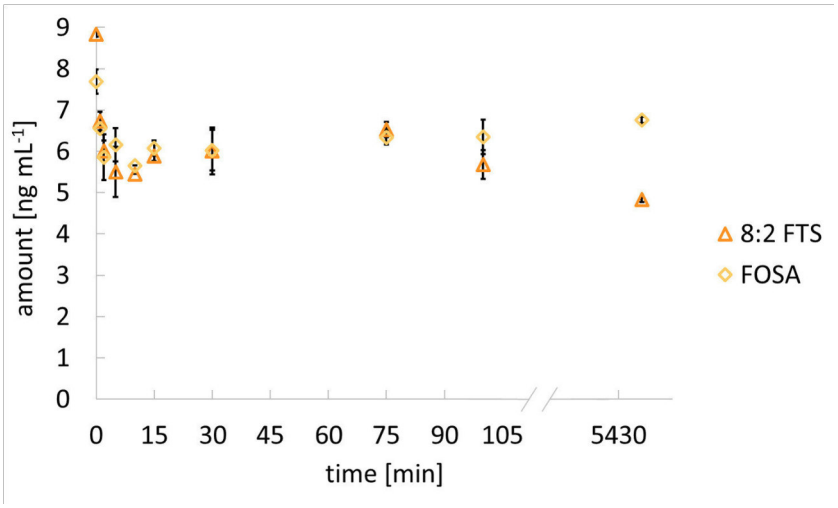

Fig. A.8: Processes of balance adjustment during the kinetic trials for the following compounds, a) PFBA, PFPeA, PFHxA and PFHpA; b) PFOA, PFNA and PFDA; c) PFUnDA, PFDoDA, PFTeDA, PFHxDA and PFOcDA; d) PFSAs e) Precursors. The shown values are the mean of relative duplicate samples, the errors are calculated as the deviation between the mean and a duplicate sample.

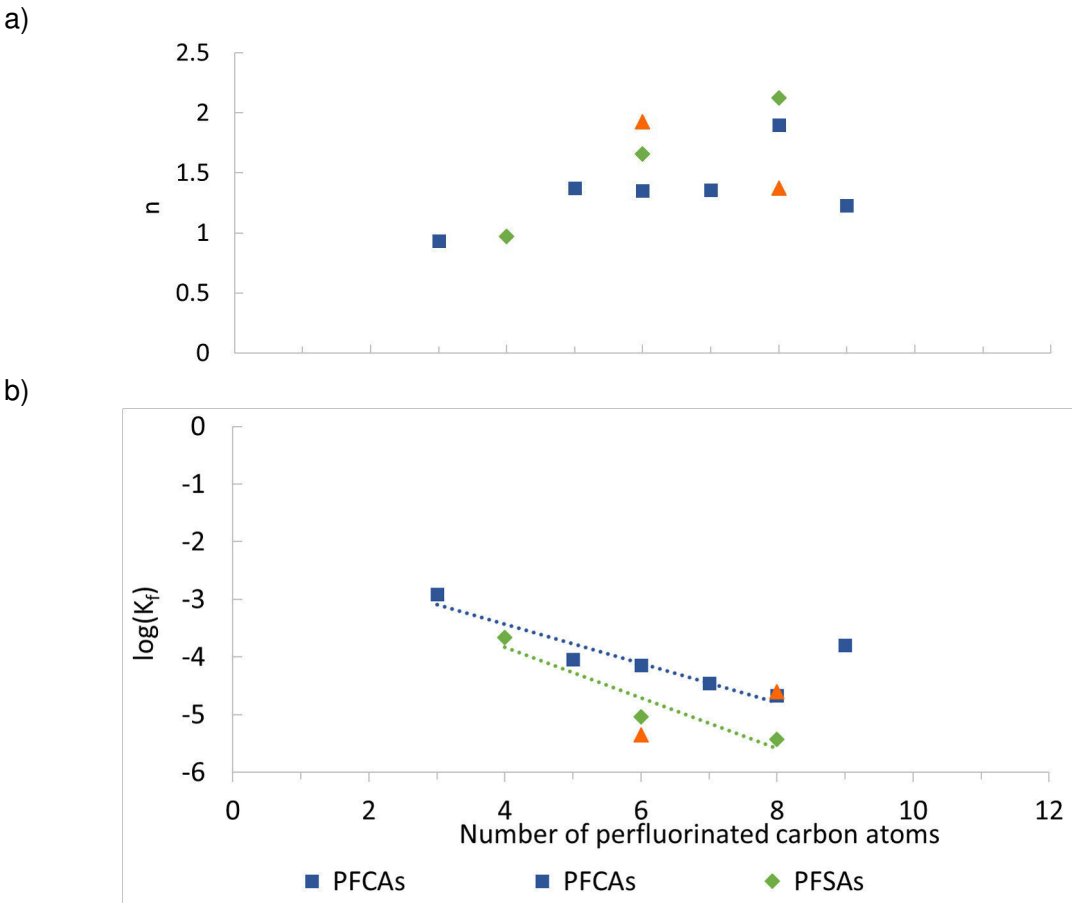

Fig. A.9: Estimated Freundlich isotherm parameters for all fitted compounds in DOC water a) adsorption intensity (n) and b) adsorption capacity (K_f)

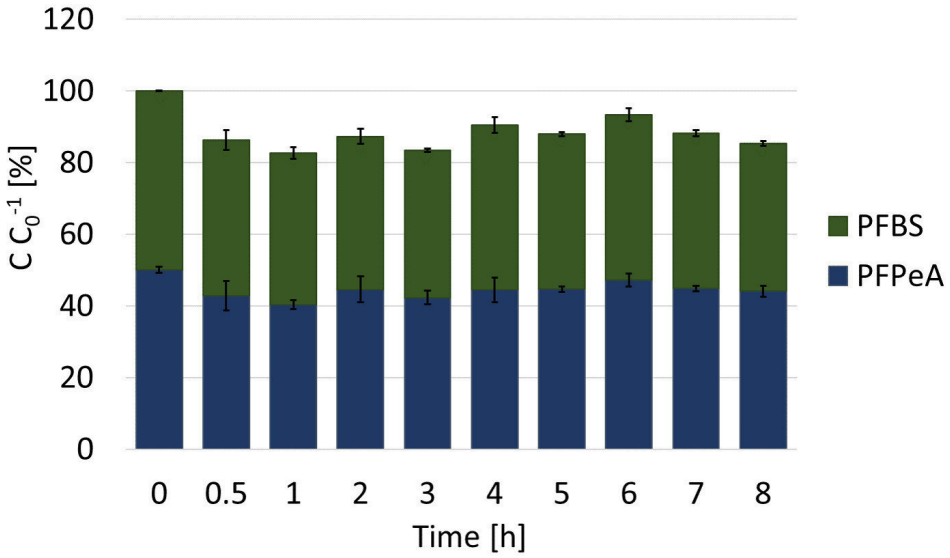

Fig. A.10: Residual concentration of compounds with four perfluorocarbon atoms during 8 h of ozonation. The sum of all relative values at the time of the 0 h sample is set as 100 %. Following values are calculated corresponding to this.

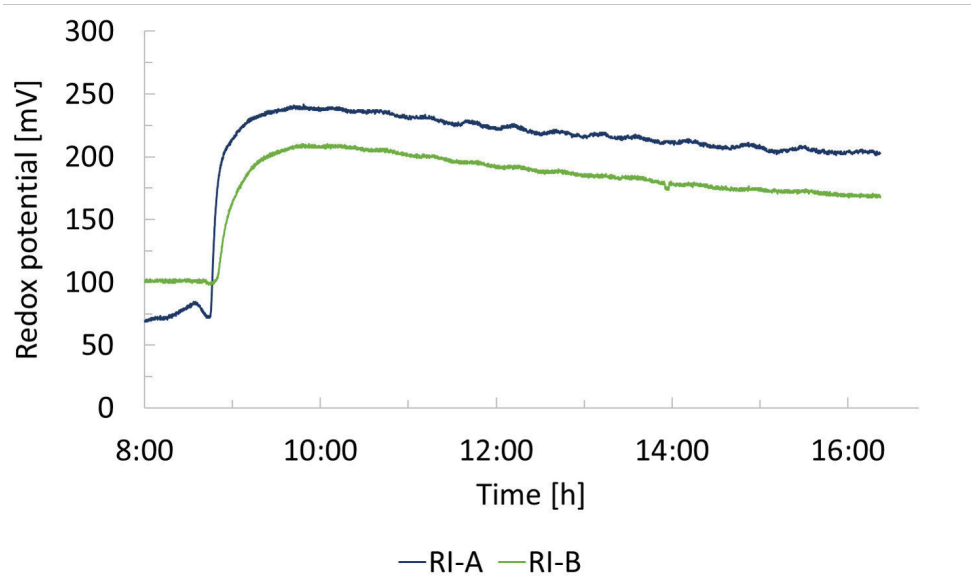

Fig. A.11: Progression of the redox potential during the ozonation. The redox potential was detected before (RI-A) and behind (RI-B) the catalytic bed.

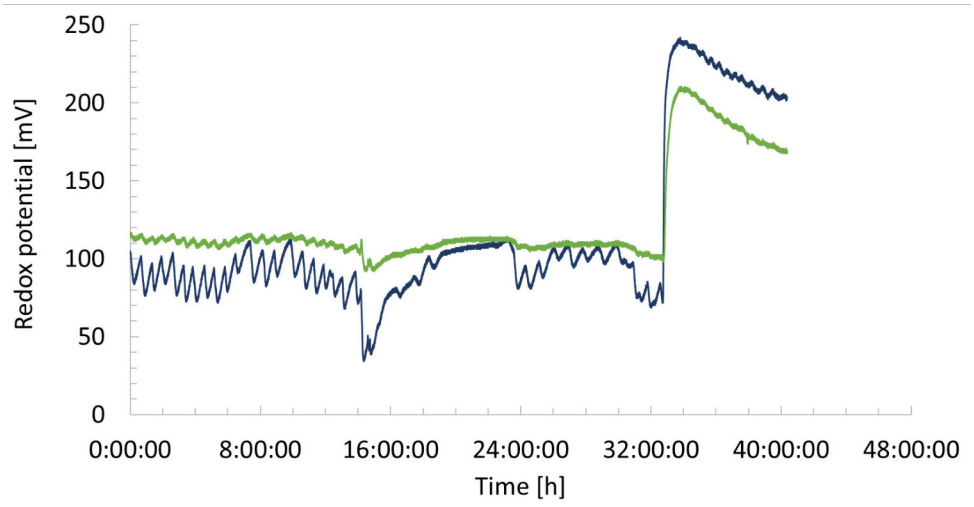

Fig. A.12: Redox potential measured during day 5 and day 6 of the pilot scale experiment.

a)

b)

c)

d)

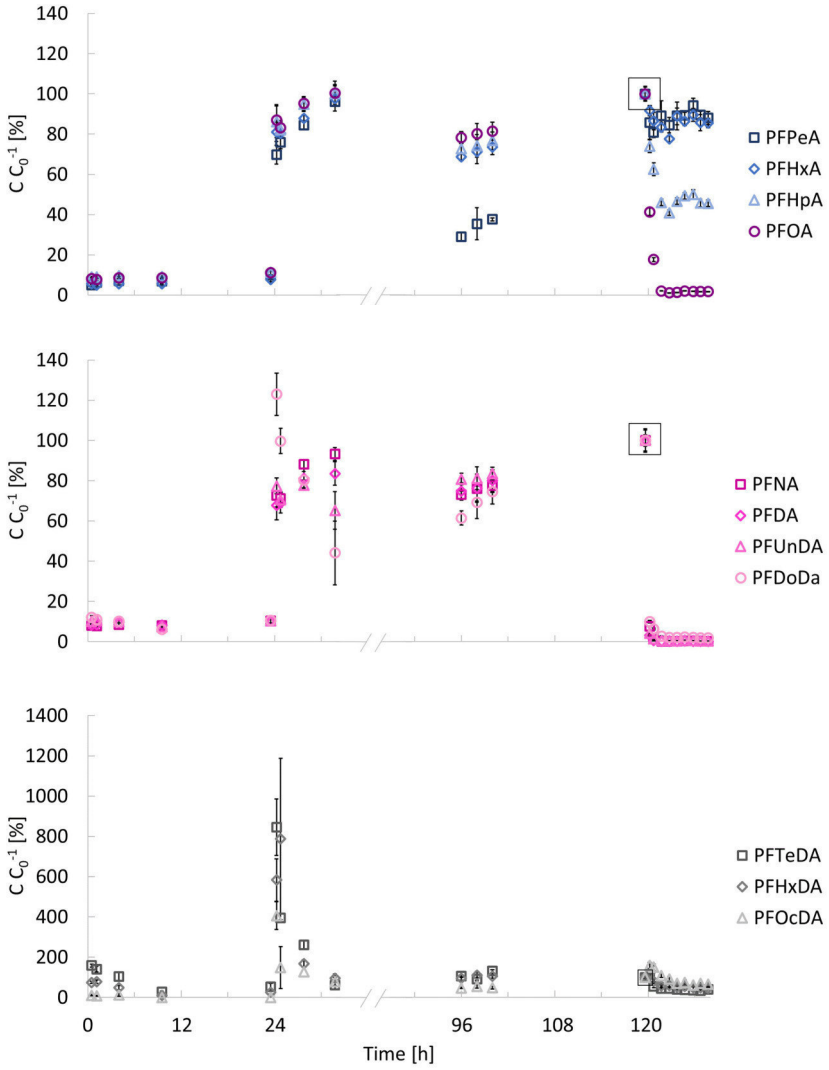
C C0-1 [%]
Time [h]
PFPeA
PFHxA
PFHpA
PFOA
PFNA
PFDA
PFUnDA
PFDoDa
PFTeDA
PFHxDA
PFOcDA
PFBS
PFHxS
PFOS

e)

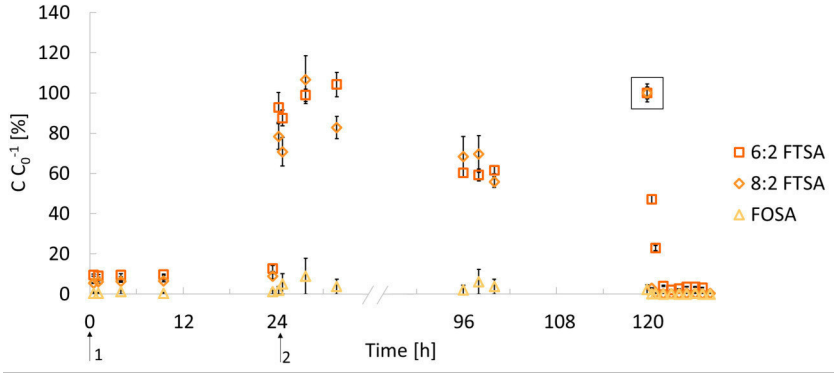

Fig. A.13: Processes of balance adjustment during the pilot scale trials for the following compounds a) PFPeA, PFHxA, PFHpA, PFOA b) PFNA, PFDA, PFUnDA, PFDoDA c) PFteDA, PFHxDA, PFOcDA d) PFBS, PFHxS, PFOS e) 6:2 FTSA, 8:2 FTSA, FOSA. Arrow 1 marks the first spike, arrow 2 marks the second spike (Tab. 4). All samples are standardized to S 14 (0h) which is marked with the black square. Please note different y-axis labelings.

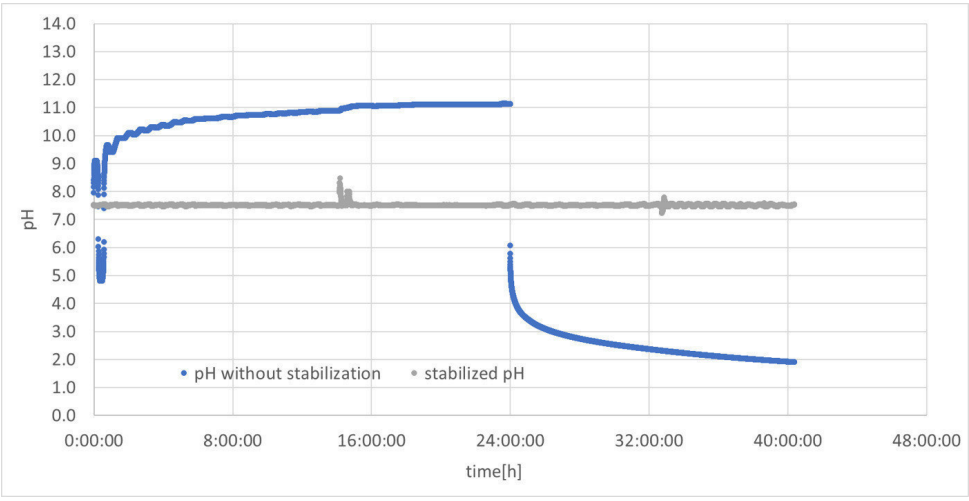

Fig. A.14: Detected pH and calculated pH of day five and six during the pilot scale experiment.

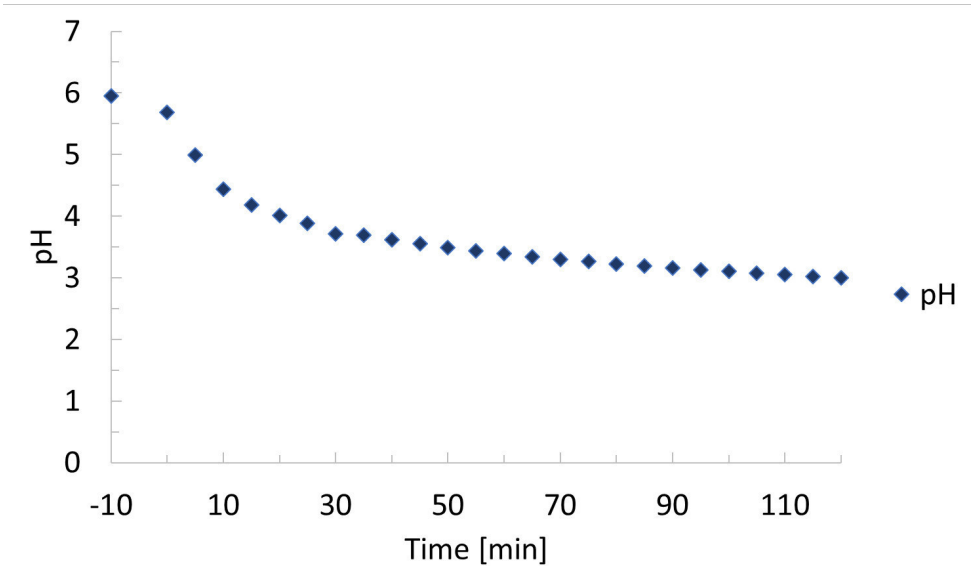

Fig. A.15: Detected pH of the positiv blank adsorption to the catalyst (2a) during the period of the lab-scale experiment.